AD NUMBER

ADC007024

NEW LIMITATION CHANGE

TO

Approved for public release, distribution unlimited

FROM

Distribution authorized to U.S. Gov't. agencies and their contractors; Administrative/Operational Use; Jan 1976. Other requests shall be referred to Office of Naval Research, Arlington, VA 22217.

AUTHORITY

ONR ltr, 3 Dec 2003

UNCLASSIFIED

AD NUMBER
ADC007024
CLASSIFICATION CHANGES
TO
unclassified
FROM
confidential
AUTHORITY
31 Dec 1983 per GDS document marking

THIS PAGE IS UNCLASSIFIED

AD NUMBER

ADC007024

CLASSIFICATION CHANGES

TO

confidential

FROM

secret

AUTHORITY

31 Jan 1978 per GDS document marking

GENERAL DECLASSIFICATION SCHEDULE

IN ACCORDANCE WITH

DOD 5200.1-R & EXECUTIVE ORDER 11652

SECRET

1

AD C007024

AD No.

DDC FILE COPY

Planning Systems Incorporated

7900 Westpark Drive • Suite 507

McLean, Virginia 22101

(703) 790-5950

SECRET

Subject to GDS
Declassify 31 Dec. 1983
Declassification date taken from bet
of contract. 1975 per Ms. Mary
Johnson, ONR/code 102.

JEC
8/23/76

SECRET

PSI CONTROL IS-391-56
7900 Westpark Drive
McLean, Virginia 22101

1

6

CHURCH OPAL: SURVEILLANCE OF SHIPPING (U)

8

by

10

Lawrence A. Turk,
Allen E. Barnes
Louis P. Solomon

12 137p.

Prepared for:

Office of Naval Research
Code 102-OSC-LRAPP
Arlington, Virginia 22217

Contract No. 15 N00014-76-C-0545 New

14 PSI-TR-036027

January 15, 1976

Submitted by:

Planning Systems Incorporated
7900 Westpark Drive
Suite 507
McLean, Virginia 22101

DD 254 dtd 15 DEC 75
CLASSIFIED by N00014-76-C-0545
SU[illegible] ICATION
SCHEDU[illegible]
AUT[illegible] AT TWO YEAR
INTERVALS
DECLASSIFIED ON DECEMBER 31, 1983

NATIONAL S[illegible] INFORMATION
unauthorized disclosure subject
to criminal sanctions

390 939 bp

SECRET

TABLE OF CONTENTS

LIST OF FIGURES

LIST OF FIGURES (cont'd)

LIST OF FIGURES (cont'd)

LIST OF TABLES

ACKNOWLEDGEMENTS

We are pleased to acknowledge the support and encouragement given to us by the Long Range Acoustic Propagation Project as personified by its Director, Dr. R. D. Gaul, CDR. T. J. McCloskey, Mr. E. L. Smith, Ms. B. J. Stephens, and the Technical Director of CHURCH OPAL, Mr. Sidney Kulek of XONICS. The technical assistance of Mr. K. W. Lackie of NAVOCEANO was of particular importance in the design of the data collection plan. The outstanding support in this data collection effort given by COMTHIRDFLT, COMPATWINGSPAC, the Operational VP Squadron VP-1 and NAVOCEANO VXN-8 is gratefully acknowledged. Finally, we are indebted to Mr. D. W. Ritchie of PSI for his assistance and computer skill in reducing the data.

0. (C) SITUATION, MISSION, AND REPORTS OF RESULTS (U)

(C) The CHURCH OPAL Exercise is one of a series of LRAPP Exercises designed specifically to acquire environmental acoustic data required for ASW program decisions. At-sea operations were conducted during September 1975 in a region of the Northeast Pacific Ocean, shown in Figure 0-1.

(C) This exercise includes the following ocean acoustic experiments related to the Moored Surveillance System (MSS), the Sound Surveillance System (SOSUS), and the Surveillance Towed Array Sonar System (SURTASS):

- (1) Noise Floor Characteristics
- (2) ASEPS Evaluation; Coherent Multi Array Processing
- (3) Horizontal Directionality of Ambient Noise; Towed Array Performance

The objective of the Noise Floor Verification Experiment is to verify the noise floor concept. The noise floor is a depth below which distance shipping noise is significantly reduced and where short range acoustic sensors could attain a substantial performance gain. The objectives of the second experiment relates to the evaluation of the propagation model component of the Automated Signal Excess Prediction System (ASEPS) and the evaluation of coherent multi array processing algorithms. The third experiment addresses the measurement of horizontal directionality of ambient noise and the assessment of towed array performance as it relates to narrow beam noise threshold and variability.

(C) CHURCH OPAL operations were centered along the CHURCH ANCHOR baseline at 143°30'W. M/V SEISMIC EXPLORER deployed the LAMBDA array for signal propagation, coherence, beam noise, and noise directionality measurements in the vicinity of Sites λ1, λ2, λA, and λB. M/V AMERICAN DELTA II deployed Vibroseis CW projectors for propagation and coherence measurements at selected locations and along tracks associated with Sites V1 to V17a. R/V MOANA WAVE made a series of environmental measurements and

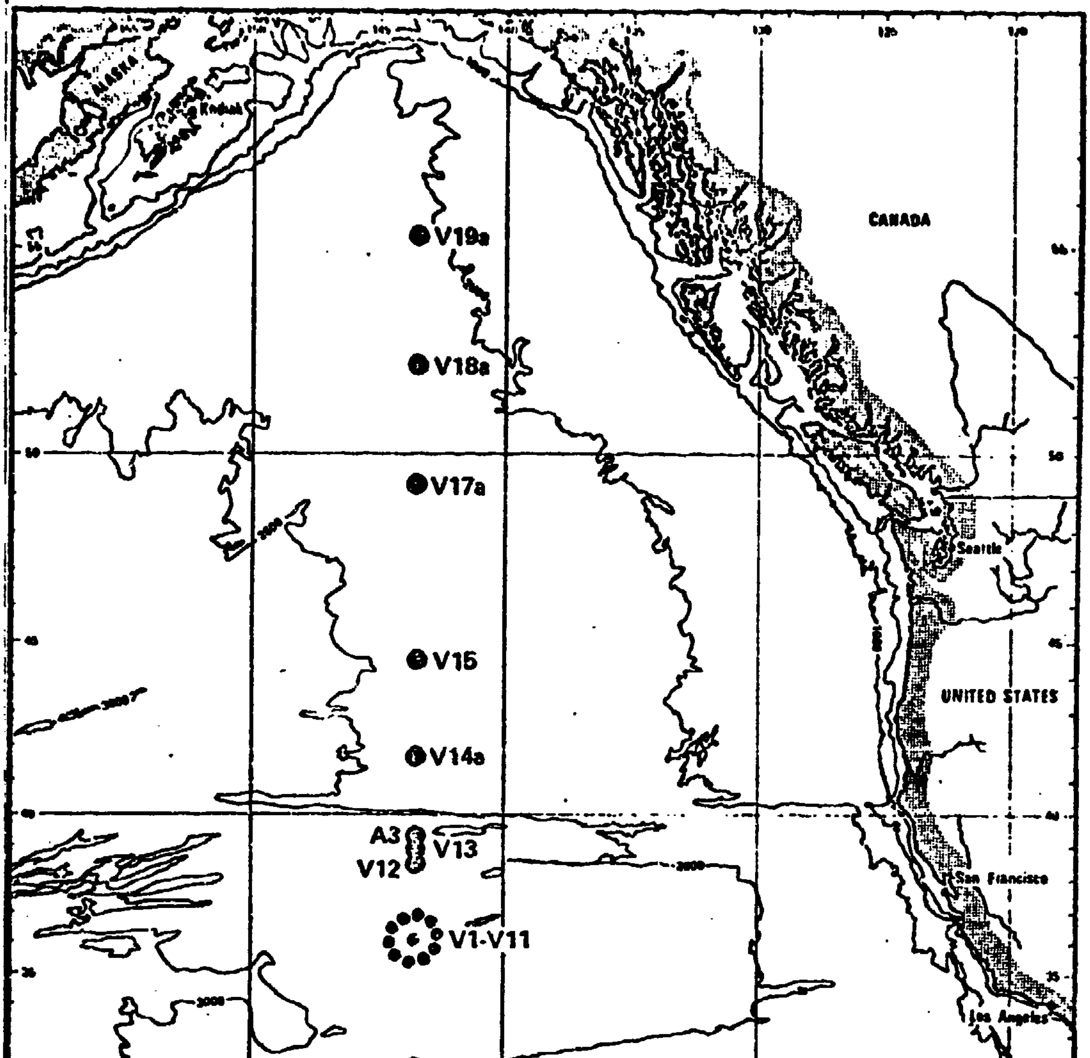

Figure 0-1. (C) CHURCH OPAL Exercise Area and Principal Reference Points (U)

deployed ACODACs at Sites A1-A3 for the purpose of making noise and signal propagation measurements at a variety of depths. The ACODAC at Site A1 was recovered; the ACODACs at Sites 2 and A3 were not. In addition to deploying the DELTA array for noise measurements at Site λB on one occasion, MOANA WAVE also deployed the backup HX-231F CW projector at selected locations and along tracks associated with Sites V13-V19a. An NRL EP-3A aircraft dropped Mark 64 SUS in the vicinity of the LAMBDA array at Site λB on four towed array deformation flights. A VXN-8 RP-3A aircraft made 12 environmental (AXBT and ART) measurement and shipping surveillance flights. Each of two (2) COMPATWINGSPAC P-3C aircraft made two (2) shipping surveillance flights. WARF and SEA ECHO OTH radars conducted surface shipping surveillance operations in limited areas. Several shore stations monitored selected Exercise events.

(C) This program is designed to provide a basis for management decisions concerning the development of undersea surveillance systems. The performance of these systems depends on the acoustic environment in which they operate. To evaluate the available options it is necessary to obtain a quantitative description of these aspects of the acoustic environment that affect system performance. The CHURCH OPAL Exercise drew deliberately on the 1973 CHURCH ANCHOR Exercise data base and thereby expanded the data base and increased acoustic prediction capability in the Northeast Pacific Ocean Basin.

(U) A Data Analysis Plan* distributed by LRAPP provided specific direction to participants for the preliminary phase of the analysis. A limited data base was defined, interpretive analytical techniques were described, priorities for reduction and analysis of the data were enumerated, and schedules and responsibilities leading to publication of preliminary analysis results in March 1976 were established. Budgetary limitations have had a

*LRAPP, October 1975, CHURCH OPAL Data Analysis Plan (U) (SECRET), prepared by Xonics, Inc.

significant impact on this limited analysis program and, as a consequence, original schedules have been extensively revised. Currently, a revised Data Analysis Plan is being prepared for subsequent analysis and reporting employing a broadened data base.

1. (S) INTRODUCTION (U)

(C) This report describes the results of surveillance of surface shipping by aircraft (A/C), comparisons of the aircraft surveillance of shipping with historical shipping data, and an investigation of the feasibility of employing over the horizon (OTH) radar for surveillance of surface shipping during the CHURCH OPAL exercise in the Northeast Pacific. The shipping surveillance portion of the exercise was conducted during September 1975, using fleet aircraft, NAVOCEANO VXN-8, the SEA ECHO, and WARF OTH radar systems.

(S) The objectives of the CHURCH OPAL Exercise as related to surveillance of shipping were three-fold: First, to obtain the nearby shipping field concurrent with LAMBDA and DELTA horizontal directionality measurements, and to determine the ships on LAMBDA beams during beam noise measurements; second, the comparison of observed CHURCH OPAL shipping distributions with theoretical models and historical shipping fields from other data sources; third, the evaluation of OTH radar systems to provide shipping distributions of adequate quality for use in theoretical models of ship distributions and ambient noise prediction.

(U) The report is organized as follows: Sections 2 and 3 present the procedure for reducing and analyzing respectively, the raw data obtained from A/C surveillance. The raw data base consists of commentary on radar and navigation performance, A/C tracks and surface ship positions given by radar range and bearing from the A/C. Appendix A presents A/C tracks and ship contacts for the 12 flights and 8 days of coverage.

(C) Section 4 outlines the procedure used to generate the instantaneous discrete shipping field. A correction procedure was applied to some of the data which allowed for a more accurate reconstruction of ship positions about the array. Appendix B presents the reconstructed shipping fields for September 14 and 16. Individual ship contacts are given by range and bearing from the array. Ship positions are also given by their latitude and longitude. The uncertainty in ship positions as determined by A/C is considered in Section 4.

(U) A comparison between model and historical shipping distributions with the CHURCH OPAL data is given in Section 5. The reduced CO shipping data is given in Appendix C and a quantitative comparison with historical data summarized in Appendix D.

(U) Section 6 presents a comparison of OTH and aircraft ship distributions. An overall comparison based upon shipping densities is made for all areas for the entire exercise period, and a detailed comparison for September 14 between WARF data and A/C data is made for WARF Area 2. A detailed comparative analysis between WARF and A/C detections was possible only on the 14th of September due to financial constraints. Nevertheless, the comparison, indicated in Figure 6-2, is representative of the problems which are encountered in attempting to make a detailed comparison. The reports of SRI and NRL on the operations of their WARF and SEA ECHO radars respectively, is given in Appendix E.

2. (C) DATA REDUCTION FOR SHIPPING DENSITIES (U)

(U) The location of observed surface vessels and the tracks flown by the surveillance aircraft plus estimates of the performance of the A/C radar system at each point where ships were observed by radar along the flight track represents the raw data base. From these raw data three numbers were derived for each five by five degree square within A/C radar range for each leg of each flight. The first is the number of contacts observed in a given square within radar range for that leg, the second is the portion of the given square within the estimated radar range of the flight path, and the third is ship density for the given square. A ship density is not calculated if less than half the square was surveyed.

(U) Overlapping areas created at A/C track turn points were apportioned approximately equally between the two legs in order not to be counted twice. From observers' comments concerning the generally good radar operation, a standard radar coverage radius of 75 nm was established and was used except in those cases where it was obvious from the observer, navigation or contact logs that a reduced or greater radar range was in effect. As a check on radar operations, a straightforward statistical test may be employed. The aircraft track is generally a sequence of rhumb line segments which crisscross the area of interest. Although a leg may parallel a shipping route for a short distance, when one considers a statistic involving the entire track, these local fluctuations are smoothed out by the law of large numbers. For each of the N ship contact $\{C_i\}_1^N$ observed on a flight, there is a distance r_i, the range of the ship from the flight track. If the radar has good coverage to 75 nm (or more), then the set of all ranges observed on the flight which were less than 75 nm should be approximately uniformly distributed, i.e., the set

$$\{r_i : 1 \leq i \leq N, \quad r_i \leq 75\}$$

should be representative of a draw from a $\mathcal{U}[0, 75]$ distribution.

If the distribution is not uniform but decreases with range, then it can be assumed that surface vessels within the coverage radius are being missed and a resultant bias is being introduced. A determination that these distributions were approximately uniform preceded the establishment of the expected radar coverage range.

(U) For each exercise day the number of contacts and the percent coverage for each five by five degree square were summed over all legs of all flights, e.g., if a flight covered 75% of a specific square on both an outbound and inbound leg then percentage coverage due to that flight would be 150% and the number of contacts would be the sum of the two observations. It is recognized that any multiple coverage thus created does not necessarily provide completely independent observations since the relaxation time is a function of the average ship transit time through the square; however, this procedure does not introduce any bias and the variance of the density estimator is reduced by any deviation from a correlation of 1.0 that might exist between observations.

(C) Ship positions and their range and bearing from the LAMBDA array on the dates of 14 and 16 September are given in Appendix B. Array location and times are given in Table B1. Due to A/C navigation limitations, it was decided that array location be determined from the M/V SEISMIC EXPLORER Satellite Navigation Log. The actual ship positions to be used in determining LAMBDA beam noise threshold levels are given in Tables B2 and B3. These ship positions were checked against the Naval Oceanographic Office (NOO) exercise reconstruction, and it was found that the positions were in agreement.

(U) Ship range was computed for each surface contact using equation (1) for the great circle distance between the array and each ship location. Bearing as measured from the array was computed using equation (2), where latitude and longitude of the array is given by (θ_a, ϕ_a) and for the surface ship (θ_s, ϕ_s).

$$D(nm) = 60 \cos^{-1}[\sin \theta_a \sin \theta_s + \cos \theta_a \cos \theta_s \cos(\phi_s - \phi_a)] \quad (1)$$

$$B = \cos^{-1}\left[\frac{\sin \theta_s - \sin \theta_a \cos(D/60)}{\sin(D/60) \cos \theta_a}\right]$$

$$B = \begin{cases} B & ; \sin(\phi_s - \phi_a) < 0 \\ 360 - B & ; \sin(\phi_s - \phi_a) \geq 0 \end{cases} \quad (2)$$

(U) The sum of the contacts for each five by five degree square is divided by the sum of coverage over that square to give the estimated ship density for the given exercise day. The results are contained in Appendix C which presents, for each measurement day:

(1) the sum of the contacts
(2) the sum of the coverage
(3) the estimated shipping density [i.e., the quotient (1)/(2)] for all 5° x 5° squares having coverage of 50% and greater.

We note that the estimates are given for shipping densities — not the number of ships in a square which are customarily estimated in historical shipping "density" charts. The two terms are identical except when land area is included within the square and for such a square an adjustment must be made before a comparison with historical data can be undertaken.

(C) The actual noise directionality is computed from a directional ambient noise model. These models, of which there are a small number, require as inputs shipping densities in some cases, and actual ship positions in other cases. In those models which require shipping densities, the data is provided in 1° x 1° squares.

That requires that the 5° x 5° square data be broken down to 1° x 1° square data. This is done using an exponential weighted smoothing algorithm.* The models then accept this 1° x 1° square data derived from the basic 5° x 5° square data and breaks it down into even smaller areas, viz., 10' x 10' square. This is obtained from the 1° x 1° square data generally by uniformly distributing the densities into the 36 - 10' x 10' squares in each 1° x 1° square. Comparisons in determining the validity of shipping surveillance data is almost always made by comparing 5° x 5° square, or even larger areas. The smaller number of ships in any 1° x 1° square generally is too variable to allow reasonable comparisons with various data and these larger areas are almost always employed. There are exceptions to this procedure, but only in very special circumstances such as in narrow seas, straits, or similar confined ocean areas.

(C) The use of shipping densities as opposed to real or specific ship positions in the ambient noise models is, to a great extent, dependent upon the system which is being studied. If a system with broad beams is being considered, then there is always a large number of ships seen within that beam. Therefore, if a few ships are excluded from consideration, the effect on the beam noise level is quite small. At the low frequencies which are being considered, the propagation loss is not of great importance to the ambient noise field, and it may be fairly argued that the integration of the shipping density over the area covered by the beam is the major effect on the beam noise level. Comparison of measured with predicted beam noise levels indicate the soundness and

*(L.P. Solomon, "CHURCH ANCHOR: AIRCRAFT SURVEILLANCE OF SHIPPING" PSI TR-004002, Pages 13-18).

validity of this approach. A direct result of this observation is the recognition that the accuracy constraints on the shipping density is 5° x 5° square is much less stringent than on a more compact density specification. Our experience with the 5° x 5° historical shipping fields as modified by at-sea exercise data indicates its dependability and utility when used by directional ambient noise models in considering broad beam systems.

3. (U) STATISTICS OF THE SHIPPING DENSITIES (U)

(U) For each 5° x 5° square let n_i be the number of ships observed on the i^{th} day ($i = 1,2,\ldots K$) and K the number of days of coverage for a given square. Define p_i to be the proportion of the area covered on the i^{th} day. If $p_i \neq 0$ then an estimate of the density of ships in the area on the i^{th} day is given by

$$d_i = n_i/p_i \tag{3}$$

The daily weighted ship densities are given in Appendix C, Figures C1 through C8. For later convenience, define:

$$s = \sum_{i=1}^{K} p_i \tag{4a}$$

$$s_2 = \sum_{i=1}^{K} p_i^2 \tag{4b}$$

(U) The weighted average has the form

$$d = \frac{1}{m}\sum_{i=1}^{K} w_i d_i \tag{5}$$

where w_i and m are constants (the constant m is introduced so that the w_i may have simpler form). In order to attach the same importance to each square mile which was covered, the weight must be proportional to the amount of area covered, i.e., $w_i = p_i$. The constant m is chosen such that d is an unbiased estimator. That is, if d_i are independent samples of a random variable (called "density") having mean μ, then m is chosen such that the expected value of d is μ, i.e.,

$$E[d] = \mu \tag{6}$$

which implies $m = s$. But $w_i d_i = p_i d_i = n_i$ so

$$d = \frac{1}{s}\sum_{i=1}^{K} n_i \tag{7}$$

(U) For similar reasons, a weighted estimator of variance is desirable. This estimator has the form

$$\hat{\sigma}^2 = \frac{1}{\hat{m}} \sum_{i=1}^{K} \hat{w}_i (d_i - d)^2 \tag{8}$$

Letting $\hat{w}_i = p_i$ gives a system consistent with equation (7). This system favors the larger area coverage, but does not place inordinate emphasis on the days with maximum coverage. Choosing m such that $\hat{\sigma}^2$ is an unbiased estimator gives

$$\hat{\sigma}^2 = \frac{s}{s^2 - s_2} \left(\sum_{i=1}^{K} n_i^2/p_i - d^2 s \right) \tag{9}$$

where $n_i^2/p_i \equiv 0$ when $n_i = p_i = 0$.

(U) Ship density statistics for 5° x 5° squares are provided if there was 50% coverage or more for the given square. The number of days K, for which A/C coverage met the above criterion for the 5° x 5° squares is given in Appendix D, Figure D1. We note that there is a variation in K between squares, which depends on the number of flights, radar range, and the extent of overlapping coverage in the given area. Weighted average densities and standard deviations for these squares are given in Figure D2 and Figure D3. Since the sums in Equations (7) and (9) are over K, our confidence in these statistics must vary accordingly.

(U) It is of interest to compare the CHURCH OPAL (CO) averaged distributions with predicted model results and other historical files. Such a comparison may be used to evaluate the model predictions, note any temporal variability in the shipping fields and to up-date the model shipping routes if necessary. The averaged shipping densities obtained in September of 1973 during the CHURCH ANCHOR (CA) exercise together with the RMS and Automated Marine

International (AMI) model distribution are given for 5° x 5° squares in Figure D3. The ratio of CA, RMS and AMI densities to CO is given in Figure D4. Analysis of these data is given in Section 5.

4. (S) AIRCRAFT PERFORMANCE AND LIMITATIONS (U)

(C) Radar coverage of surface vessels was provided on eleven days during the CHURCH OPAL Exercise. On each of two high priority LAMBDA beam noise measurement days (14 and 16 September), three flights covered the surrounding area. OTH radar provided overlapping coverage on the 14th for the region labeled Area 2 in Figure E1.

(C) Appendix A gives the actual tracks for each flight and Table A1 gives the schedule of flights for each exercise day. Reliable data were not obtained on Flight PB on the 14th due to radar malfunction. The flight was intended to provide far-field shipping data for the region 18-22°N, 137-158°W. Fortunately, excellent radar conditions prevailed, and flight PA was able to provide partial coverage in this region. Ship contacts were obtained in this region which are over 950 nm from the array. Flights on September 26, 29 and October 1 were at very high and low altitudes, and not primarily intended for shipping surveillance, but for airborne radiation thermometry measurements. Consequently, no statistics are provided on these dates; the other eight days were extensively analyzed.

(U) Flight Commanders were requested to fly at altitudes consistent with both good radar coverage and low clutter rate for the prevailing conditions. A scientific observer on each flight was responsible for the collection of the radar contact logs and navigation logs as well as for a personal log in which he was to document any deviations from the scheduled operations, e.g. radar malfunctions, changes in flight plan, bad weather conditions, etc.

(C) For each flight an overall mission effectiveness is given in Table A1. These evaluations are assessments over the entire duration of the flight. Weather conditions may have varied dramatically over certain portions of the track. Therefore, these performance estimates provide a measure of the mean effectiveness for a given flight. Accordingly, we judge overall A/C surveillance for these eight days of coverage to have been very good. The crews of both VXN-8 and VP-1 were excellent and their performance is responsible for the overall success of the missions. Of particular merit was the outstanding performance of personnel at the Tactical

Support Center, Barbers Point.

(S) In the following we delineate the procedure used to generate the Array and Ship Position Tables B1, B2 and B3. The reference times given in these tables for 14 and 16 September are the times A/C contact was made of the M/V SEISMIC EXPLORER (SE). Using data from the SE Satellite Navigation Log (SATNAVLOG) for ship position and speed, the position of SE was determined at the reference times by dead reckoning (DR). Ship logs showed that SE did not change course or speed during the time interval over which the DR computation was made so that we have high confidence in the SE positions given in Table B1 which for 2336A 14 September was

31.6378° N, 143.0780° W.

The position of SE determined by VXN-8 flight TE on the 14th from a range of 75 nm using APS-80 radar at the same time was

31.6055° N, 142.9521° W

Thus the two positions differ in latitude by $\Delta L = 0.0323°$ and longitude by $\delta\lambda = 0.1259°$. The difference in range δr between the two positions [using Equation (1)] is 6.72 nm. Assuming no uncertainty in dead reckoning the SE position from Satellite Navigation data, this distance can be thought of primarily as the error in the aircraft's track. The array, of course, is used in the post-exercise reconstruction as a tie point.

(S) On 14 September VXN-8 navigation was dependent upon a combination of LORAN-C (which was noted to be very poor for the above contact), celestial and radio fixes. On 16 September VXN-8 employed the LITTON-51 inertial navigation system. Contact of the SE was logged at a range of 19 nm. An analogous computation gave differences in latitude $\delta L = 0.0591°$ and longitude $\delta\lambda = -0.0010°$. This positional discrepancy represents a range difference of $\delta r = 3.54$ nm between the two locations.

(C) For all surface contacts logged by VXN-8 on the above dates the corresponding latitude and longitude differences, δL,

$\delta\lambda$ were added to all A/C ship positions. This correction is only valid for VXN-8 contacts; ship positions reported by fleet A/C were not altered. The shift in position of the VXN-8 contacts allowed a more accurate reconstruction of the shipping.

(U) Tables B2 and B3 are intended to provide the instantaneous discrete shipping fields for times 2336Z 14 September and 2259Z 16 September 1975, respectively. The positions of all surface contacts were not determined simultaneously, but over a period of several hours during which the shipping field did not remain stationary. Since surface ship speeds and bearings were not obtained, precise reconstruction of the discrete shipping field is not possible. Estimates however, can be made that provide an upper bound to the uncertainty introduced into the range and bearing of ship positions as measured from the array.

(U) Uncertainty in position of a surface contact with respect to the array will be introduced into Table B2 and B3 if there occurred relative motion between the contact and array over the time interval between A/C recording of the contact and the reference time given in the tables. If the relative motion was transverse, we approximate the upper limit in bearing uncertainty δB by

$$\delta B = v(\Delta t)/x \qquad (10)$$

where v is the surface ship speed, Δt the time interval between A/C determination of contact and the reference time, and x the radius vector from array to surface contact. Had the relative motion been entirely radial, the range uncertainty δR is

$$\delta R = v(\Delta t) \qquad (11)$$

(C) As representative examples we take from Table B2 entries 1, 16 and 20 and compute δB, δR for these cases. The results are summarized in Table 4.1 Entrees 1, 20 and 16 are for ship contacts in the far, middle and near shipping fields respectively. They are 919.1, 130.6 and 14.7 nm from the array. Assuming these contacts were moving transverse to the SE and therefore parallel to the array, the maximum bearing uncertainties are 3.1, 3.5 and 0.78° respectively. Thus we could write for entry 16 a bearing of 38.0769 ± 0.7802° (bearing has been measured from 0° T.

Had the motion been entirely longitudinal, the range would be given by 14.6680 $\pm$ 0.2000 nm. These examples illustrate the gross bearing and range resolution uncertainties that may be expected and the possible limitations of the discrete shipping fields given in Tables B2 and B3.

Table 4.1 (C)

Maximum Range and Bearing Uncertainties due to Ship Movement for Table B2 Entries 1, 16 and 20* (U)
(Reference time 142336 Z)

Table B.2 Entry	Range from Array (nm)	Time Logged (DTG)	δR^{+} (nm)	δB^{++} (deg.)
1	919.0800	141931	48.96	3.0539
16	14.6880	142337	0.200	0.7802
20	130.6212	150016	8.000	3.5093

* Assumes surface ship speed of 12 knots

$^{+}$ Assumes relative motion is entirely radial

$^{++}$ Assumes relative motion is entirely transverse

5. (U) COMPARISON WITH MODEL AND HISTORICAL SHIPPING DENSITIES (U)

(U) In this section we examine the variability in shipping densities for the CHURCH OPAL Exercise are examined. The weighted CO densities are compared with historical CHURCH ANCHOR, model RMS and AMI shipping fields.

(U) Examination of Figures C1-C8 shows that the individual CO weighted ship densities [d_i of Equation (3)] within a given 5° x 5° square may be highly variable. Furthermore, it seems that this variability can be associated with coastal and open ocean regions alike. From Figures D2 and D3 for the weighted average density and standard deviation (SD), we note a density variation in range of over 100% from squares of low and high standard deviation.* Therefore, it would appear that in the near-field, i.e., within a 5° x 5° square, the shipping distribution may be well respresented as a stochastic process.

(U) The overall ship densities computed during CHURCH ANCHOR and CHURCH OPAL show remarkable agreement. To study the results in detail we consider two regions, separated by the 35°N latitude. Above this line the squares with common (i.e., CA and CO) coverage generally had greater coverage during the CHURCH ANCHOR exercise than during the CHURCH OPAL. Conversely, those south of 35°N had far better coverage during CHURCH OPAL (indeed, many of the lower squares shown in Figure D4 had no coverage during CHURCH ANCHOR). In the southern region+ the CHURCH OPAL estimates gave a total of 57 ships, as compared with 62 for CHURCH ANCHOR. However,

*Write the average weighted density as $\bar{d} \pm$ SD and define per cent variation for a square as (SD/$\bar{d}$) x 100. Using Figures D2 and D3 for squares 20-25°N, 140-145°W; 30-35°N, 145-150°W the per cent variation in density is 5.69 and 106.98 respectively. Therefore the range of the variation (in percent) between these squares is 101.29.

+To compare CO and CA densities throughout the CO region, it was necessary to use CA densities extended to include roughly the area 20-30°N, 140-160°W. The algorithm used to extend these densities to areas not covered during the CA exercise is given by L.P. Solomon (PSI Report TR-004002). Figure C3 and D1 of this reference were used to give the AMI and CA extended densities.

there was a significant difference in the distribution of these ships between the squares. The shipping in the neighborhood of Hawaii and Northwest of the islands is distributed over a somewhat broader region than either the CHURCH ANCHOR or RMS fields show (both of these distributions show rather narrow shipping lanes from Hawaii to the mainland). It must be remembered that the shape of the CHURCH ANCHOR distribution (but not the total numbers) in this area was determined from the AMI data, since there was no shipping surveillance coverage during that exercise in the immediate vicinity of Hawaii. This data tends to confirm the thesis that shipping lanes in the open ocean are not as "narrow" as is generally believed. Other exercises have also illustrated this phenomenon. In particular CHURCH ANCHOR showed that the West Coast-Japan route was much broader and dynamic than indicated by the synthesized shipping fields.

(U) In the region north of 35°N, CHURCH OPAL gives a total of 56.95 ships versus 56.12 for CHURCH ANCHOR. When comparing densities (Figure D4) it is seen that in the three coastal squares the CHURCH OPAL figures are lower than those of CHURCH ANCHOR. These in turn are lower than the RMS numbers for these squares, which are (generally) less than the AMI numbers. The CHURCH ANCHOR data base was extensive in these coastal squares, but CHURCH OPAL was quite light; thus the small sample does not justify a conclusion that coastal traffic is changing.

(U) In conclusion, the shipping fields from the CHURCH OPAL exercise (Sept. 1975) agree remarkably well with those of CHURCH ANCHOR (Sept. 1973). The CHURCH OPAL data in the vicinity of Hawaii indicates the actual nature of the Hawaii-mainland shipping lanes, superseding the previous synthesized distributions.

6. (S) COMPARISON OF OTH AND AIRCRAFT SHIP DISTRIBUTIONS (U)

(C) The location of the CHURCH OPAL Exercise Area allowed for surveillance of surface shipping by the SEA ECHO Over-The-Horizon (OTH) radar system at San Clemente Island and the Wide Aperture Research Facility (WARF) at Los Banos, California. Surveillance of the relatively large ocean areas (5° x 5° square) required strategic scanning and subsequent doppler processing to discriminate individual ships from the sea return. The detection criterion is based on measurement of the radial component of ship velocity, for which below a threshold value, the ship will not be observed. For the SEA ECHO radar, ships having a radial velocity of less than approximately 13 knots would be below the detection threshold. Thus OTH radar may underestimate the ship density according to the directional distribution of the shipping density.

(C) On September 14, 22 and 24 there was mutual coverage of shipping by OTH radar and A/C in the areas shown in Figure E1. The WARF OTH-B system provided surveillance on the 14th and SEA ECHO radar system on the 22nd and 24th. Table E1 summarizes the results of OTH and A/C shipping surveillance operations for the three areas on the above dates.

(S) Analysis of WARF+ shipping distributions (J. R. Barnum, Ship Density Determination with High Resolution Skywave Radar Surveillance (SECRET), October 1975) indicates the presence of 12 ships within WARF Area 2. Aircraft coverage in Area 2 for time comparable with OTH gave a total of 11 surface contacts. Since A/C radar conditions were excellent on 14 September, the confidence level for these contacts is >90%. Most of these contacts appear to have been observed on OTH; others were not. There are 10 probable correlations. Reliability of OTH data will suffer unless sufficient time for on-line analysis and verification of each possible contact is provided. A plot of contacts for 14 September obtained from multiple sources (VP, VXN-8, and

+See Appendix E.

OTH) is given in Figure E2. Correlation of multiple source contacts is a demanding exercise in judgment.

(C) SEA ECHO coverage+ (R. W. Bogle, OTH Radar Ship Distribution Measurements; September 1975) on the 22nd and 24th is shown in Figures E3 and E4. The three OTH contacts were dead reckoned 3-4 hours assuming 12 knot ship speed and corresponded to 3 of VXN-8's contacts. The two outside OTH contacts were dead reckoned to points outside of VXN-8 radar range. The remaining four VXN-8 contacts were not detected by OTH, and they were too far from the edge of the area to have moved "into the region" during the time difference. Weather for VXN-8 was quite poor.

(C) On September 24 OTH found 4 contacts in the area — 4 others immediately outside. VXN-8 found 3 contacts in the area. Since the time difference is so great and only radial velocity was detected, it is not possible to make an accurate comparison. However of the 8 OTH contacts, it could be that 5 were spotted by VXN-8 (3 in the square and 2 outside), and 1 moved out of the area, leaving 2 OTH contacts which could not have moved out of VXN-8's range but were not detected by them.

+See Appendix E.

Table 6.1 (C) OTH and A/C Ship Densities (U)

Date	Coverage Times (Z) (OTH/Aircraft)	Ships Observed (OTH)	Ships Observed (A/C)	Weighted Ship Densities (A/C)
14 Sept.	1639-0102 2130-0033	2-3	11	5.95 ± 0.63
22 Sept.	1800-1830 2157-2312	3	7	10.43 ± 0.70
24 Sept.	1430-1500 2319-2335	4	3	6.13 ± 2.65

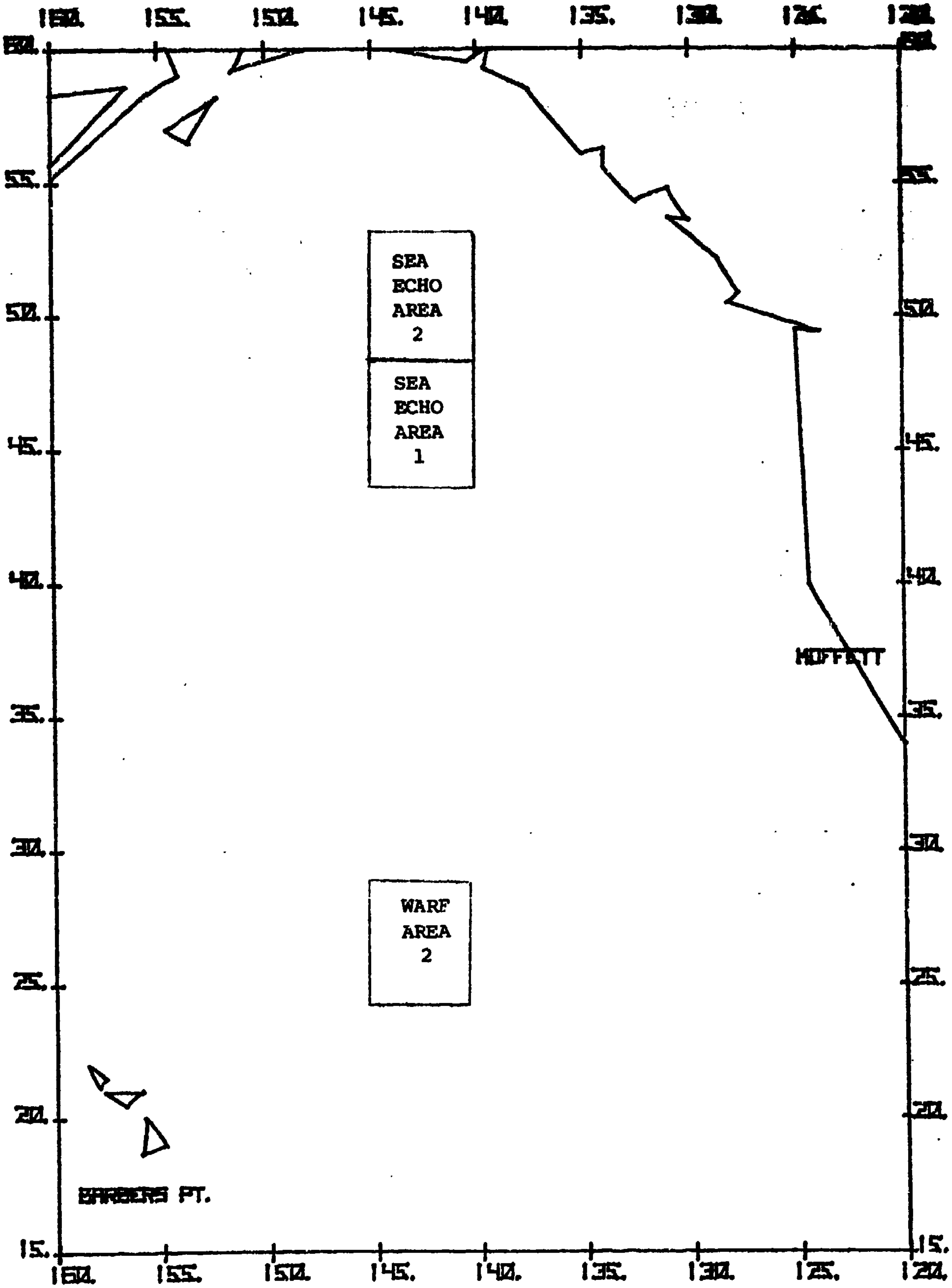

Figure 6-1 (C) Mutual OTH Radar and Aircraft Coverage Areas (U)

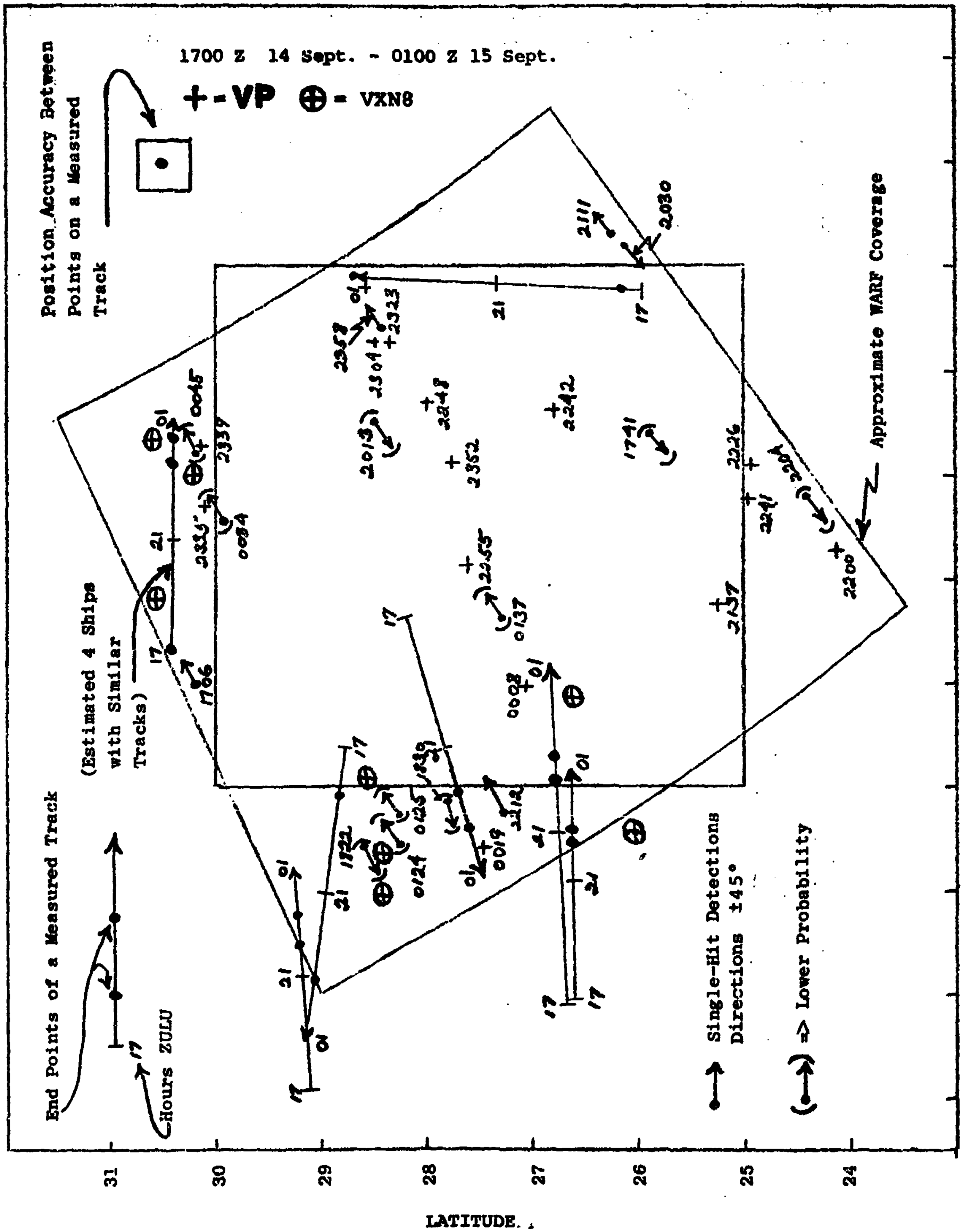

Figure 6-2 (U) Comparison of VP, VXN8, and OTH Contacts (U)

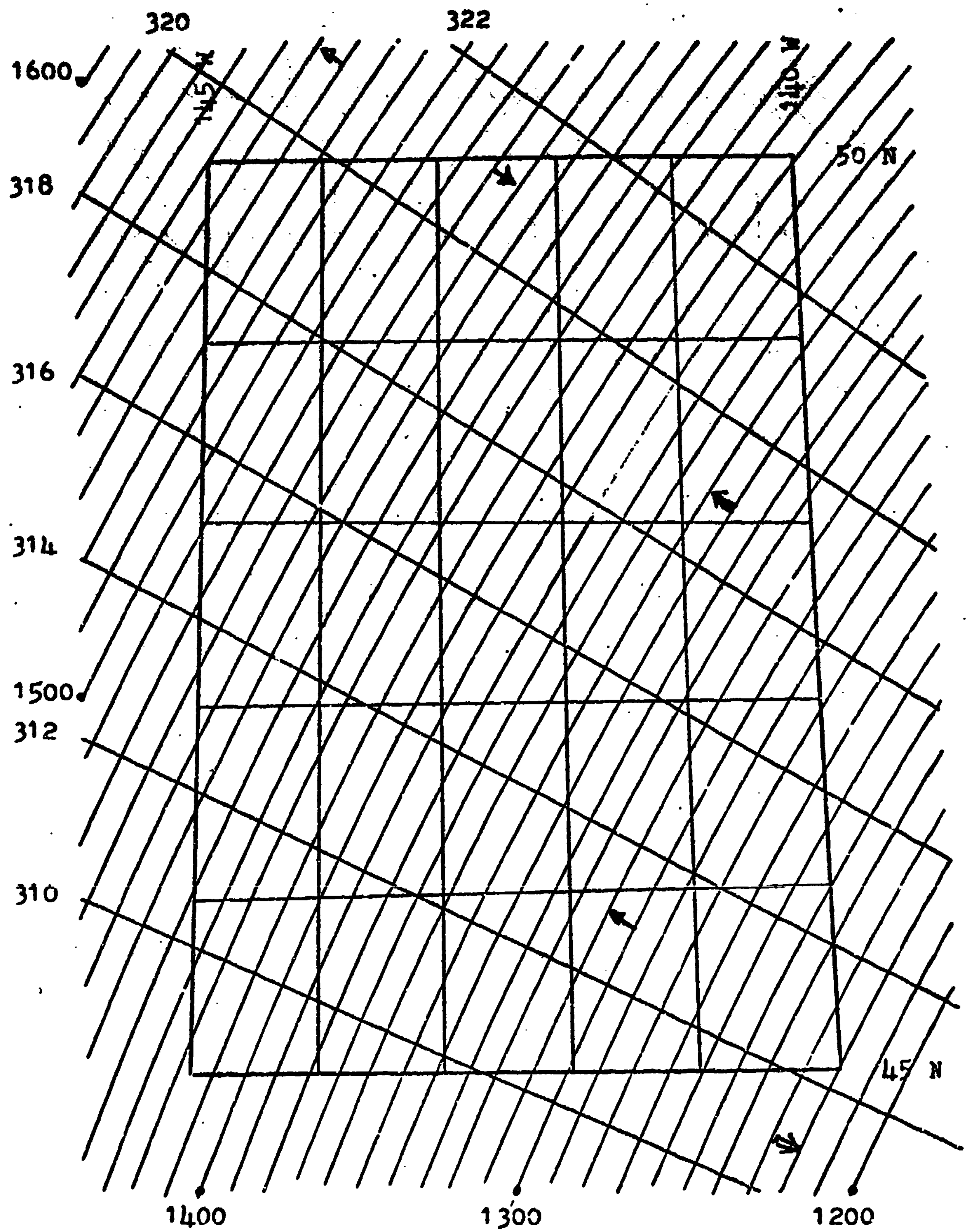

Figure 6-3 (C) SEA ECHO Coverage of Area 1 on 22 September, 1800-1830 Z. (U)

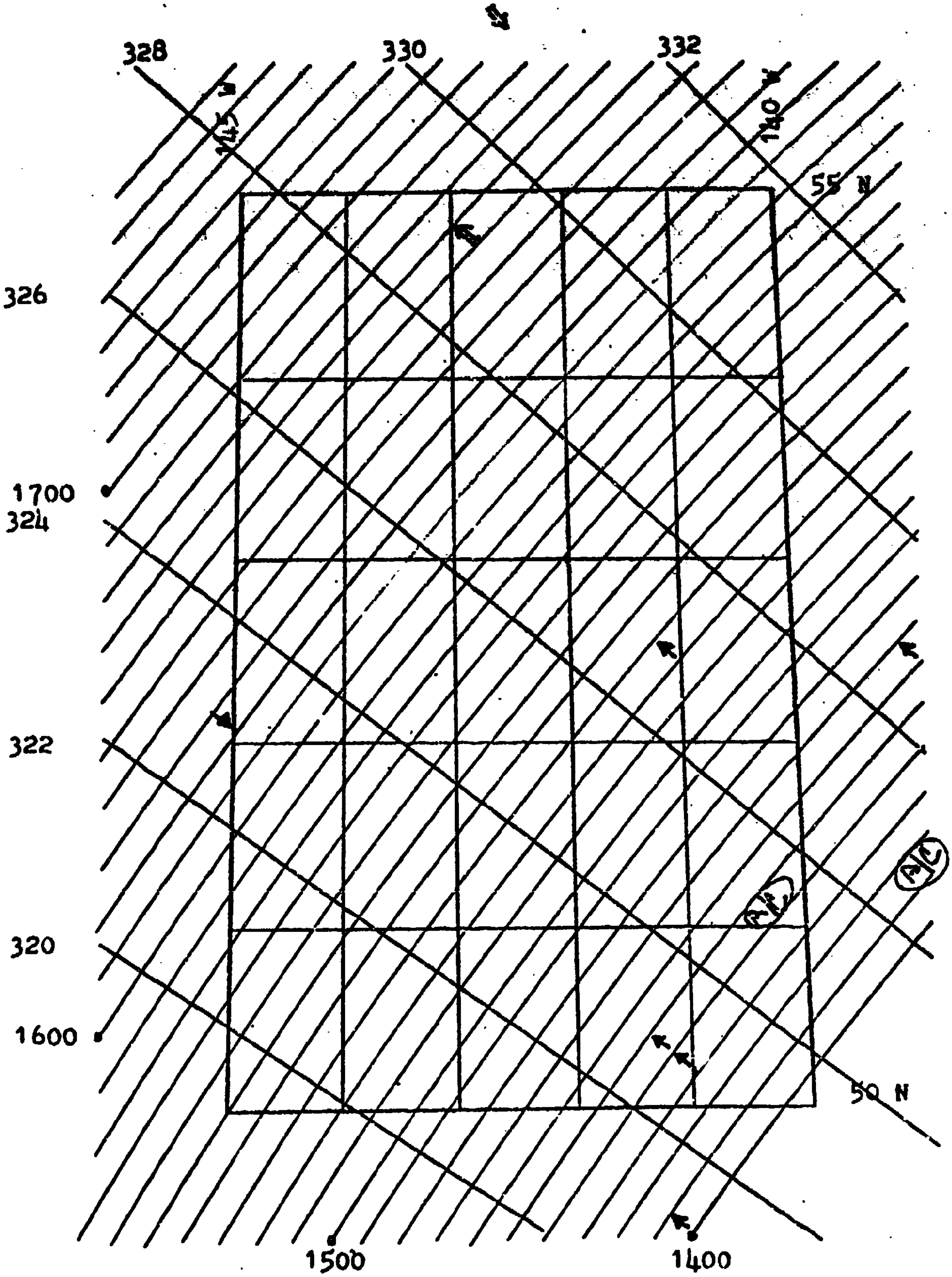

Figure 6-4 (U) SEA ECHO Coverage of Area 2 on 24 September, 1430-1500 Z. (U)

7. (S) CONCLUSIONS (U)

(S) The objectives of the CHURCH OPAL Exercise as related to surveillance of shipping were three-fold: first, to obtain the nearby shipping field concurrent with LAMBDA and DELTA horizontal directionality measurements, and to determine the ships on LAMBDA beams during beam noise measurements; second, the comparison of observed CHURCH OPAL shipping distributions with theoretical models and historical shipping fields from other data sources; third, the evaluation of OTH radar systems to provide shipping distributions of adequate quality for use in theoretical models of ship distributions and ambient noise prediction.

(S) The conclusions which can be drawn from this study can be divided into three major areas: data obtained from aircraft determination of the discrete shipping fields; data generated from the statistics of the shipping distributions as contrasted with observed, historical and model predictions; and data used for comparative assessment of OTH radar.

(1) On the two high priority beam noise measurement days, errors in ship positions were small with known bounds.

(2) Operational conditions were such that overall surveillance on the eight days of aircraft coverage was good.

(3) The ship densities from the CHURCH OPAL Exercise (Sept. 1975) are consistent with those of CHURCH ANCHOR (Sept. 1973). Both CHURCH OPAL and CHURCH ANCHOR shipping densities are in good agreement with the RMS distribution, except near the coasts where greater variation was expected.

(4) During the summer, the historical shipping density (RMS) in the Northeast Pacific is judged to be sufficiently precise to serve

as an input to present open ocean low frequency broad beam directional ambient noise models.

(5) The OTH radar is a potentially valuable tool for shipping density estimation, but should presently be utilized only in conjunction with aircraft surveillance. There is a problem of correlation between aircraft and OTH contacts. Resolution problems remain with OTH; however, these may be sharply alleviated by increased dwell time.

APPENDIX A

TABLE A1 (C) FLIGHT SUMMARY (U)

Date	Flight Track	Originations	Destination	Mission Status*
10 Sept.	TC	Moffett	Barbers Pt.	2
12 Sept.	TD	Barbers Pt.	Barbers Pt.	2
14 Sept.	TE	Barbers Pt.	Barbers Pt.	1
14 Sept.	PA	Barbers Pt.	Barbers Pt.	1
14 Sept.	PB	Barbers Pt.	Barbers Pt.	NC
16 Sept.	TE	Barbers Pt.	Barbers Pt.	1
16 Sept.	PA	Barbers Pt.	Barbers Pt.	2
16 Sept.	PB	Barbers Pt.	Barbers Pt.	2
18 Sept.	TG	Barbers Pt.	Moffett	1
20 Sept.	TA	Moffett	Elmendorf	PC1
22 Sept.	TH	Elmendorf	Moffett	PC2
24 Sept.	TA	Moffett	Elmendorf	1

*General Status codes for overall flight effectiveness are:

1 = Overall excellent radar and navigation; coverage along entire track

2 = Overall good radar and navigation; coverage along entire track

3 = Overall poor radar and navigation; coverage along entire track

PC1 = Excellent radar coverage along 95% of track; no coverage along the track through 35-36°N, 135-138°W

PC2 = Excellent radar coverage along 60% of track; no coverage over remainder

NC = No coverage

FIGURE A1 (U) TRACK TC ON 10 SEPTEMBER (U)

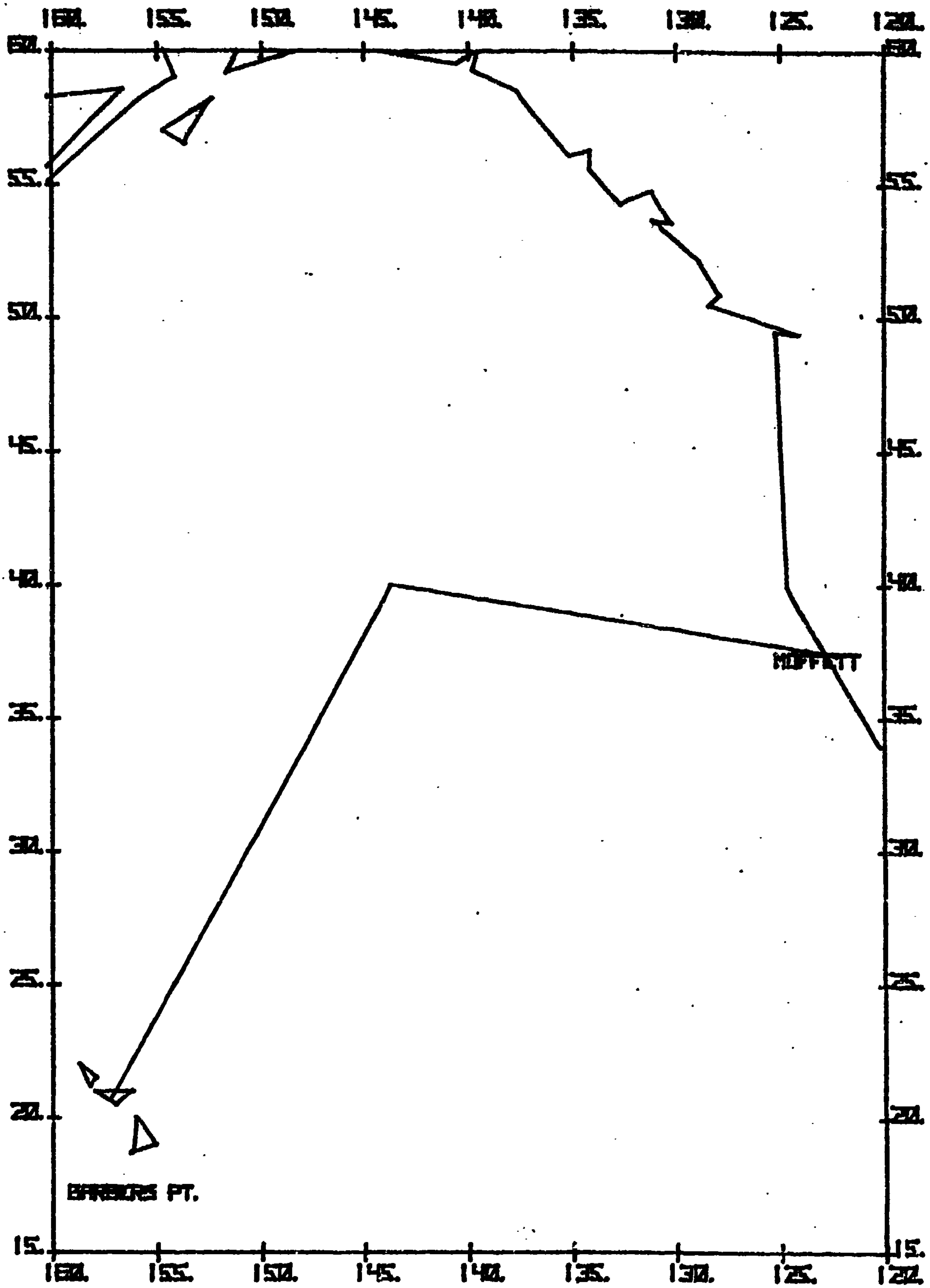

FIGURE A2 (U) SURFACE CONTACTS ON 10 SEPTEMBER (U)

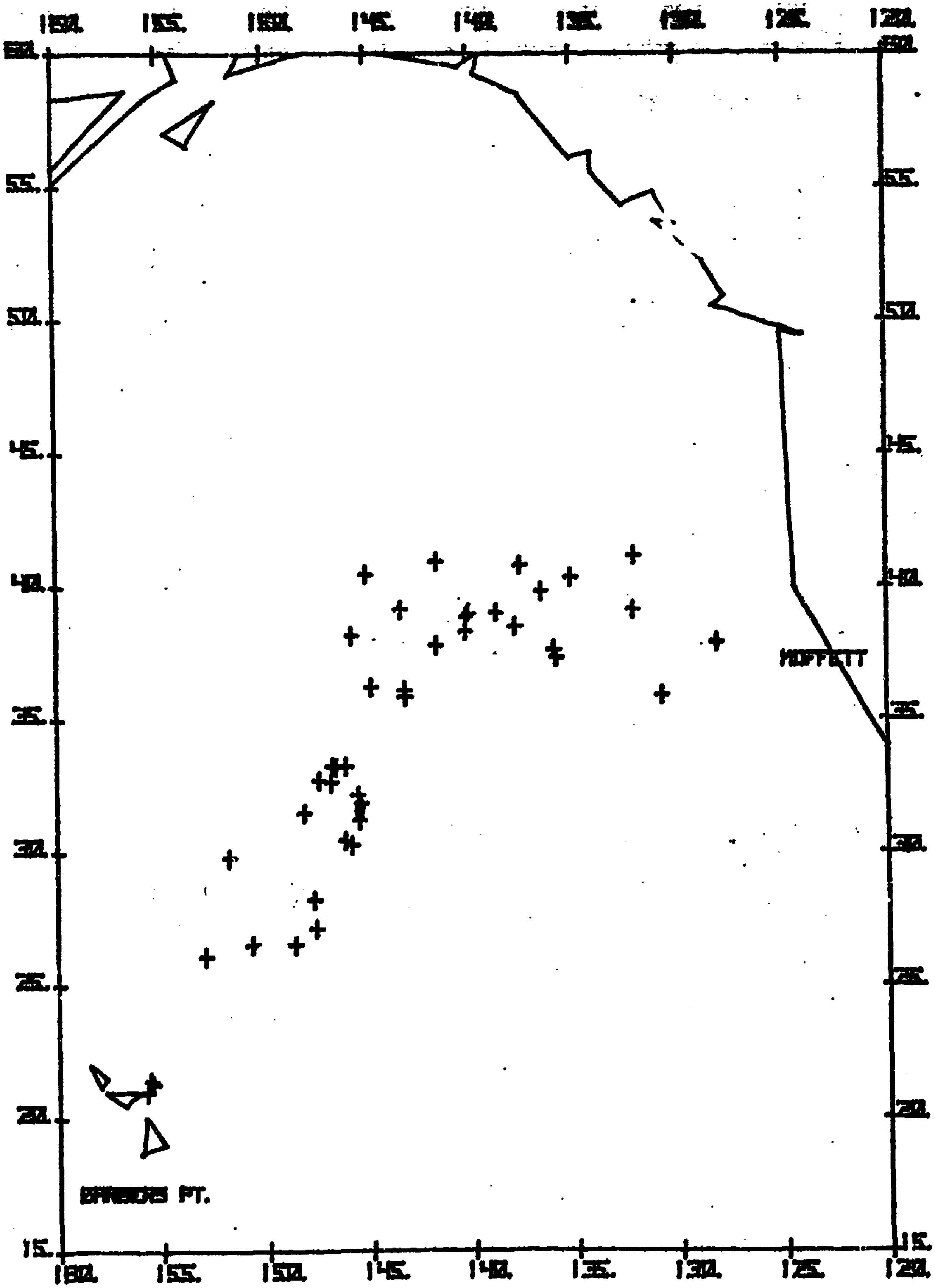

FIGURE A3 (U) TRACK TD ON 12 SEPTEMBER (U)

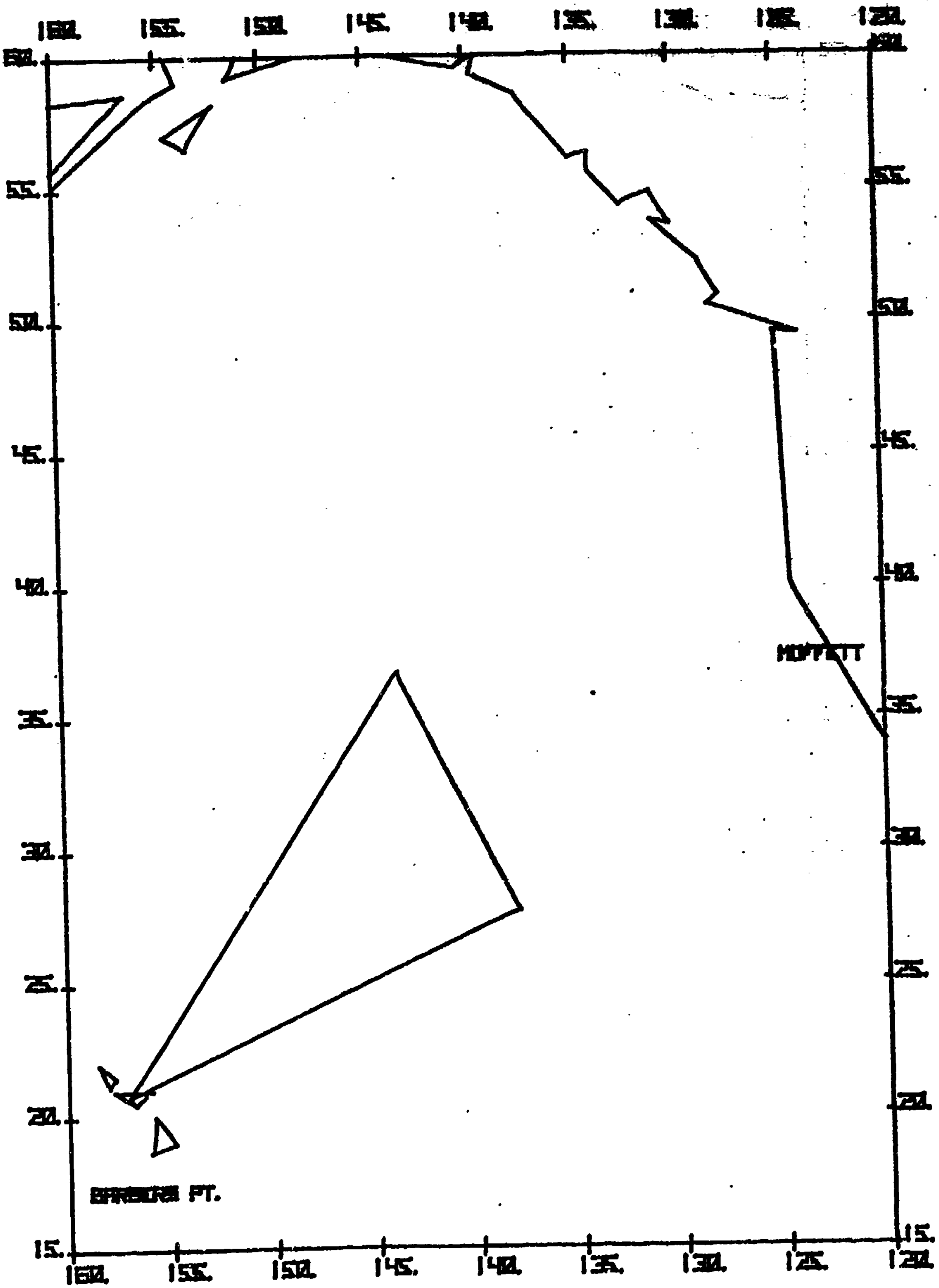

FIGURE A4 (U) SURFACE CONTACTS ON 12 SEPTEMBER (U)

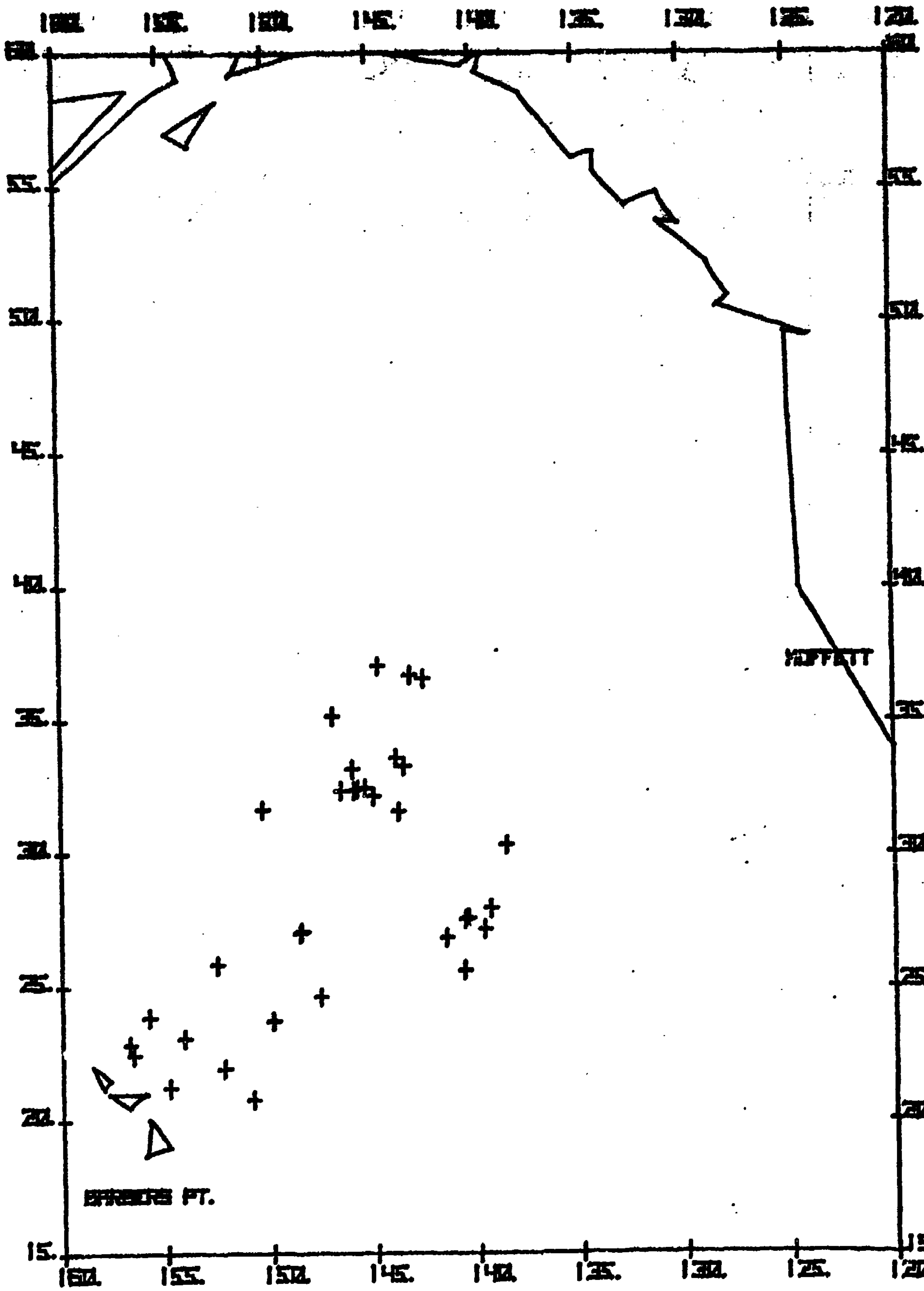

UNCLASSIFIED

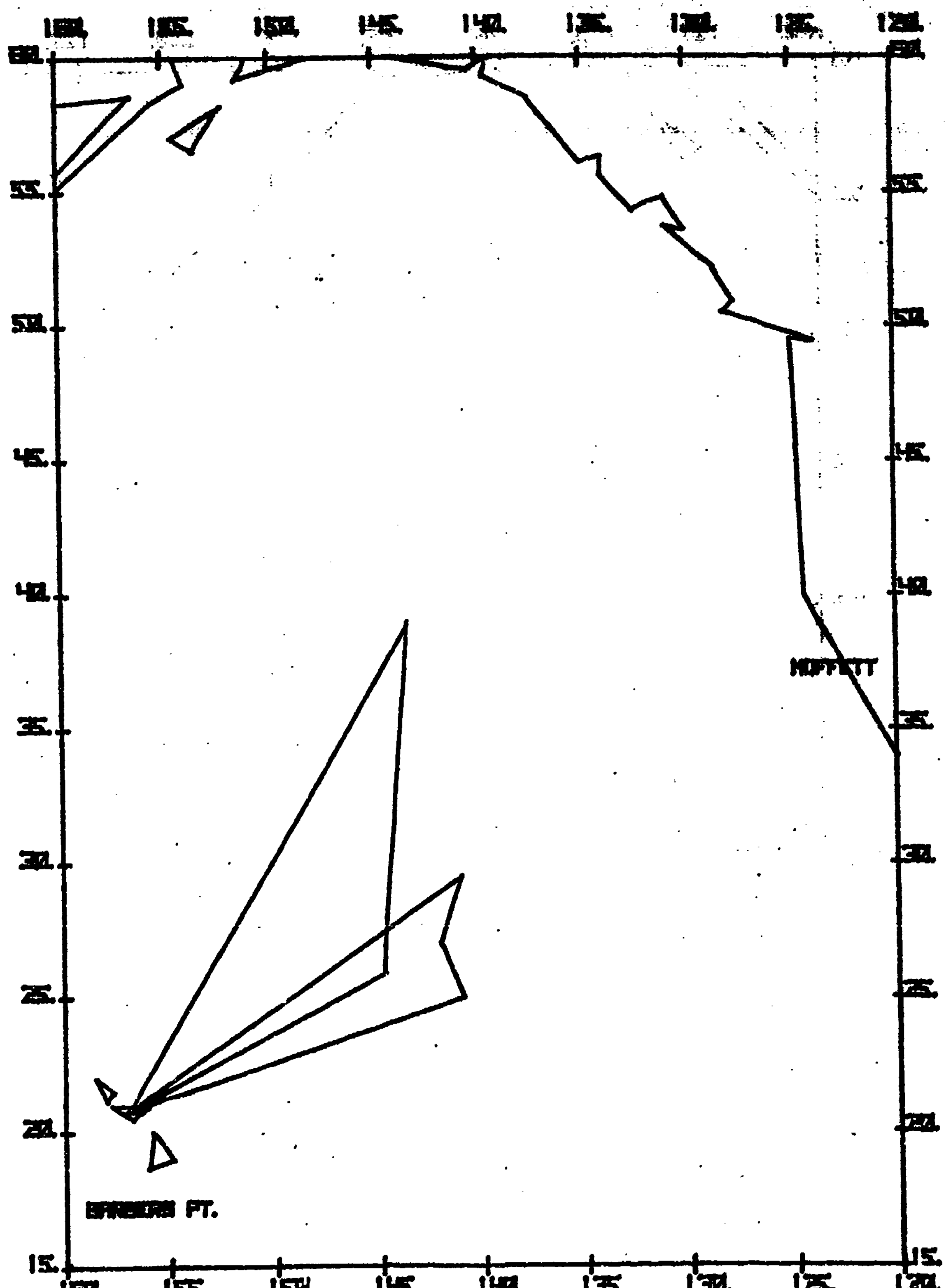
160.
155.
150.
145.
140.
135.
130.
125.
120.
60.
55.
50.
45.
40.
35.
30.
25.
20.
15.
MOFFETT
BARBERS PT.

FIGURE A6 (U) SURFACE CONTACTS ON 14 SEPTEMBER (U)

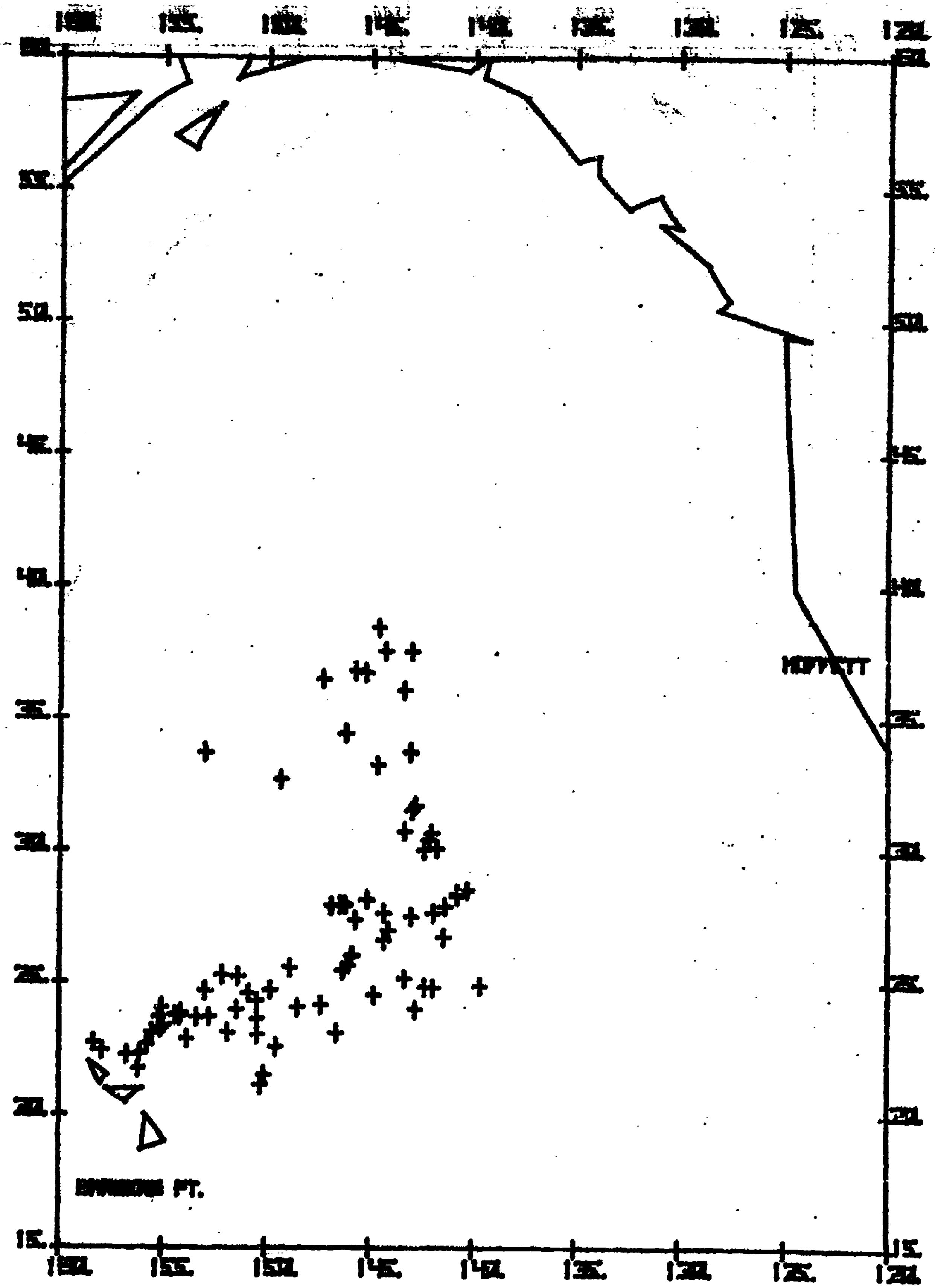

FIGURE A7 (U). TRACKS TE, PA, PB ON 16 SEPTEMBER (U)

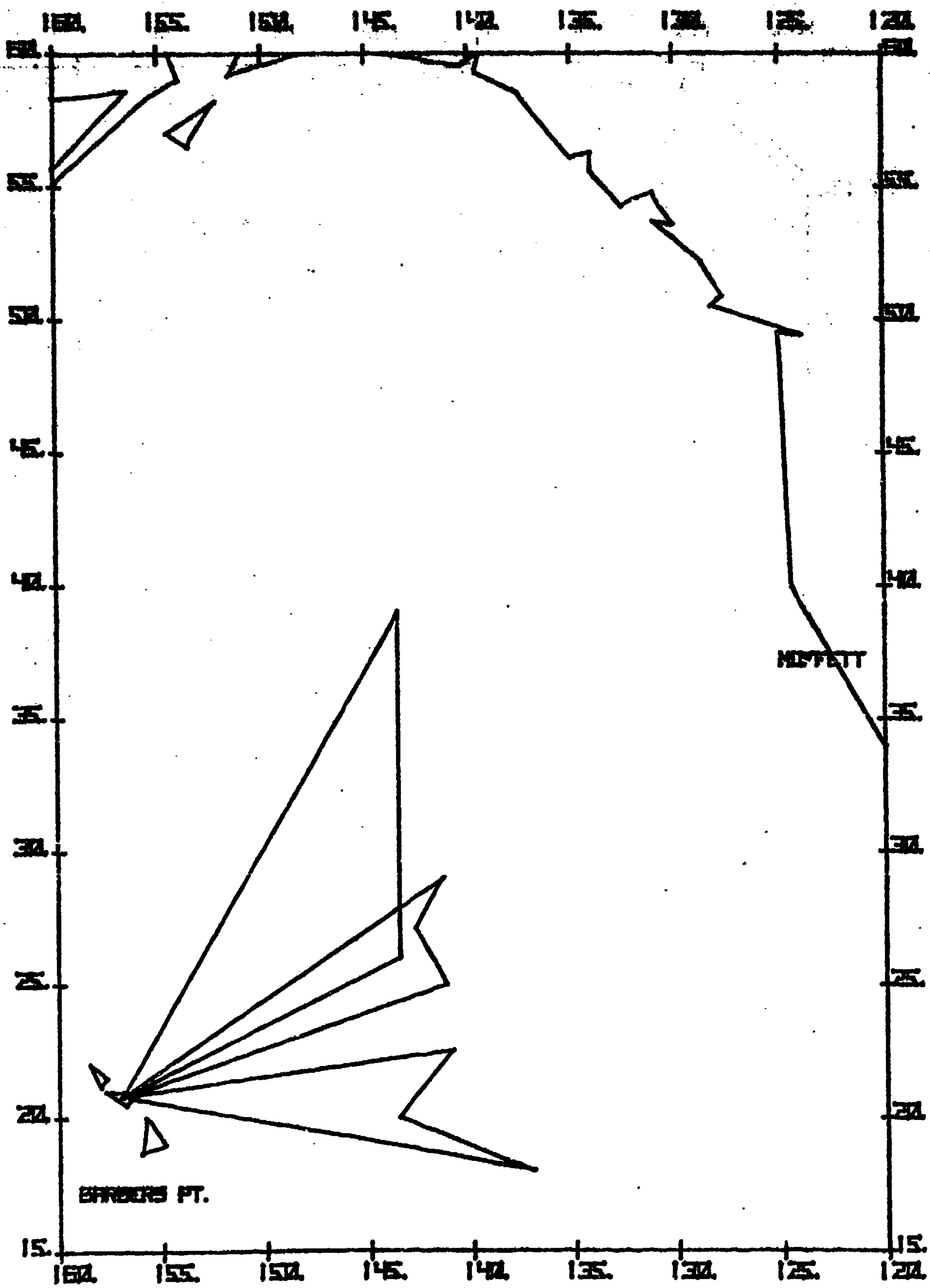

FIGURE A8 (U) SURFACE CONTACTS ON 16 SEPTEMBER (U)

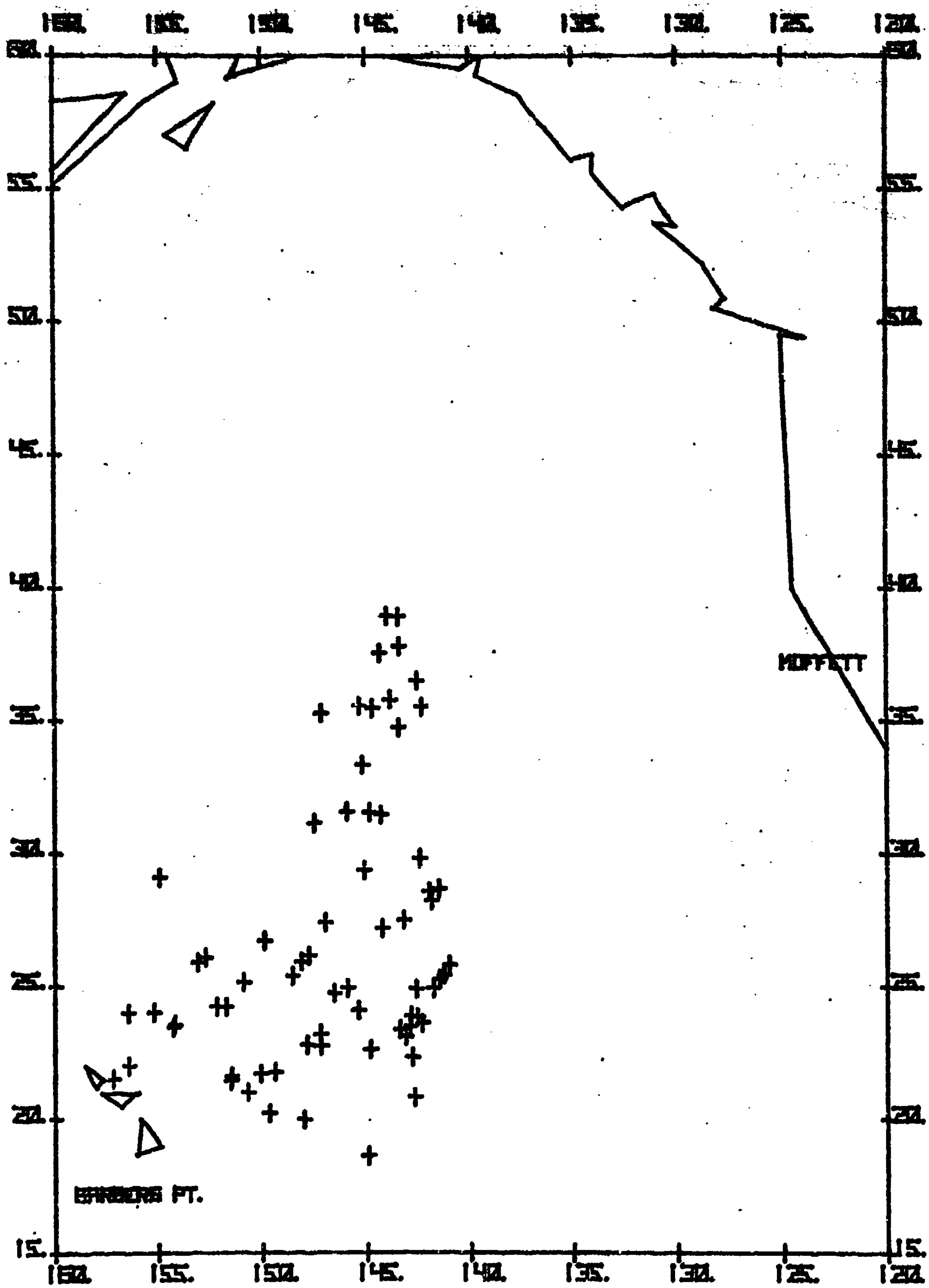

FIGURE A9 (U) TRACK TG ON 18 SEPTEMBER (U)

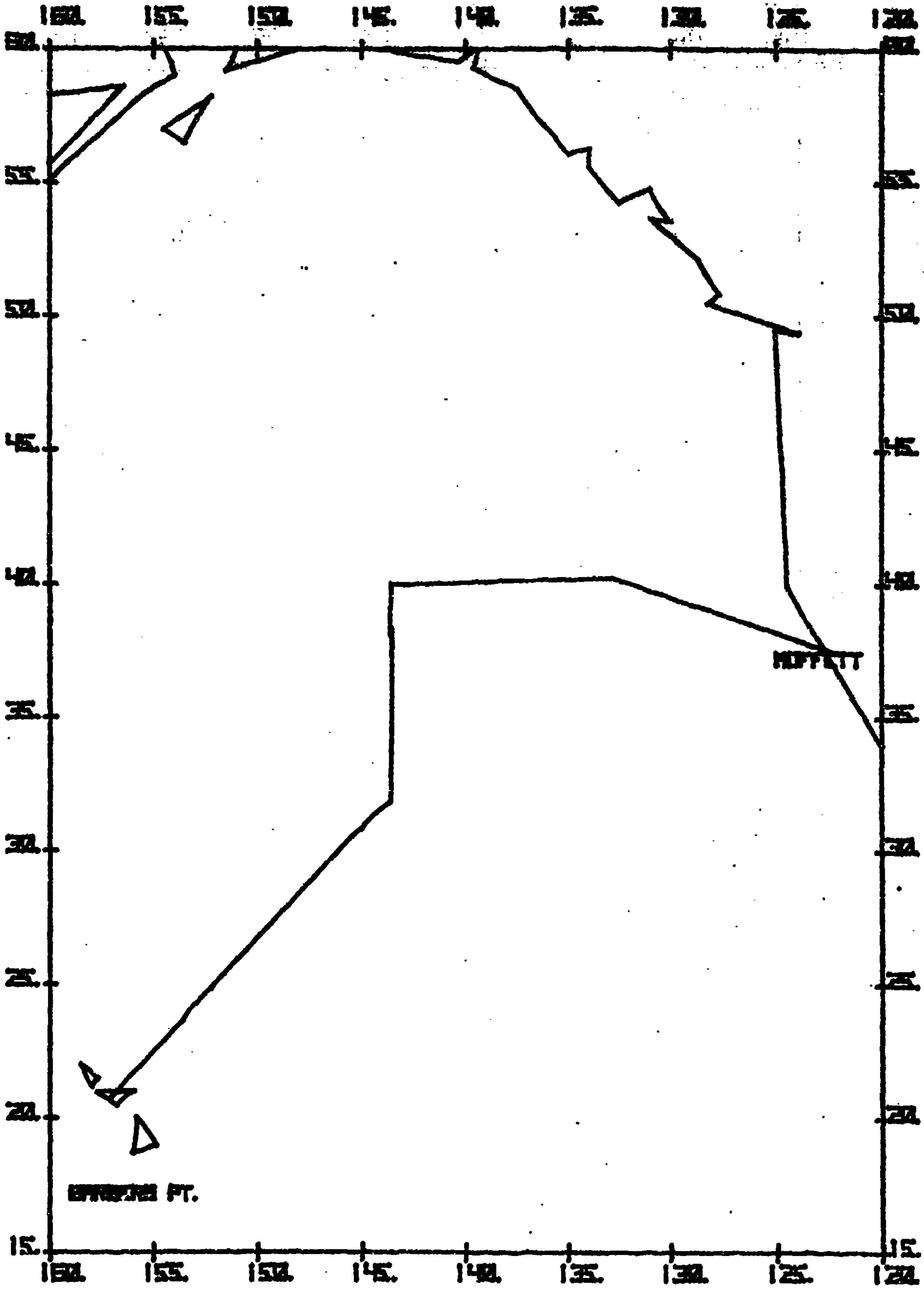

FIGURE A10 (U) SURFACE CONTACTS ON 18 SEPTEMBER (U)

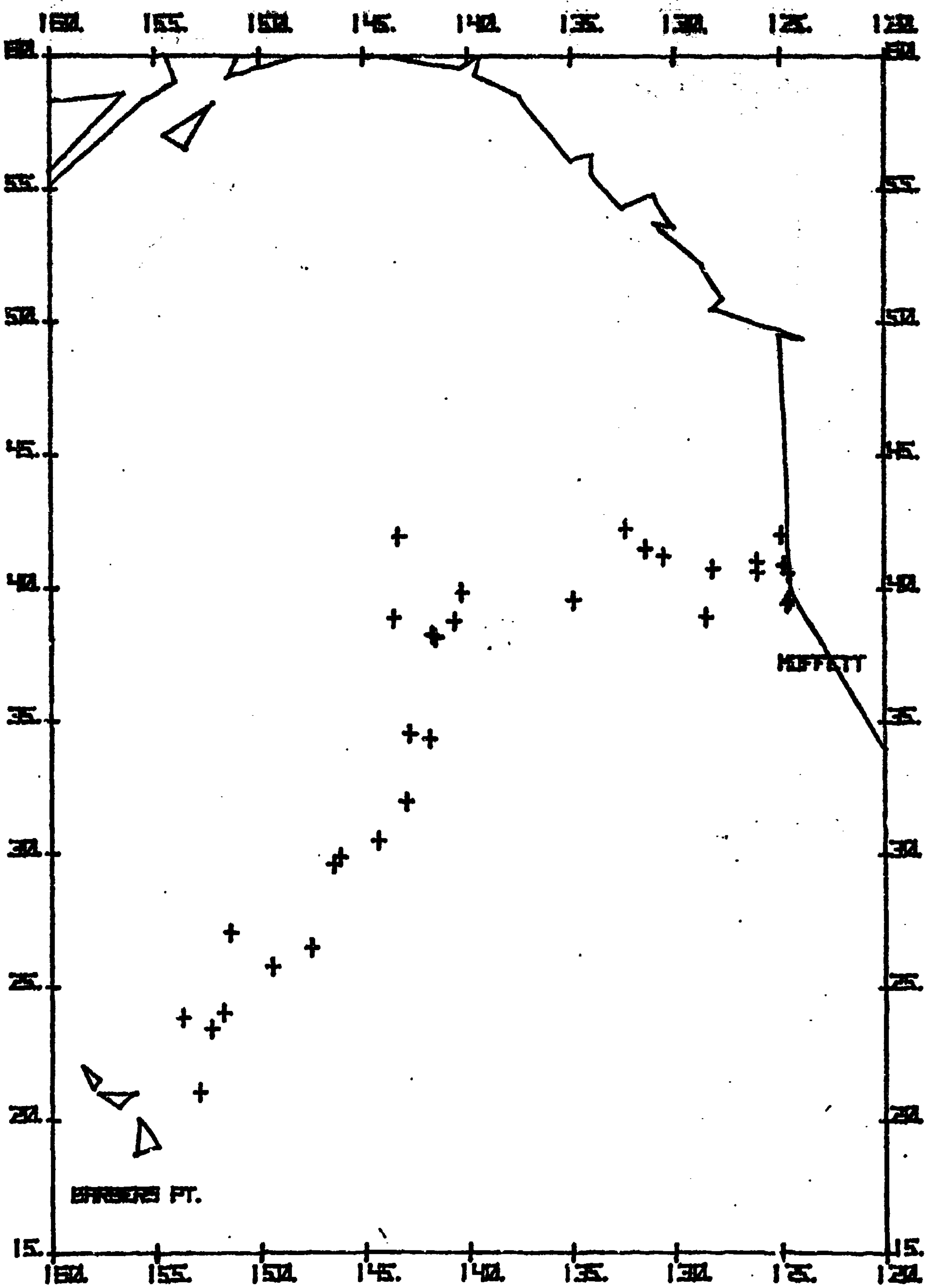

FIGURE A11 (U) TRACK TA ON 20 SEPTEMBER (U)

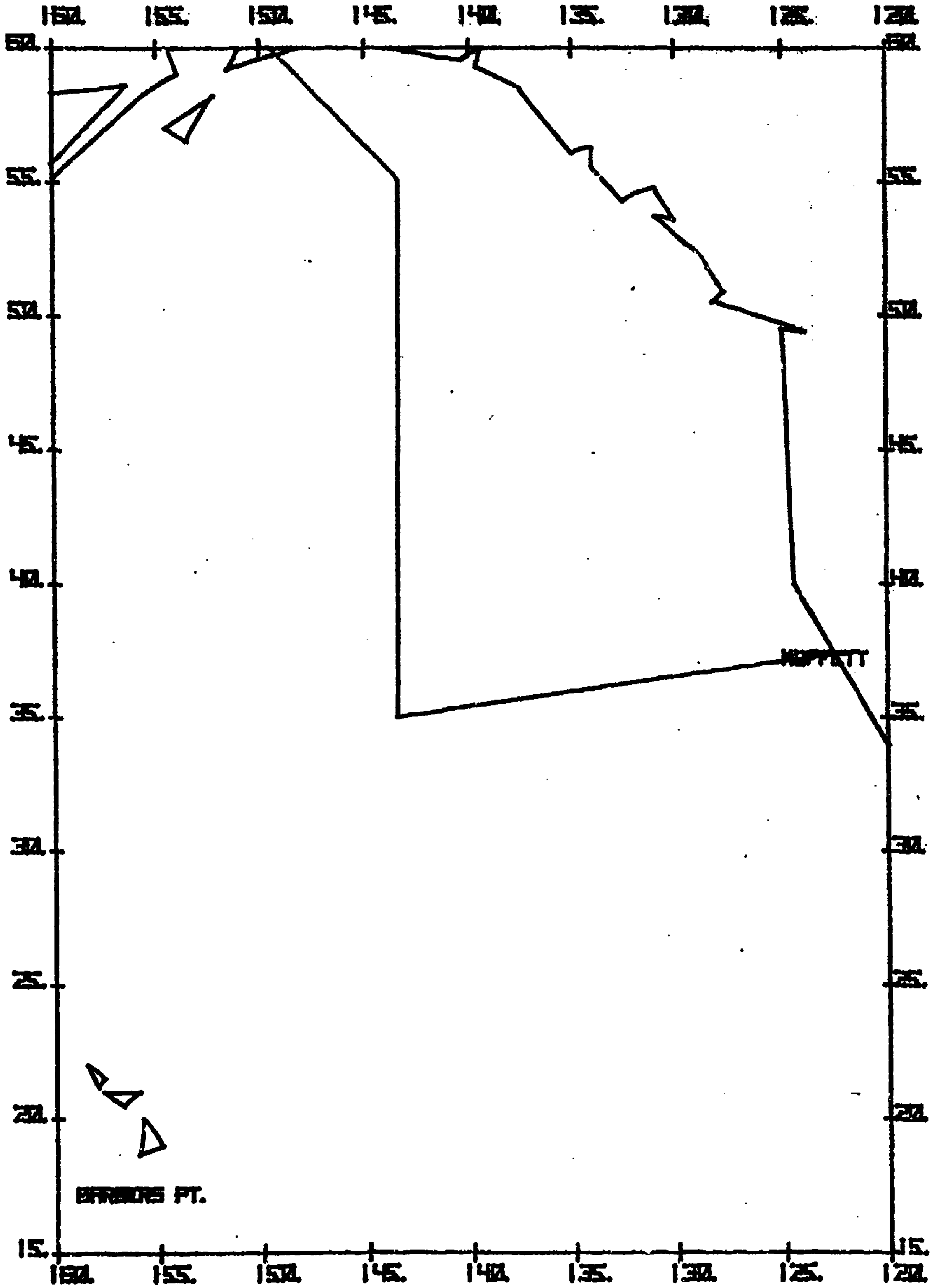

FIGURE A12 (U) SURFACE CONTACTS ON 20 SEPTEMBER (U)

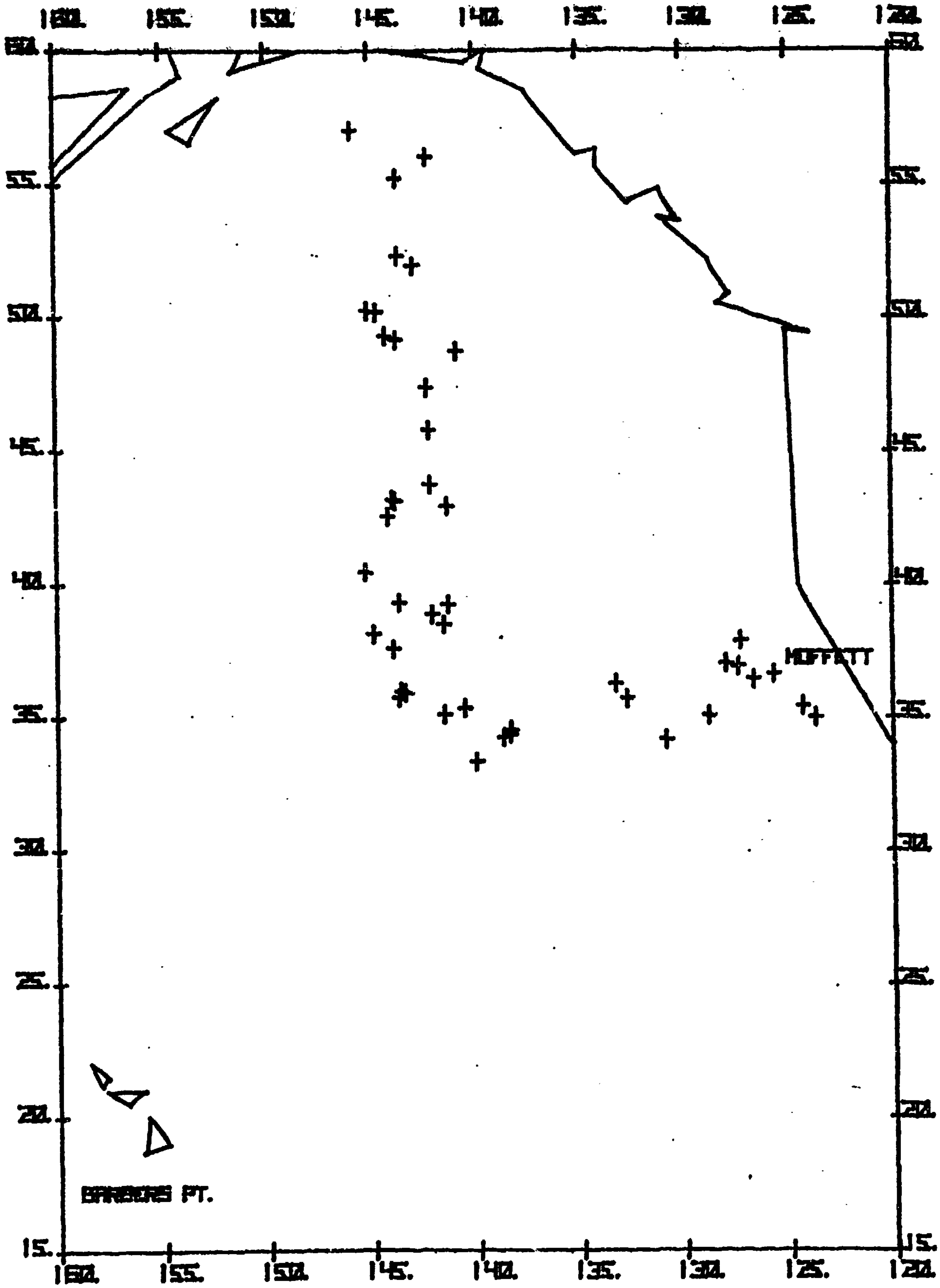

FIGURE A13 (U) TRACK TH ON 22 SEPTEMBER (U)

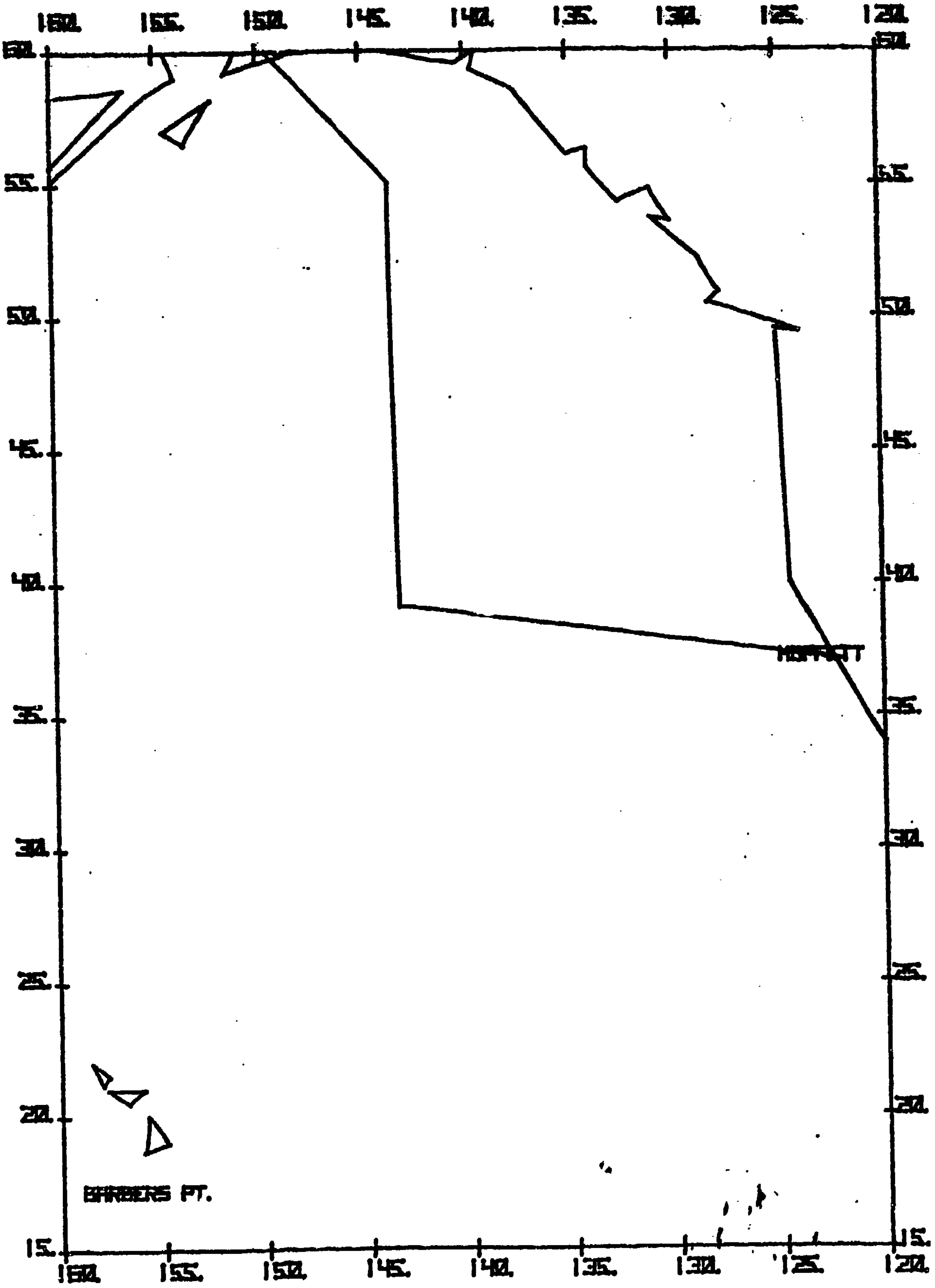

UNCLASSIFIED

FIGURE A14 (U) SURFACE CONTACTS ON 22 SEPTEMBER (U)

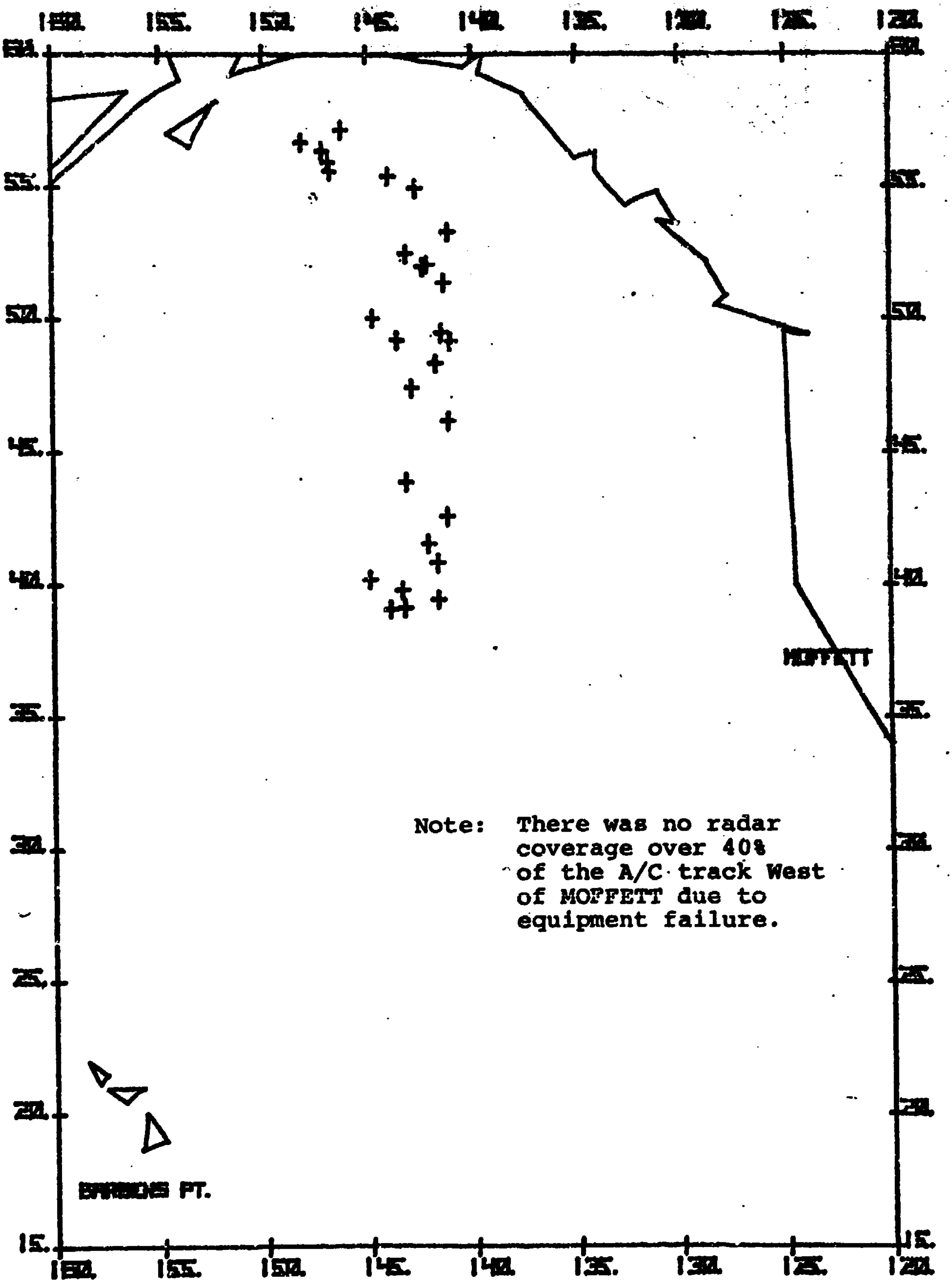

UNCLASSIFIED

FIGURE A15 (U) TRACK TA ON 24 SEPTEMBER (U)

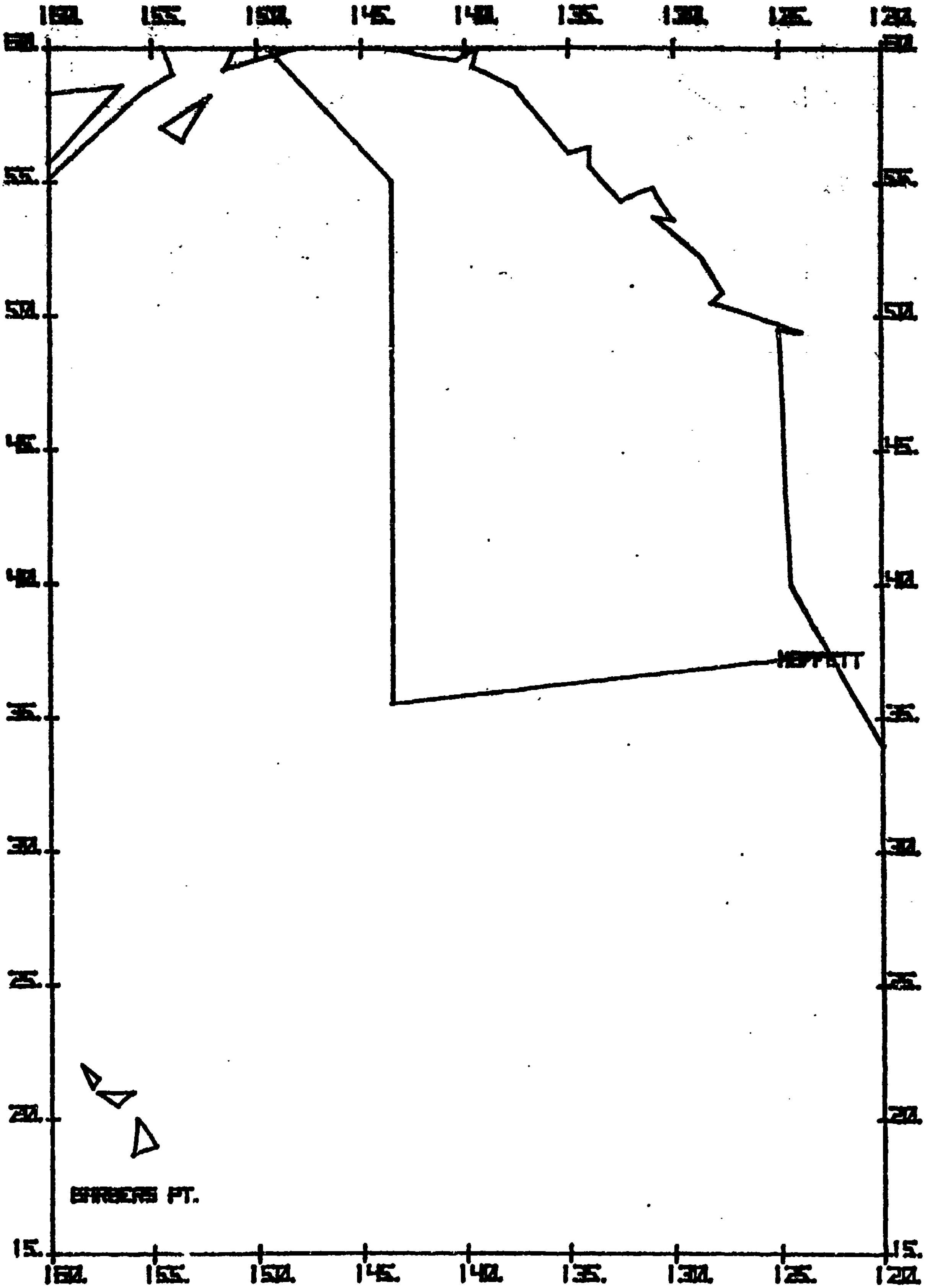

FIGURE A16 (U). SURFACE CONTACTS ON 24 SEPTEMBER (U)

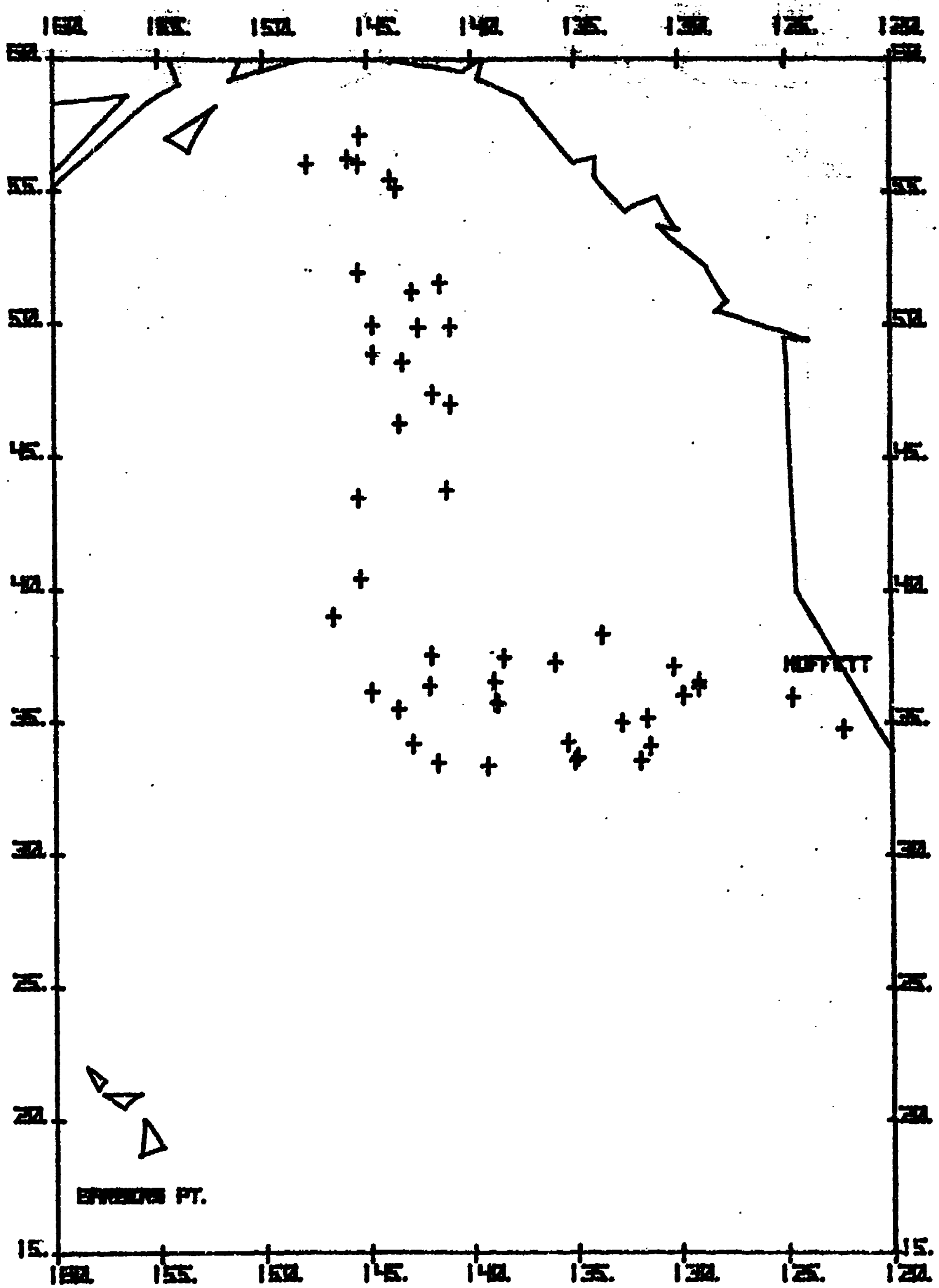

APPENDIX B

DATE	TIME (Zulu)	LOCATION (Latitude, Longitude)
14 September	2336	31.6378°N, 143.0780°W
16 September	2259	31.5452°N, 144.2988°W

TABLE B1 (C) Location of LAMBDA Array Used to Determine Ship Ranges and Bearings (C)

latitude =	22.4146	28.0641	33.3704	32.7766
longitude =	156.8408	146.9560	144.7761	149.4486
range =	919.0800	294.4000	134.8675	330.4972
bearing =	236.3570	224.2457	320.8790	283.6165
	21.8804	28.2842	33.8378	33.8395
	156.2793	145.2608	143.1749	153.0624
	916.7118	230.9841	132.0920	520.6806
	233.5348	209.9708	357.9061	287.3590
	22.4613	27.7647	36.1822	25.3460
	156.2211	144.4480	143.4636	151.4575
	891.1066	243.0990	273.3364	580.7850
	235.0659	197.4218	356.0793	231.5608
	23.4135	26.7249	37.6280	23.9630
	155.2076	144.4448	143.0780	154.2361
	811.4156	303.3305	359.4104	749.3706
	235.5446	193.9904	0.0000	234.8554
	23.8456	28.0590	37.6513	24.1739
	154.2561	146.3160	144.3681	155.1730
	754.7797	272.9149	366.3736	781.2983
	234.4990	218.9409	350.3533	238.0367
	23.7131	31.8304	36.8357	23.8494
	150.5433	142.9004	145.3183	155.3176
	618.8106	14.6880	331.0484	799.5397
	221.6388	38.0769	341.0106	237.2727
	24.8522	30.5210	38.5929	22.8404
	153.0656	142.2978	144.6903	158.4916
	666.0836	78.0847	424.7223	975.4359
	234.8179	148.9036	349.7207	241.0397
	24.8425	30.7932	36.9144	22.7644
	149.8821	142.1440	145.8155	155.6997
	543.3826	69.7507	344.4132	857.3819
	223.0799	136.3527	337.5561	234.7193
	24.2905	30.9156	36.5892	23.2019
	147.4502	143.4926	147.3855	155.4531
	497.8768	48.2616	366.0192	829.9396
	208.7813	206.2395	325.4248	235.4759
	26.6072	33.8137	34.5371	23.8419
	144.6695	143.1620	146.2541	154.3256
	313.1344	130.6212	236.0912	757.8174
	195.8425	358.1648	318.3105	234.[illegible]760

[illegible]	[illegible]	[illegible]	[illegible]
685.7206	382.2241	234.5487	636.6875
224.5776	181.4015	140.0157	213.8194
24.6692	24.0958	30.1119	23.8053
150.7653	142.7408	142.3283	152.6714
582.8910	452.8691	99.3572	692.5345
226.0841	177.6558	156.9404	229.6438
24.0614	24.9972	30.1761	25.3786
151.3428	139.5786	141.7217	152.0469
631.1062	439.1368	112.1004	603.4346
225.9728	154.2619	141.1226	233.7623
21.2186	24.9119	27.7333	23.7814
150.1872	141.8947	141.9033	153.2708
732.1046	408.3553	242.1310	717.1751
213.0835	170.9062	165.0574	231.4337
21.6078	24.9439	27.0881	23.4747
150.0167	142.2869	144.0564	154.8847
707.1235	403.7977	277.7309	795.4900
213.3606	173.8675	190.8575	234.9182
24.1544	26.8158	27.4800	22.9625
148.4039	141.3931	145.6253	153.7467
530.2255	302.4558	282.6504	770.1820
213.4558	162.6229	208.6913	230.1079
23.2053	27.9811	28.0453	22.5064
146.5494	141.3203	146.3633	157.9086
538.5653	237.7077	275.0908	961.7020
200.8970	156.9168	219.2526	238.9160
25.7386	27.6131	25.6611	
145.9717	142.9464	148.7797	
385.2754	241.5809	467.4952	
203.9913	176.3382	221.3414	
25.5519	28.4825	24.3919	
146.2350	140.7200	150.3806	
401.1778	225.4498	581.5632	
205.2599	146.5065	223.4382	
24.6292	28.3597	23.1225	
144.7483	140.7383	150.3550	
429.6817	231.2071	640.9430	
192.2712	147.6860	218.9350	

latitude = [illegible]	[illegible]	[illegible]	[illegible]
longitude=154.1699	148.1508	143.4494	147.5337
range =706.1143	387.5504	251.4282	166.6127
bearing =230.3438	212.4499	9.4871	264.7308
24.0845	23.3131	35.6381	31.6834
156.4569	147.2220	145.3606	145.9668
784.3776	517.8066	251.2328	85.6266
238.2172	198.1862	348.0971	275.9927
24.1191	24.1918	35.3680	29.2026
155.2021	145.4252	143.8789	154.9421
729.4729	445.2249	260.2054	568.3192
235.0567	187.9807	4.5052	258.4252
23.5569	27.5042	35.6175	25.2766
154.2322	147.0110	142.3557	150.8612
712.7239	280.7504	262.9130	511.0254
230.1922	210.9633	21.1484	224.2479
21.7024	25.9006	36.5841	21.6050
151.4458	141.0524	142.5895	157.2165
703.6050	379.2604	314.0235	913.0576
214.6631	152.4379	15.2238	232.3567
24.3380	27.6159	37.6162	24.2772
151.7335	143.2209	144.3749	152.0889
584.6971	242.3735	364.2763	600.2352
224.1484	166.3115	359.4306	225.3372
26.1924	28.7610	37.8918	24.7600
152.6892	141.5502	143.4401	146.5269
545.1220	219.6241	383.1361	423.7997
236.0152	138.8161	6.1047	196.6842
25.9971	29.4627	39.0103	24.9467
153.0586	145.1253	144.0451	145.8947
568.0233	132.0519	448.0725	404.7838
236.3263	199.0869	1.5173	192.4123
25.4924	31.6398	38.9919	23.6586
148.5497	144.8554	143.4910	142.3261
426.6414	29.0025	448.5386	484.6538
212.7171	281.4249	4.8320	167.0323
26.8048	27.7574	35.5481	23.8719
149.8825	142.4706	144.7190	142.5450
407.8640	246.4452	241.0876	469.7064
227.1970	156.7858	355.1162	168.1423
22.8895	33.4342	35.3524	24.9225
147.8464	145.2125	147.1819	142.5844
552.6541	122.4009	270.1666	407.5494
200.8624	338.0502	328.4981	166.7382

CONFIDENTIAL

TABLE B3 (C) Ship Positions on 16 September at 2259 Z. (cont'd)(U)

23.9039	21.4664	22.7492	
142.8617	151.4708	147.2178	
464.7772	716.4397	550.2157	
170.2050	214.1641	197.1376	
24.9439	20.2292	21.7706	
141.7767	149.6703	149.4092	
417.8726	737.9595	647.0868	
160.7874	204.3521	206.2359	
25.4292	19.9944	21.7172	
141.2675	148.0131	150.0683	
400.2164	721.3589	665.6214	
155.7217	196.9925	209.0362	
25.2853	18.6106		
141.4722	144.9367		
404.0835	776.8514		
157.6524	182.6986		
28.2400	20.8400		
141.8617	142.7089		
235.3568	647.9674		
146.7951	172.0449		
28.5919	23.3786		
141.9769	143.4169		
214.3119	492.2376		
145.1798	174.3178		
27.1892	23.4906		
144.2258	142.9447		
261.3946	488.6098		
179.1445	171/1987		
27.0267	23.1067		
147.7375	143.1406		
325.3464	510.0554		
214.4299	172.7742		
24.0319	22.3439		
150.6431	142.8181		
562.4042	557.7144		
218.2910	171.4900		
22.0239	22.6214		
156.3961	144.8447		
862.6623	536.2239		
231.4802	183.2450		

APPENDIX C

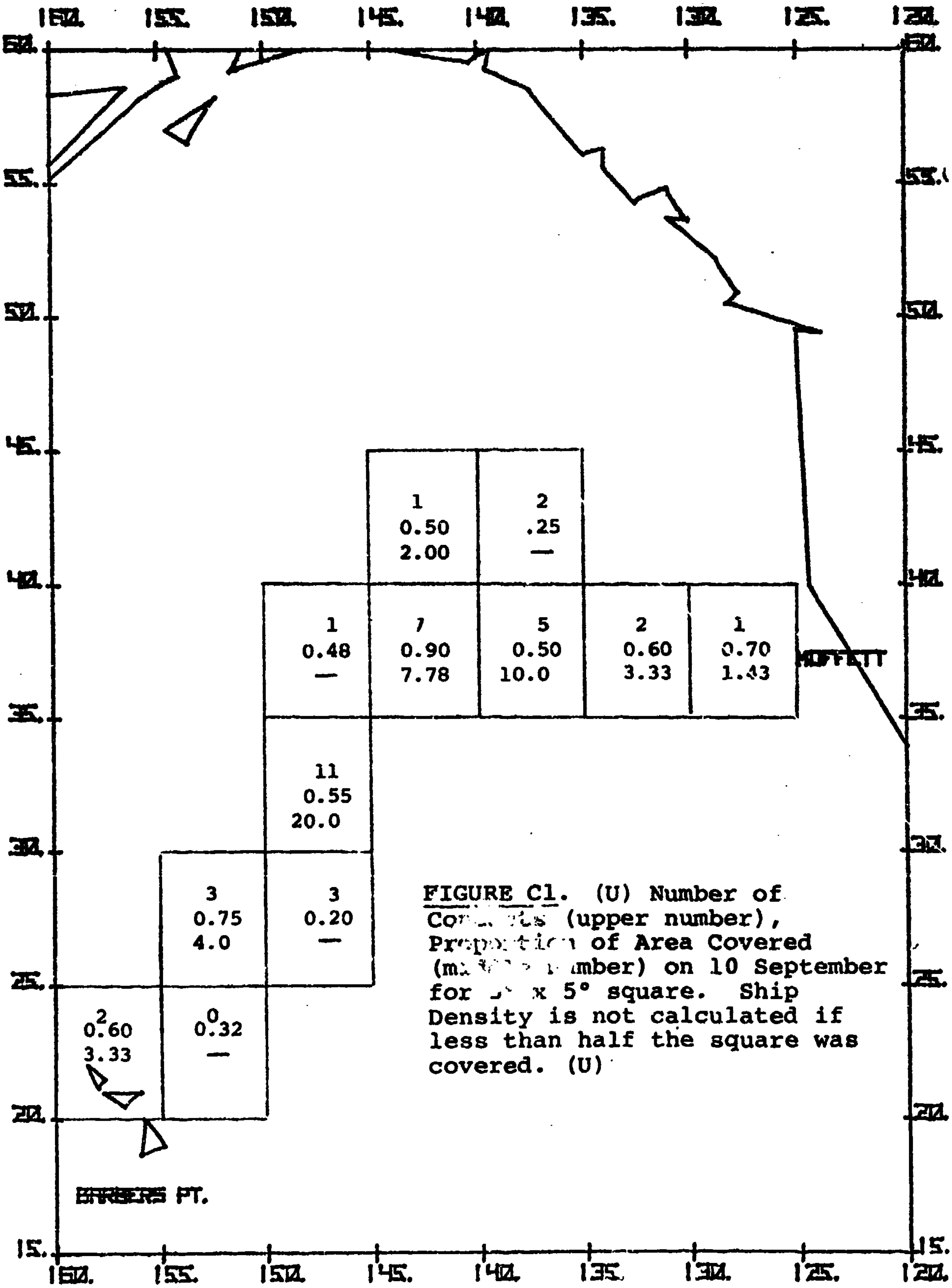

FIGURE C1. (U) Number of Contacts (upper number), Proportion of Area Covered (middle number) on 10 September for 5° x 5° square. Ship Density is not calculated if less than half the square was covered. (U)

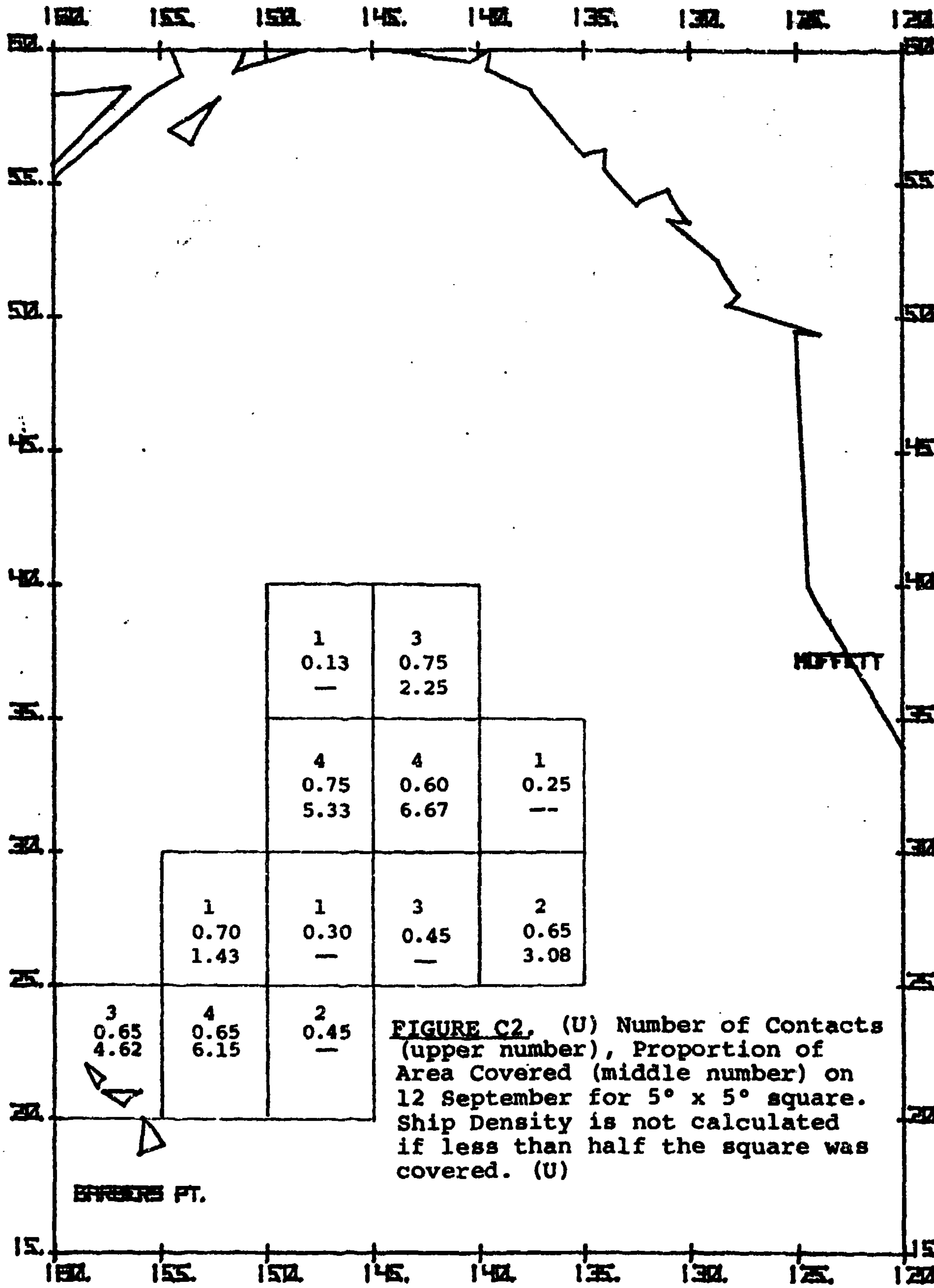

FIGURE C2. (U) Number of Contacts (upper number), Proportion of Area Covered (middle number) on 12 September for 5° x 5° square. Ship Density is not calculated if less than half the square was covered. (U)

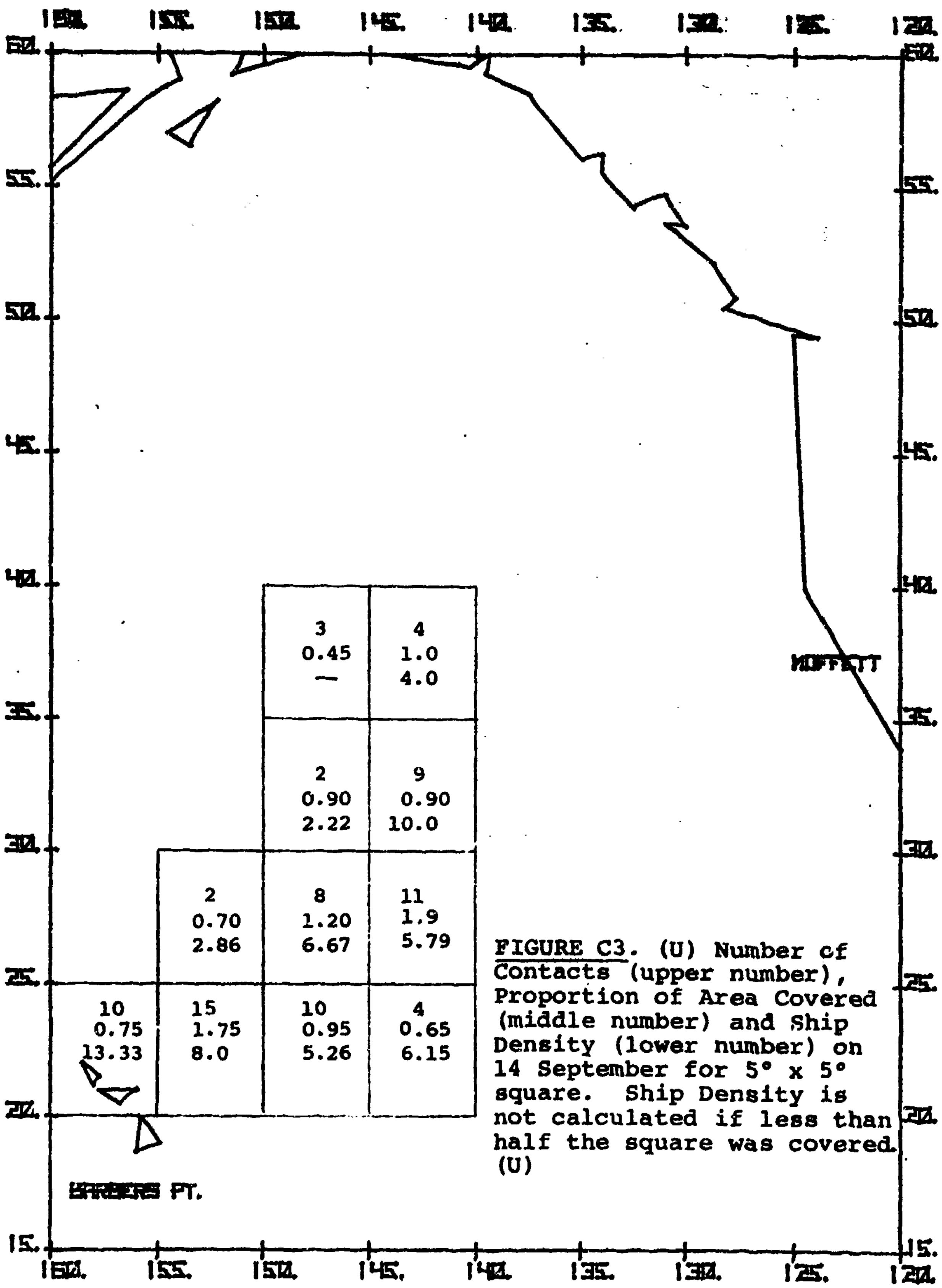

FIGURE C3. (U) Number of Contacts (upper number), Proportion of Area Covered (middle number) and Ship Density (lower number) on 14 September for 5° x 5° square. Ship Density is not calculated if less than half the square was covered. (U)

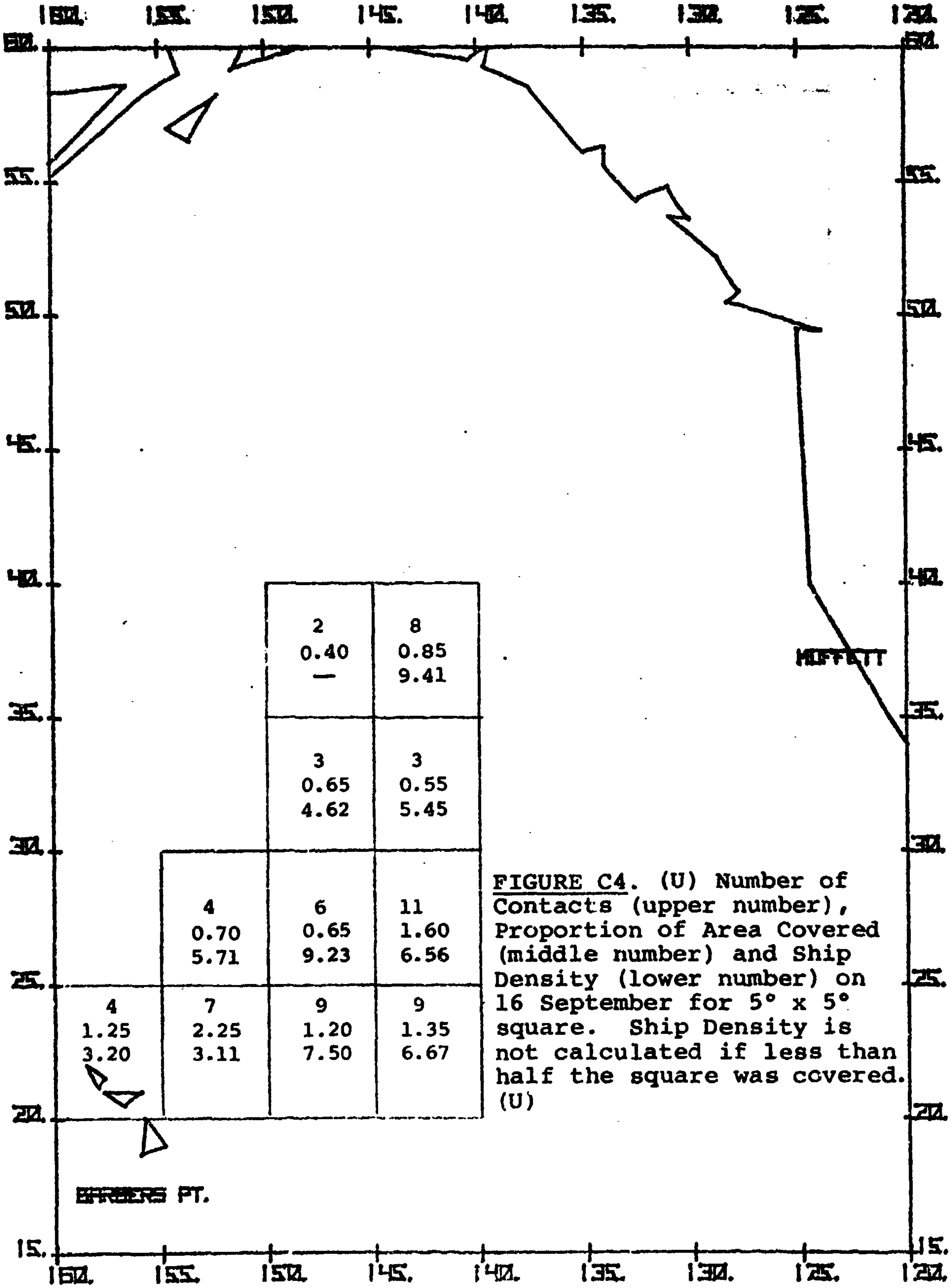

FIGURE C4. (U) Number of Contacts (upper number), Proportion of Area Covered (middle number) and Ship Density (lower number) on 16 September for 5° x 5° square. Ship Density is not calculated if less than half the square was covered. (U)

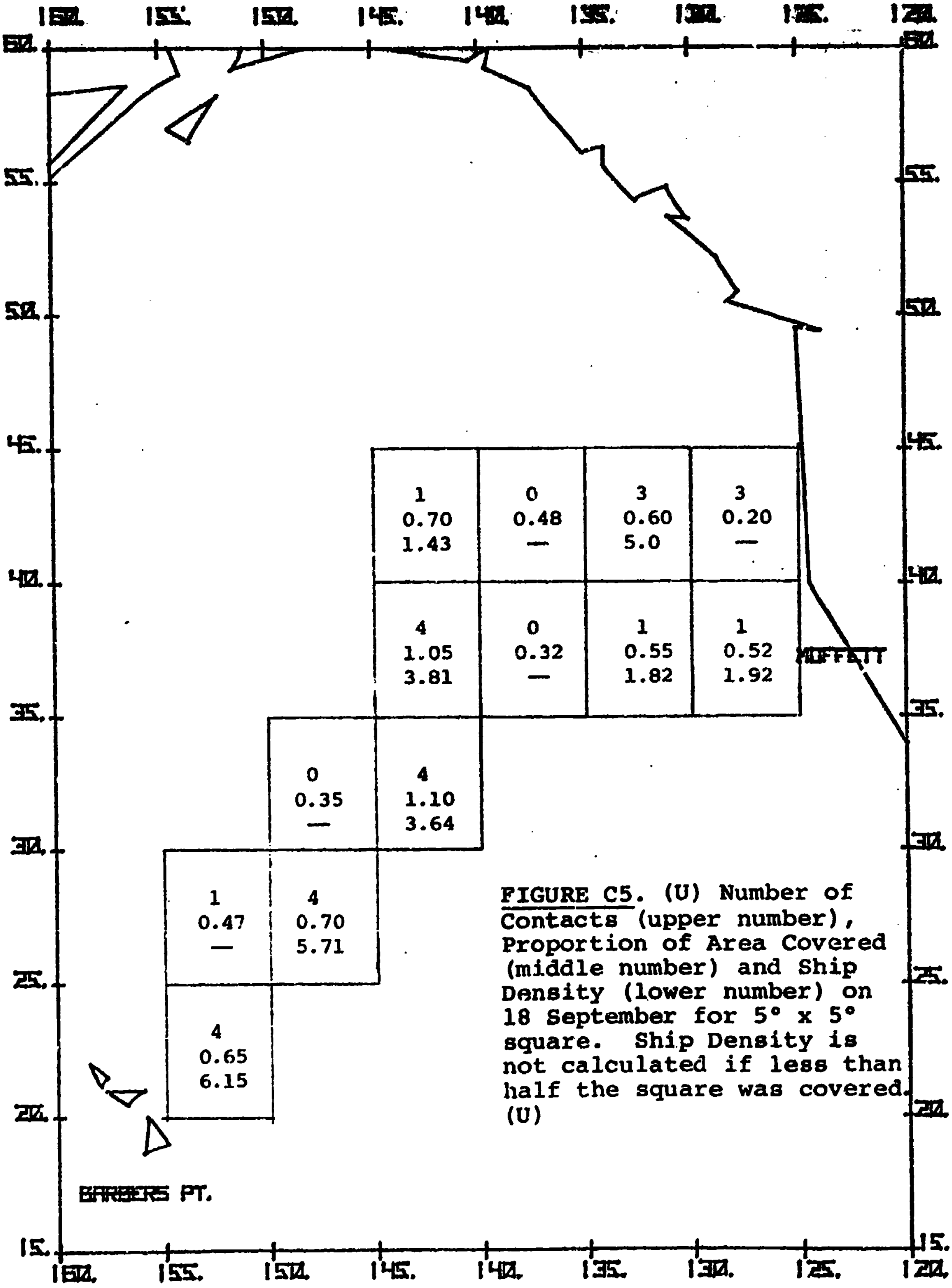

FIGURE C5. (U) Number of Contacts (upper number), Proportion of Area Covered (middle number) and Ship Density (lower number) on 18 September for 5° x 5° square. Ship Density is not calculated if less than half the square was covered. (U)

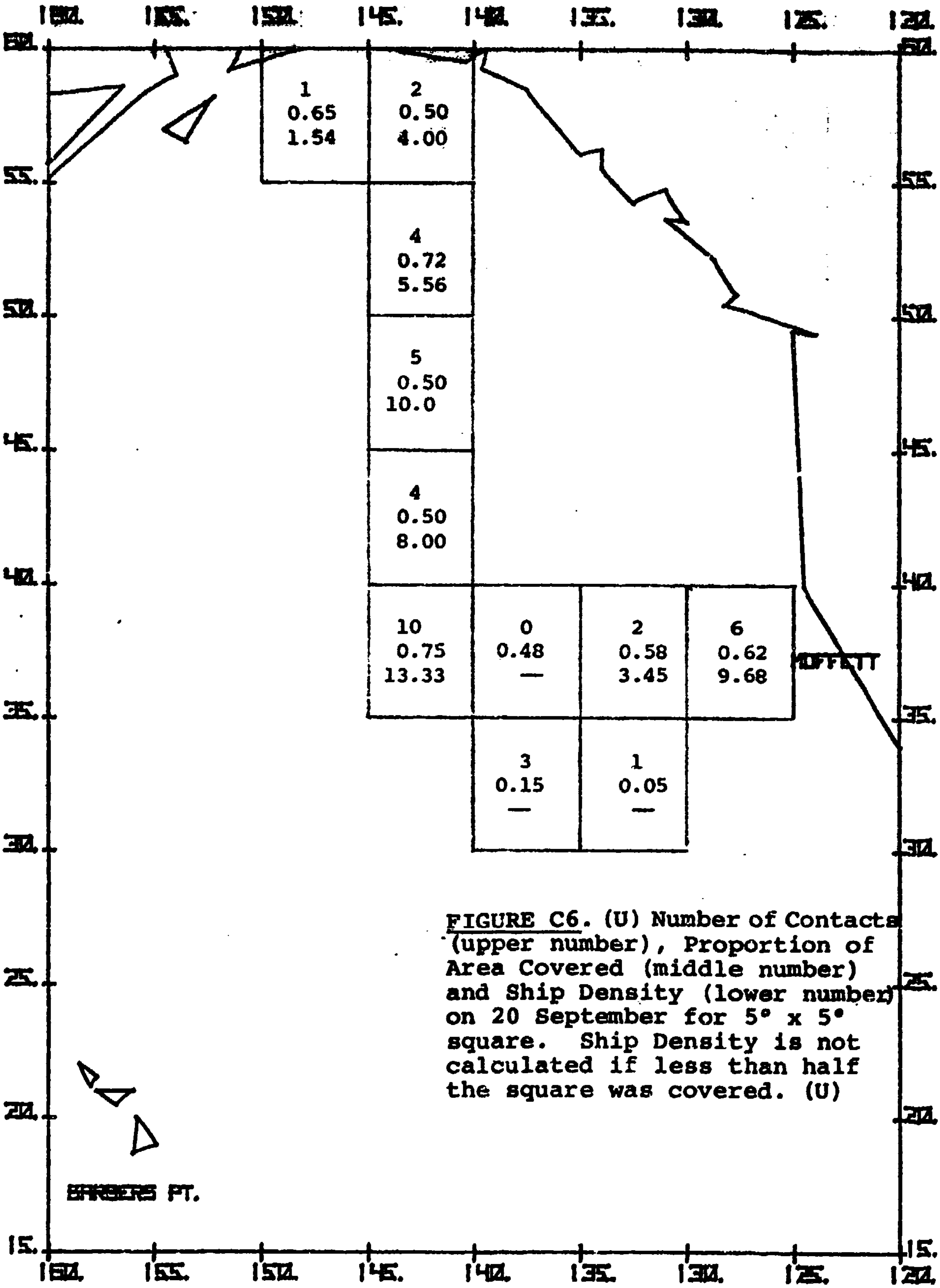

FIGURE C6. (U) Number of Contacts (upper number), Proportion of Area Covered (middle number) and Ship Density (lower number) on 20 September for 5° x 5° square. Ship Density is not calculated if less than half the square was covered. (U)

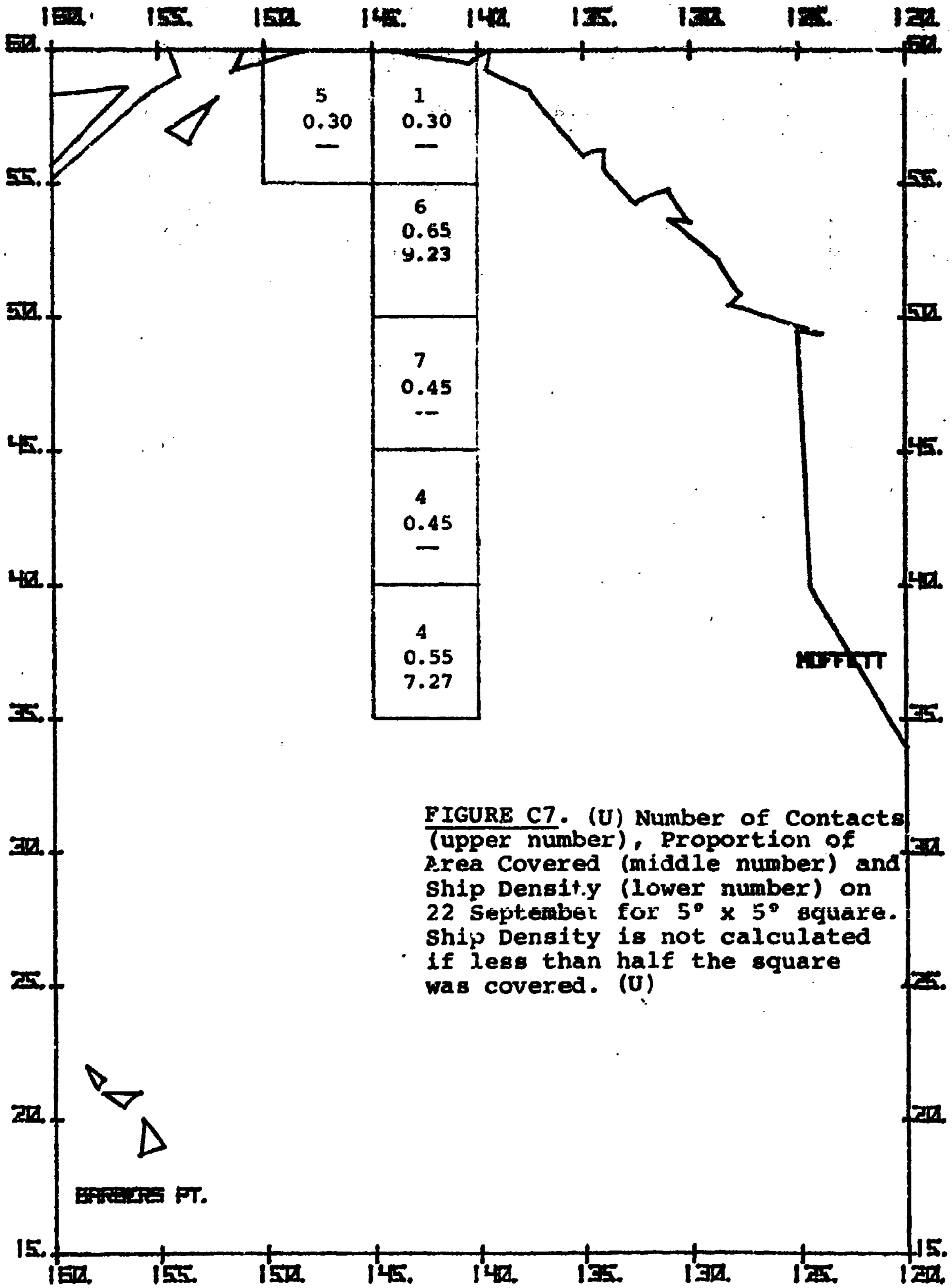

FIGURE C7. (U) Number of Contacts (upper number), Proportion of Area Covered (middle number) and Ship Density (lower number) on 22 September for 5° x 5° square. Ship Density is not calculated if less than half the square was covered. (U)

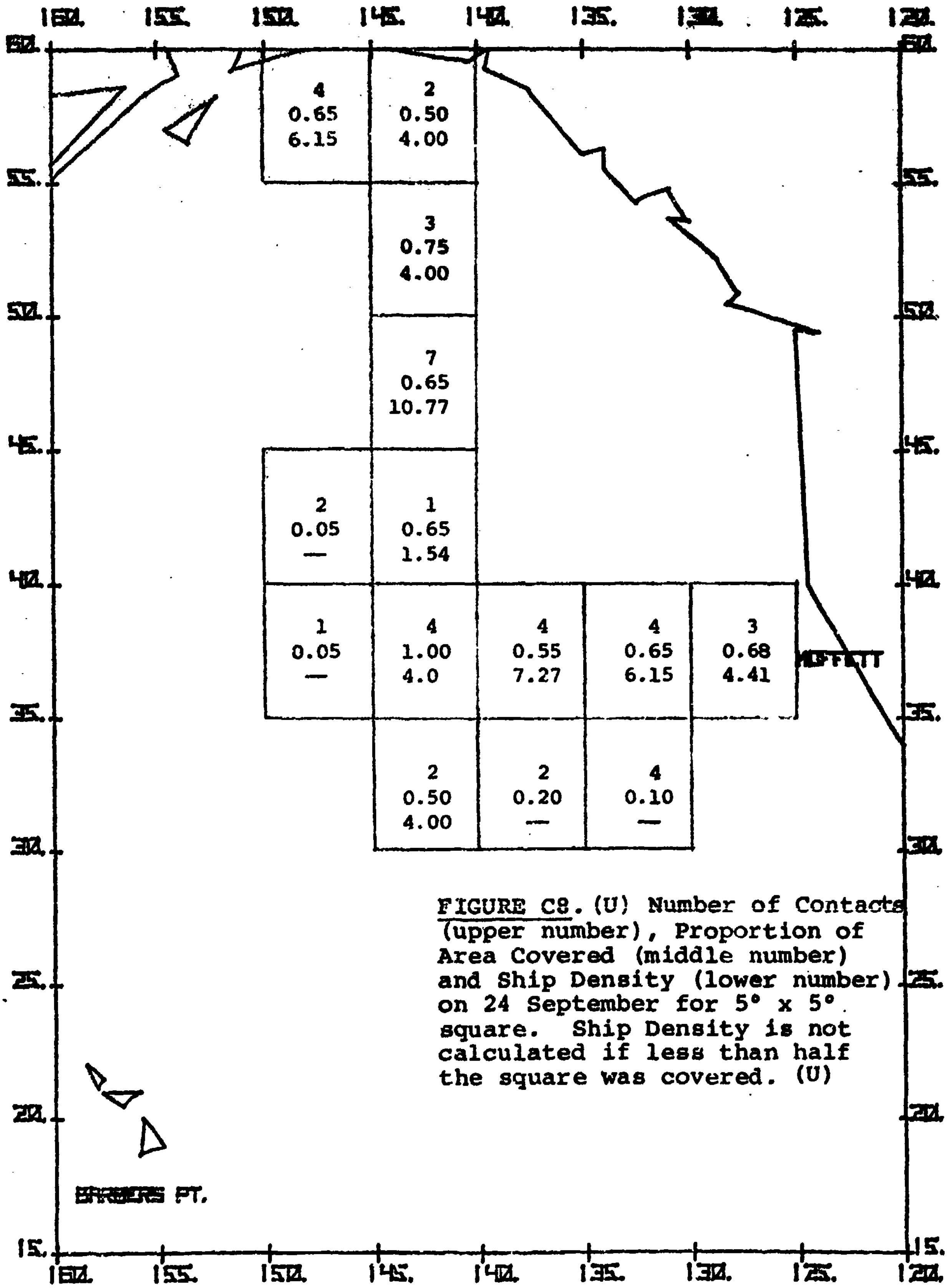

FIGURE C8. (U) Number of Contacts (upper number), Proportion of Area Covered (middle number) and Ship Density (lower number) on 24 September for 5° x 5° square. Ship Density is not calculated if less than half the square was covered. (U)

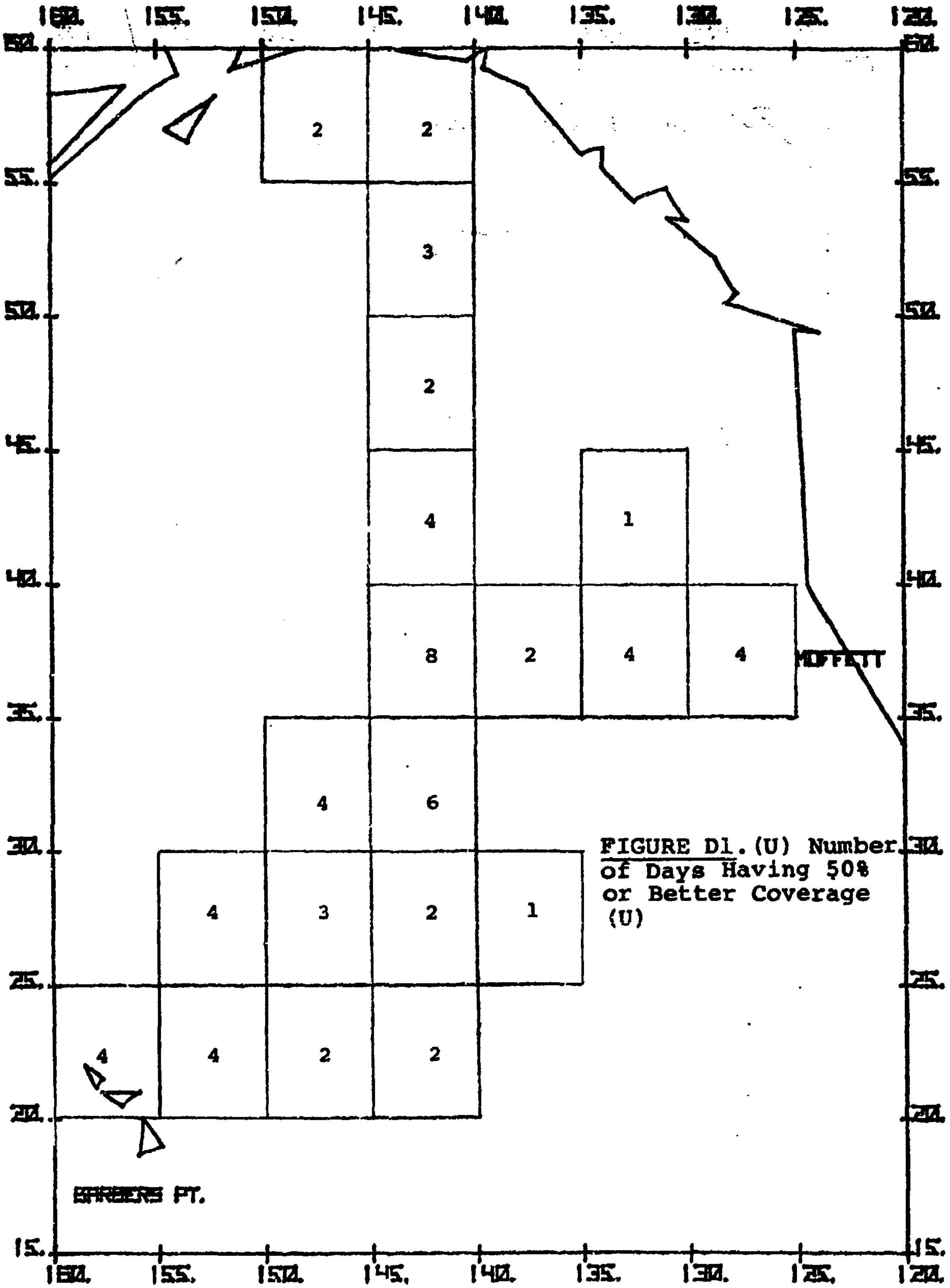

FIGURE D1. (U) Number of Days Having 50% or Better Coverage (U)

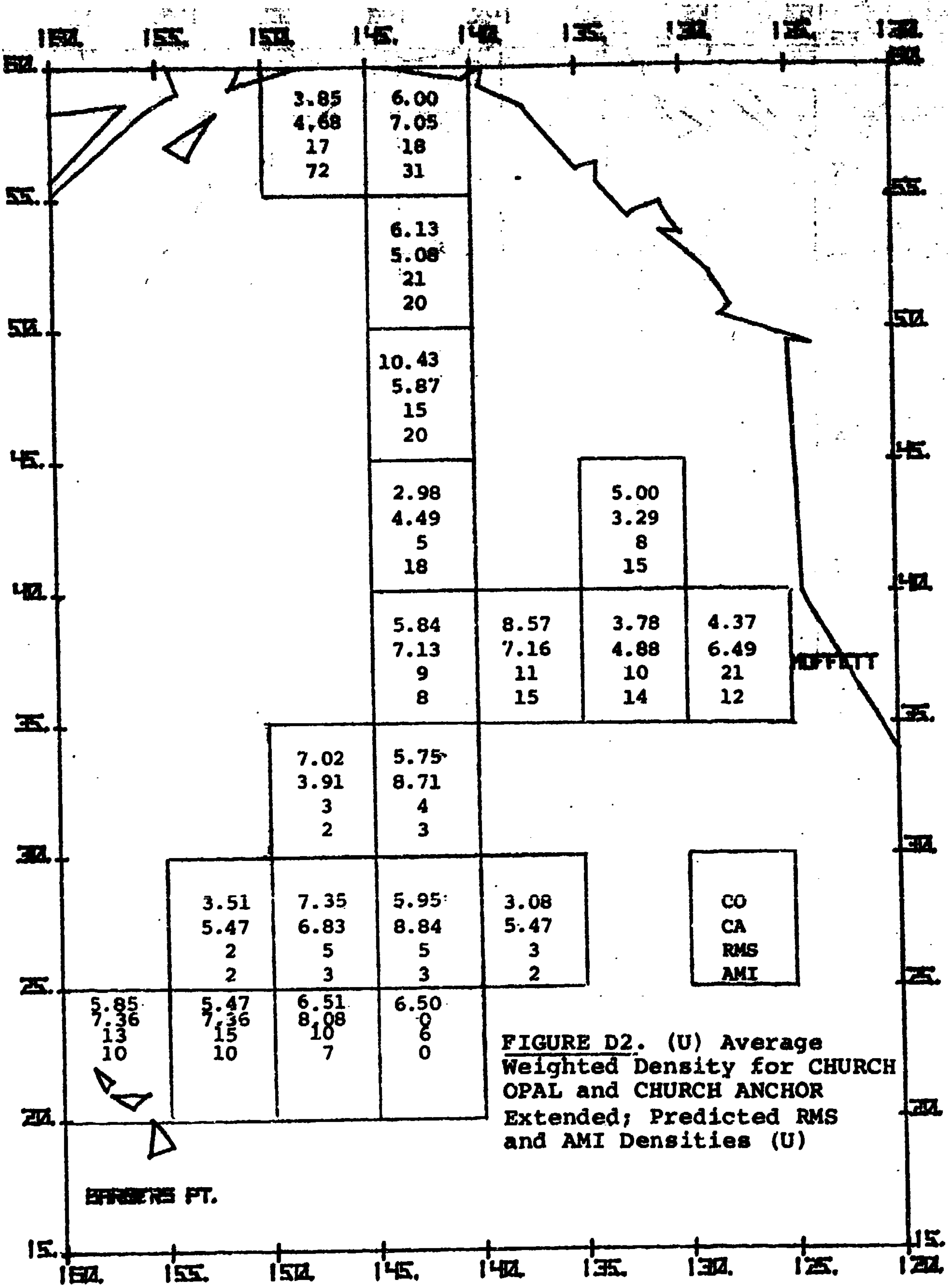

FIGURE D2. (U) Average Weighted Density for CHURCH OPAL and CHURCH ANCHOR Extended; Predicted RMS and AMI Densities (U)

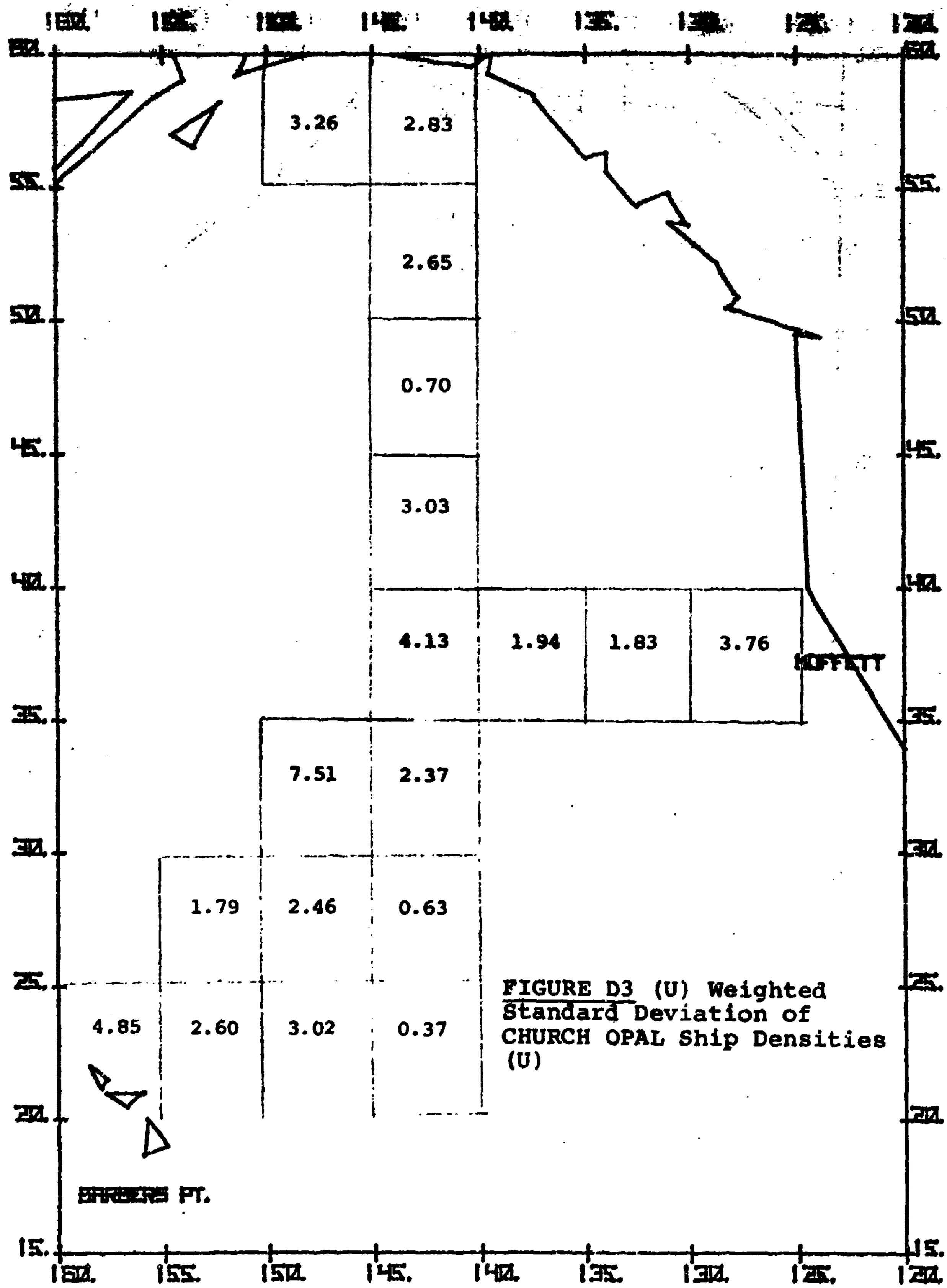

FIGURE D3 (U) Weighted Standard Deviation of CHURCH OPAL Ship Densities (U)

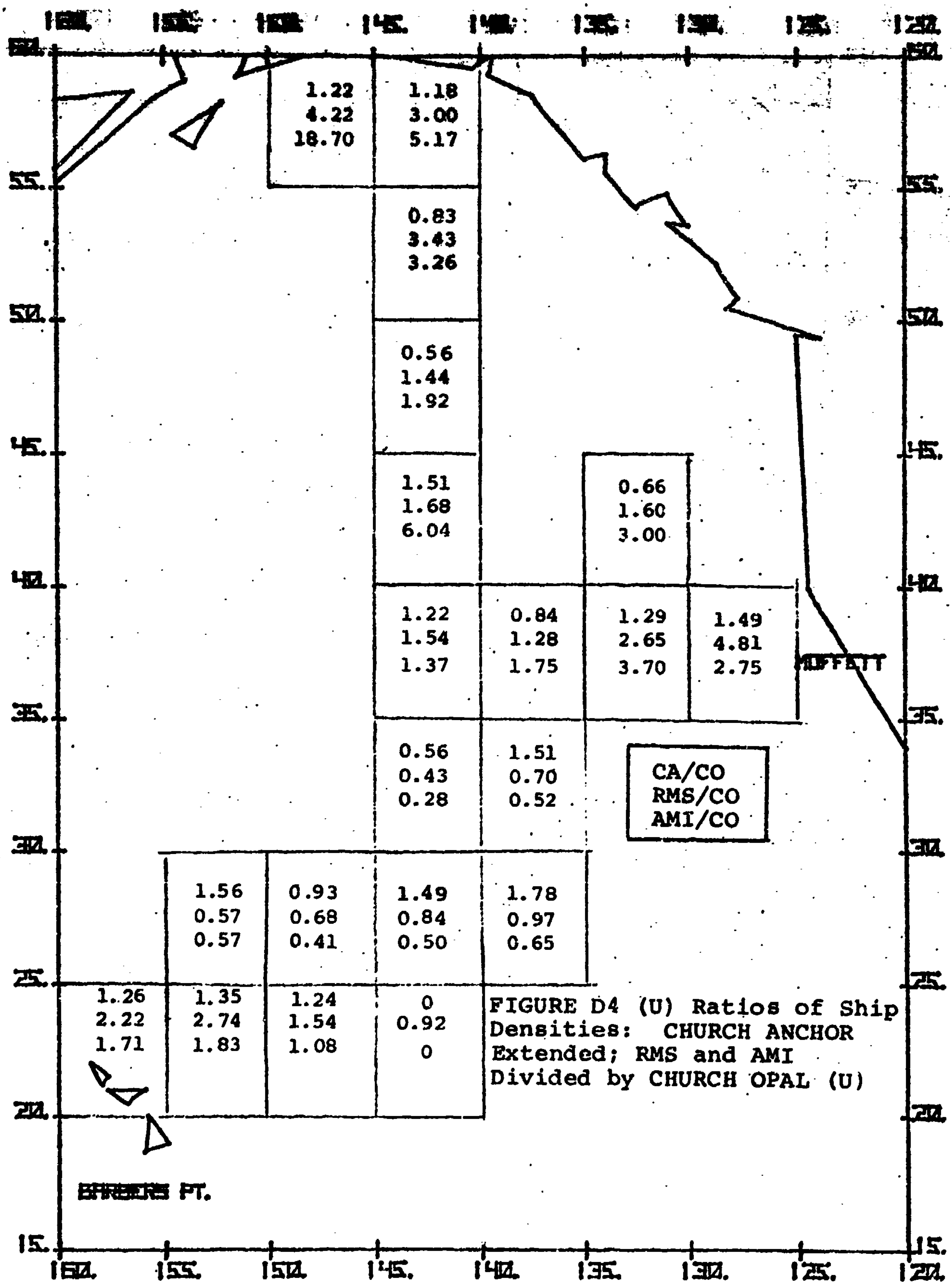

FIGURE D4 (U) Ratios of Ship Densities: CHURCH ANCHOR Extended; RMS and AMI Divided by CHURCH OPAL (U)

APPENDIX E.1

APPENDIX E.1

SHIP DENSITY DETERMINATION WITH HIGH RESOLUTION SKYWAVE RADAR SURVEILLANCE: REPORT OF FEASIBILITY EXPERIMENT (U)

1. (C) INTRODUCTION (U)

(C) The Wide Aperture Research Facility (WARF) high-resolution OTH-B radar was operated over the period of 10 September 1975 through 14 September 1975 for the purpose of detecting ships in the Pacific Ocean. This mission was identical to that described in the CHURCH OPAL Exercise Plan. The total area of coverage is illustrated in Figure E.1-1. Daily ship surveillance was performed in areas exceeding 5° latitude x 5° longitude that were centered on the following locations:

10 September 1975: 35° - 40°N and 140° - 145°W
11,12 September 1975: 30° - 35°N and 140° - 145°W
13,14 September 1975: 25° - 30°N and 140° - 145°W

The radar was operated for a period to time close to 10 hours on each day.

2. (C) RESULTS (U)

2.1 (C) DATA SUMMARY (U)

(C) Approximately 55,000 individual ocean surface cells were sampled each day for the purpose of detecting ships. Each cell measured 7.5 km in radar range depth and approximately 13 km in radar azimuth width, or about 100 $(km)^2$ per cell. The ocean area surveyed per day measured about 400,000 $(km)^2$. This area accounts for 4,000 of the 55,000 sampled cells. On the average, over half of the radar dwells were usable on each day; thus, each 5° x 5° area was sampled several times (some portions more than others). When necessary, many dwells were devoted to the verification of ship targets by concentrated sampling of single areas. The unusable radar dwells contained meteor echoes (which camouflage ships), insufficient signal strength (necessitating radar frequency changes) or unusually spread sea clutter due to disturbed ionospheric conditions.

(S) Summaries of the ocean areas surveyed on each day with good data are presented in Figures E.1-2 through E.1-6. The area corresponding to each radar dwell is outlined (approximately rectangular). Each of these dwells contained 105 individual (but slightly overlapping) 100 $(km)^2$ cells that were recorded simultaneously. Some areas were sampled more often and thus have higher probability for determination of ship density. (The number of overlapping dwells did not reproduce in the figures.) Approximately 4 good dwells on an area were necessary in this experiment to insure detection of ships of approximately 400 feet and larger, at radial speeds in excess of 9 or 10 knots. Smaller ships may or may not have been detected.

2.2 (S) SHIP TRACKS (U)

(S) The tracks of ships detected on the 5 days are presented in Figures E.1-7 to E.1-37, in chronological order measured to the beginning of each track. The date of the track is printed at the top of each map. (To simplify software developed recently for this test the maps were produced with varying scale ratios for latitude and longitude.) Except where noted, each ship track is drawn on the map with an arrow denoting the direction of travel. Data pertinent to each track are printed on each figure.

- The top line gives the begin and end time (GMT) of the track, the track duration, and the begin and end positions in decimal degrees).
- The third line gives the average observed <u>radial</u> speed (kts).
- The fourth line gives the average estimated radar cross section (AVG RCS).
- The fifth line gives the calculated true speed (kts) and course heading at the end of the track.

For a few tracks (e.g., Figure E.1-9) the true speed and heading has been omitted because either too few hits were present or the time span too short to establish an accurate cross-range rate. In those cases we have labeled each track as "inbound" or "outbound", relative to central California, based on the sign of the radial speed. The accuracy of the track end points is within 20 km (10 nmi).

2.2.1 (S) Probability Estimates (U)

(S) A probability has been associated with each track and is printed on the lower right-hand corner of each figure. This probability is based on the number, time spacing, and consistency of radar contacts. These probabilities are rough estimates, and may be defined as follows:

- >90% means the track is almost undoubtedly a ship.
- >50% means that something less than half of all the tracks with this probability are probably only coincidental correlations of false echoes produced by noise, meteors, clutter enhancements, and/or aircraft.
- <25% means that probably less than one fourth of the tracks with this probability are ships.

In some hypothetical strategic situations, the radar operator would surely pass all the 90% tracks, and probably the 50% tracks. Further sensor verification of the 25% tracks would be necessary to give them reasonable validity.

2.2.2 (S) Track Combinations and Multiple Targets (U)

(C) In two cases, Figures E.1-21 and E.1-31 (each in three parts), we had two tracks spaced by two and seven hours, respectively, that could be combined into one track. In each case, this conclusion was based on the consistency of both the target's radial speed and the final speed estimate.

(U) For Figure E.1-21 we would use only the combination track (Figure E.1-21-C).

(S) Figure E.1-31 is much more complicated. We have high probability for both the begin and end tracks (spaced by seven hours), and very good consistency for the final track. However, we probably had more than one ship in a group of 2 or 3 (spaced by tens of km) in each of the two tracks. Whether or not the same ships that were together on the first track (Figure E.1-31-A) were also together on the second track (Figure E.1-31-B) is uncertain. Owing to the long time between tracks, we would recommend that the two tracks be left separate, with two ships per track. Figure E.1-31-C would be ignored unless other sensor information can help relate the two separate tracks.

(C) The detection log that formed the track of Figure E.1-8 also suggested the presence of two or three closely spaced ships. We would recommend the association of two ships for this track.

2.2.3 (S) Target Size (U)

(S) The ship size is roughly related to its average RCS estimated from the data and printed beneath each track. This estimate is based on an estimate of the sea clutter cross section which has been found to be surprisingly predictable. Based on measurements of both full-size and scale model ship cross sections, we would divide the ship sizes as follows:

- Small (<400 feet) for RCS<35 dB_m^2
- Medium (400 to 600 feet) for $35 \leq RCS \leq 40$ dB_m^2
- Large (>600 feet) for RCS>40 dB_m^2

3. (S) CONCLUSIONS AND RECOMMENDATIONS (U)

(S) A total of 32 tracks (containing a total of 34 ships were derived by means of surveillance by high resolution OTH-B radar during the period of 10-14 September 1975. The surveillance areas are outlined in Section 1 of this report. Of these tracks we attach very high confidence (>90%) and medium confidence (>50%) as follows:

(S)

10 September		2 tracks, 3 ships (>90%)
		2 tracks, 2 ships (>50%)
	TOTAL	4 tracks, 5 ships
11 September		2 tracks, 2 ships (>90%)
		2 tracks, 2 ships (>50%)
	TOTAL	4 tracks, 4 ships
12 September		1 track, 1 ship (>90%)
		1 track, 1 ship (>50%)
	TOTAL	2 tracks, 2 ships
13 September		4 tracks, 4 ships (>90%)
		2 tracks, 2 ships (>50%)
	TOTAL	6 tracks, 6 ships
14 September		5 tracks, 7 ships (>90%)
		2 tracks, 2 ships (>50%)
	TOTAL	7 tracks, 9 ships

On 10 September one track had two ships closely spaced, and on 14 September two tracks had two ships in a group. Tracks remaining of the 34 had a confidence of less than 25% and are included herein only for academic purposes (e.g., if another sensor could verify them). The position accuracies for all tracks are 20 km (10 nmi).

(S) Ship radial speeds ranged from 10.8 to 22.6 kts, while estimated true ship speeds ranged from 14.0 to 24.6 kts. Both inbound and outbound ships were tracked. The accuracy of the radial speed is about 5%. The course and true speed accuracy is primarily determined by the time span between track end points when the 20 km position accuracy is applied.

(C) Several new area-surveillance ship tracking methods were developed as a result of this feasibility experiment. Heretofore, (with one exception) we have employed WARF for the tracking only of specific (single) ships of high interest either to SRI or the

U.S. Fleet. The surveillance of relatively large areas with high resolution requires rather careful planning to insure efficient target hit-to-hit correlation. New correlation procedures were developed in the CHURCH OPAL exercise, and better software is now being written to automate much of what was done manually after the experiment (this work is part of a separate ONR-supported task). Additionally, we are now prepared to suggest new scanning procedures, possibly a fence concept, for any future experiments with LRAPP. A suitable blend of scanning strategy and hit-to-hit correlation procedures would yield target tracks all of high confidence. Tracks of initially lower confidence would be verified.

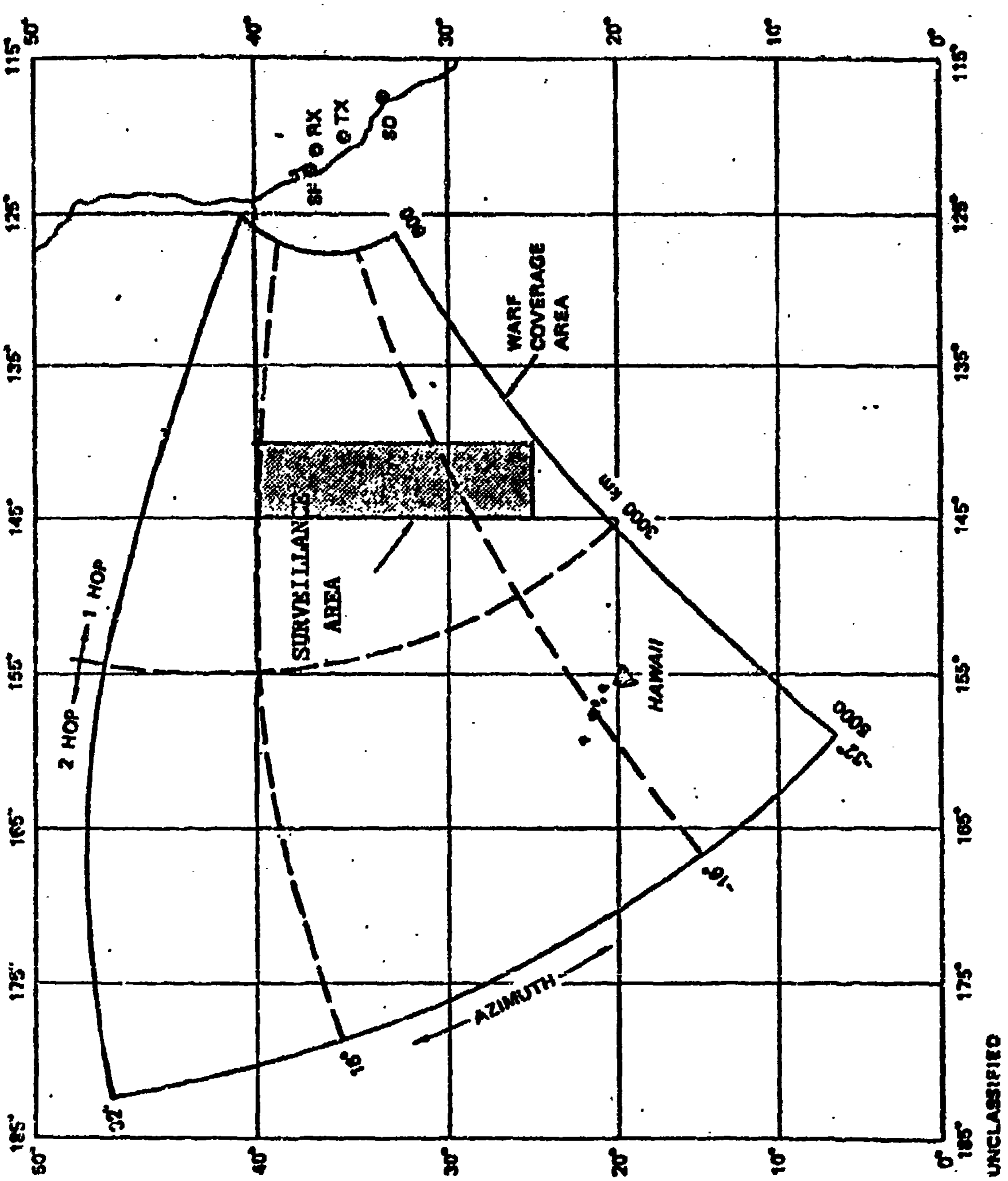

SURVEILLANCE AREA FOR LRAPP SHIP DENSITY STUDY
WITH WARF RADAR (U)

Figure E.1-1

LRAPP: START 10 SEPT 75 1723:36Z END 10 SEPT 75 0239:16Z

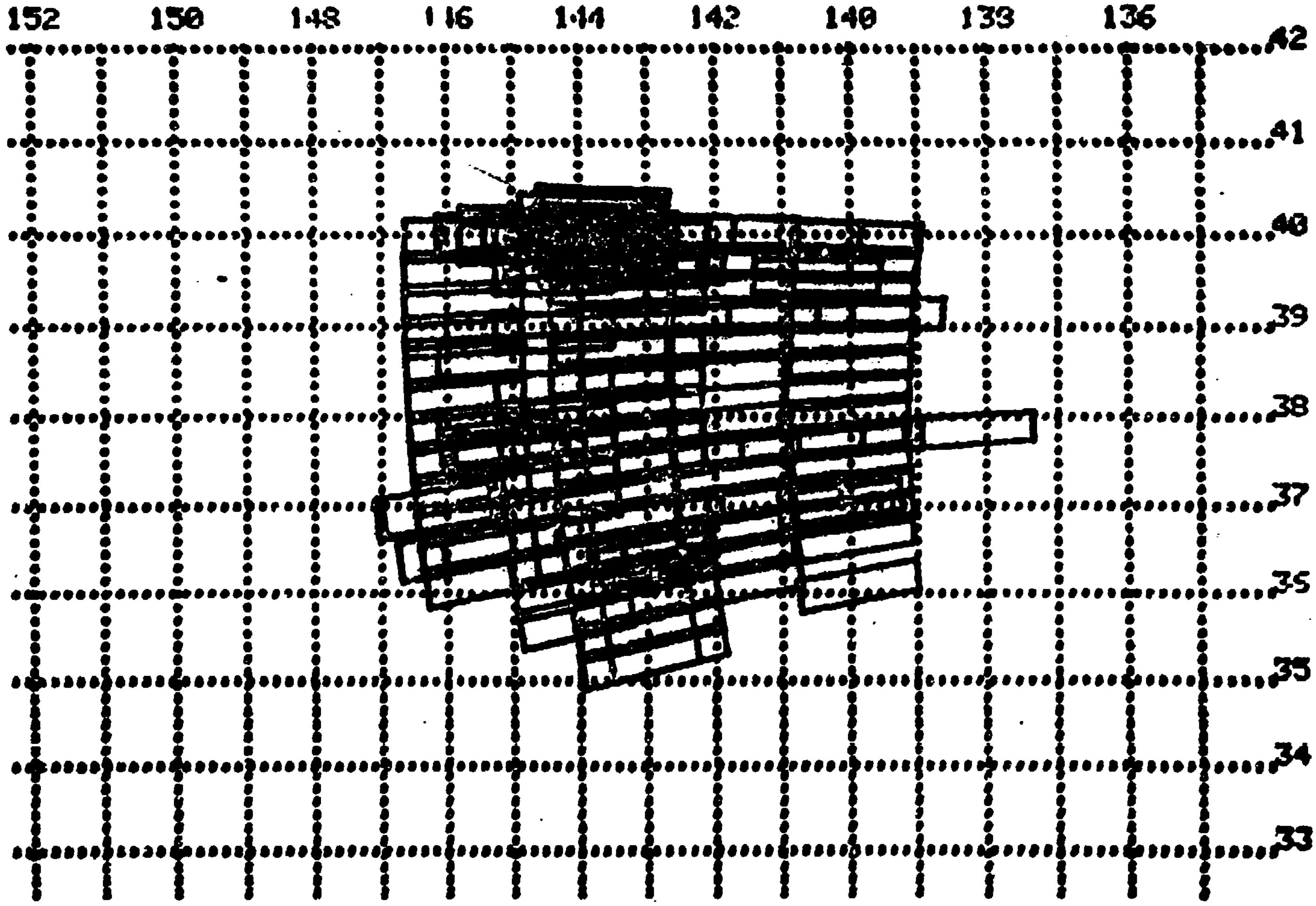

NOTE: EACH COVERAGE RECTANGLE CONTAINS 105 RESOLUTION CELLS

Figure E.1-2

LRAPP: START 11 SEP 75 1727 16Z END 11 SEP 75 0223:16Z

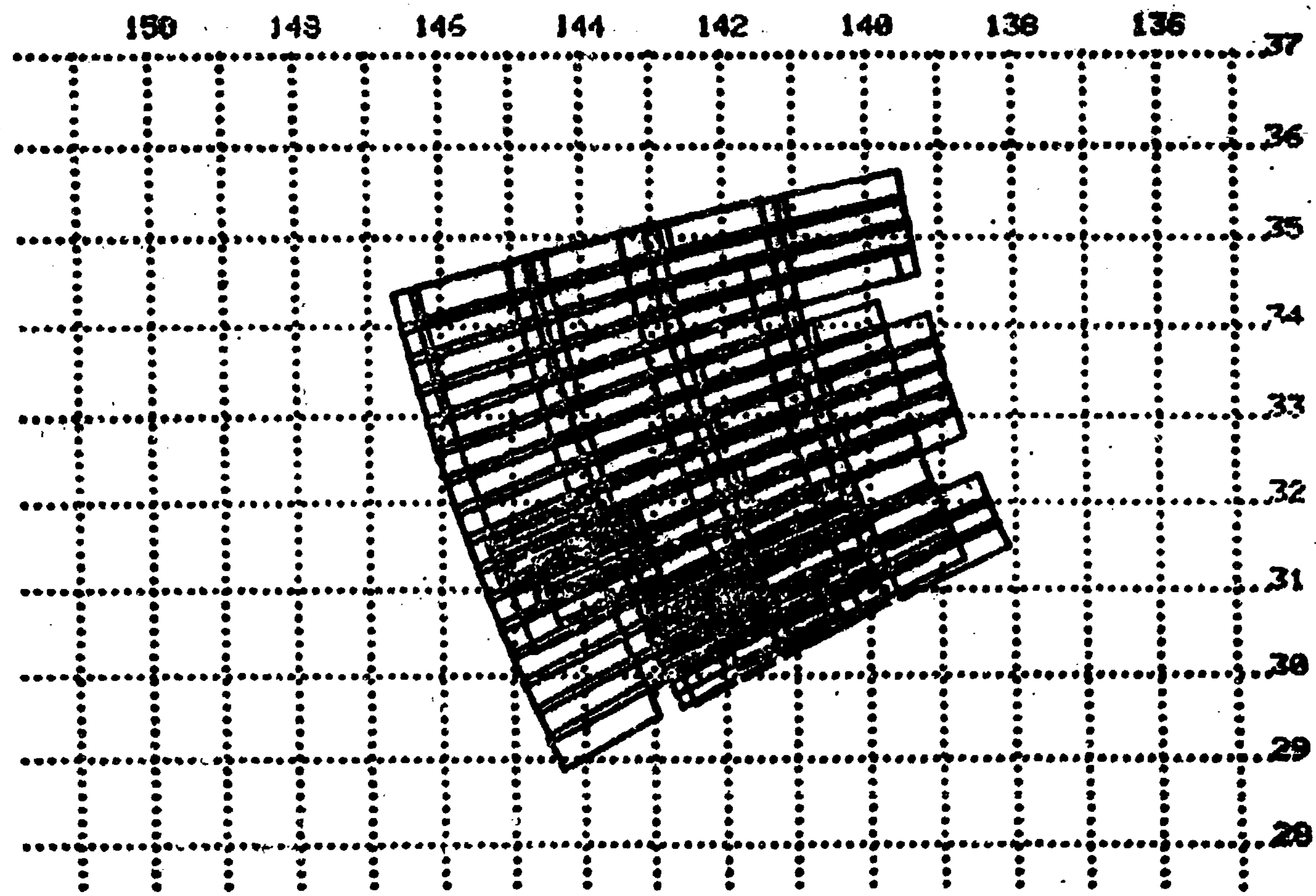

NOTE: EACH COVERAGE RECTANGLE CONTAINS 105 RESOLUTION CELLS

Figure E.1-3

LRAPP: START 12 SEP 75 1723:26Z END 12 SEPT 75 0212:15Z

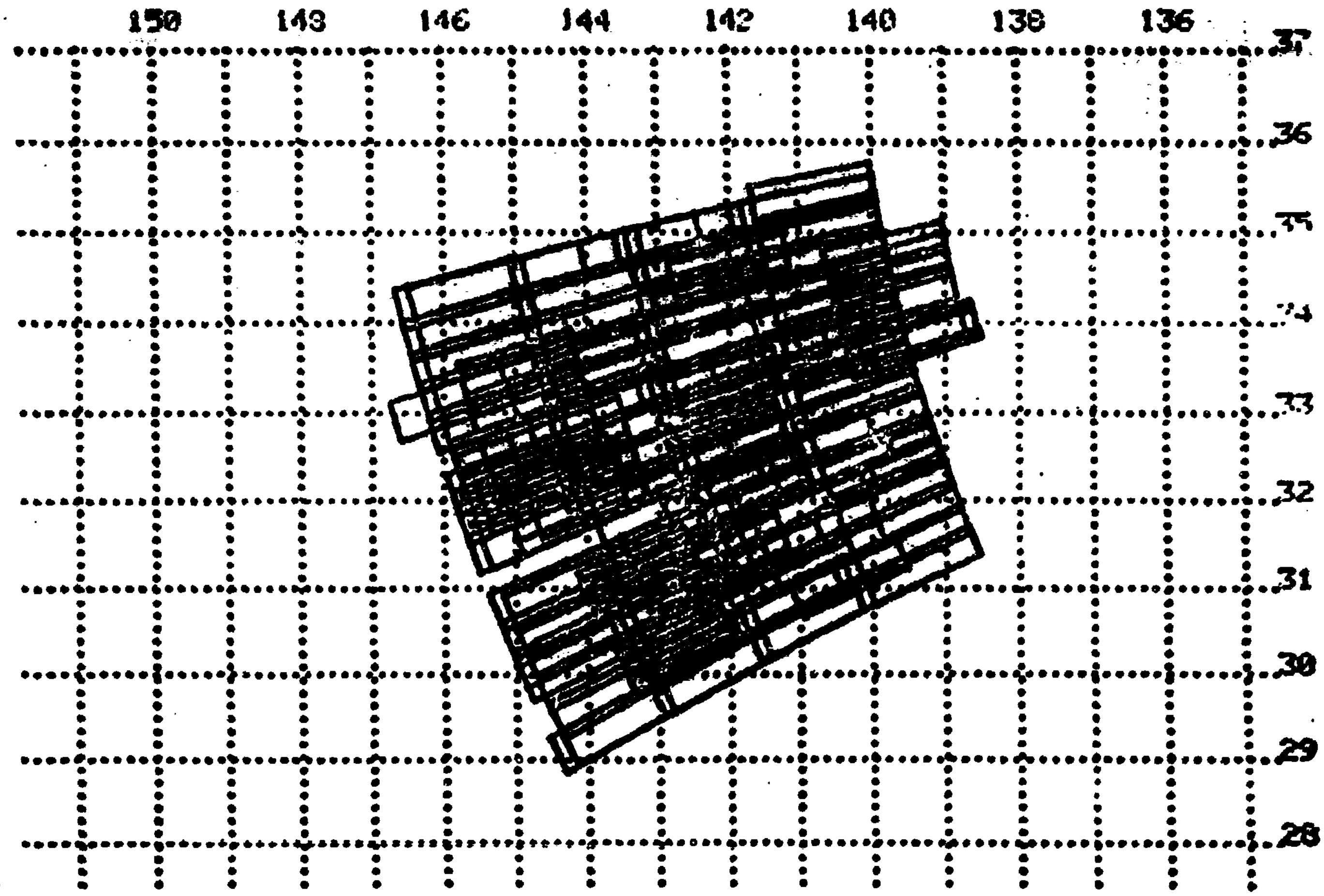

NOTE: EACH COVERAGE RECTANGLE CONTAINS 105 RESOLUTION CELLS

Figure E.1-4

LRAPP: START 13 SEPT 75 1634:16Z END 13 SEPT: 75 0237:39Z

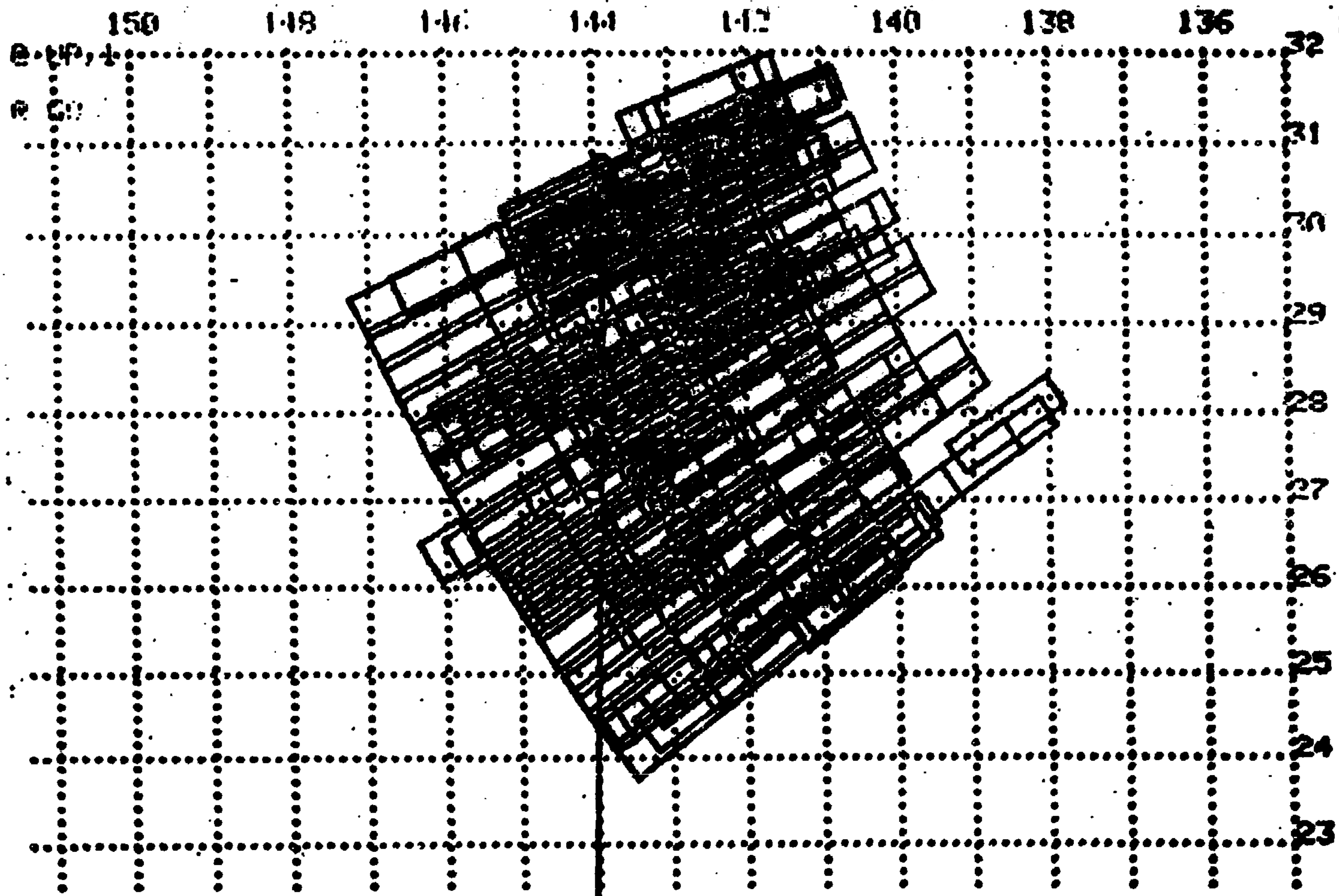

NOTE: EACH COVERAGE RECTANGLE CONTAINS 105 RESOLUTION CELLS

Figure E.1-5

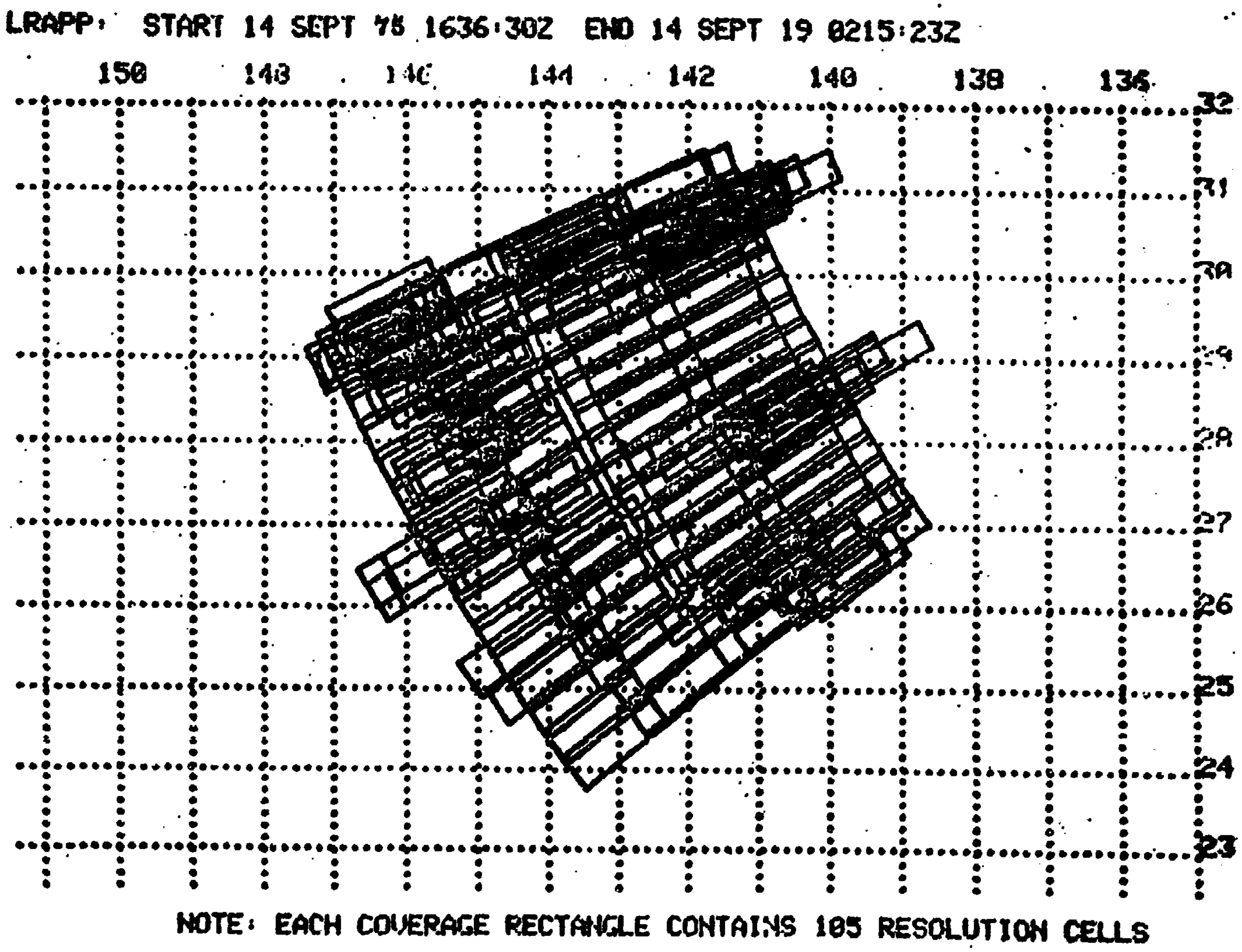
LRAPP: START 14 SEPT 75 1636:30Z END 14 SEPT 19 0215:23Z
150
148
146
144
142
140
138
136
32
31
30
29
28
27
26
25
24
23
NOTE: EACH COVERAGE RECTANGLE CONTAINS 105 RESOLUTION CELLS

Figure E.1-6

SEP 10 1975

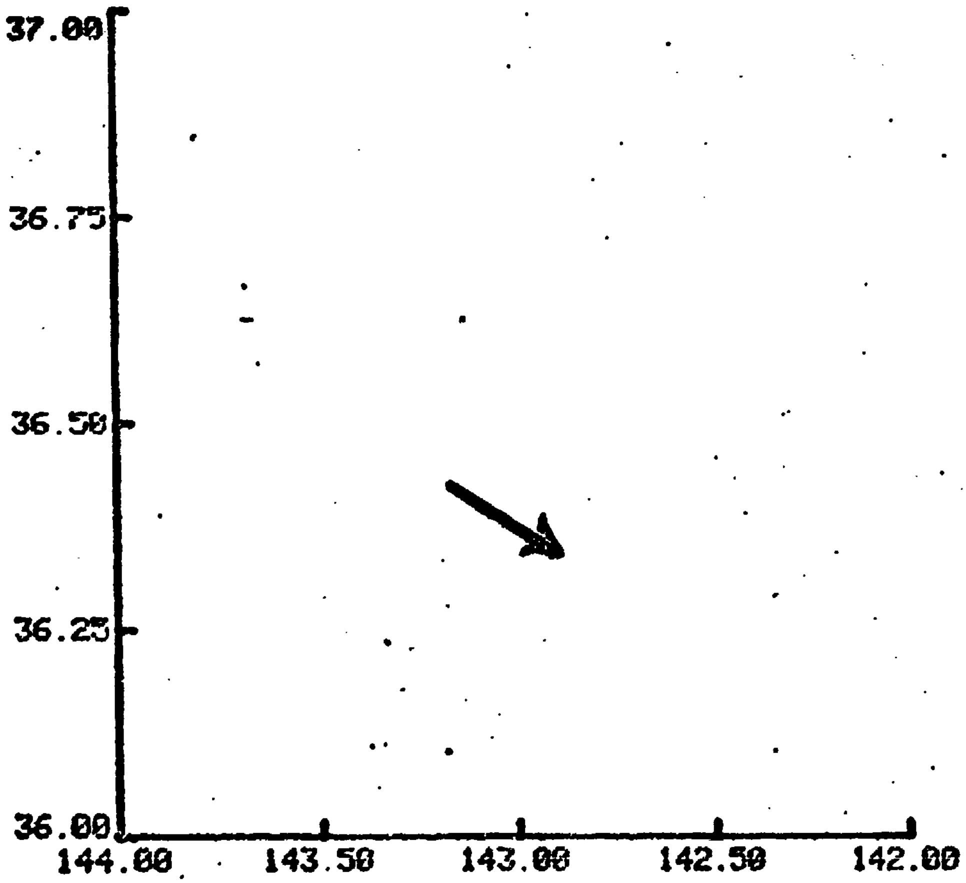

FILES 236 268 TIME 21:49:00 22:18:22 .49 HOURS 36.42 143.15
SPEED RANGE 20.8 22.3 MIN SNR 13.8 36.35 142.92
AVG SPEED= 21.7 SPEED FROM LSQ 20.9
AVG SNR= 14.5 AVG RCS= 43.1 RCS S.D.M= -2.0 AVG SPEED
SPEED FROM LAT/LON= 24.6 HEADING 106.5 DEGREES

> 90%

Figure E.1-7

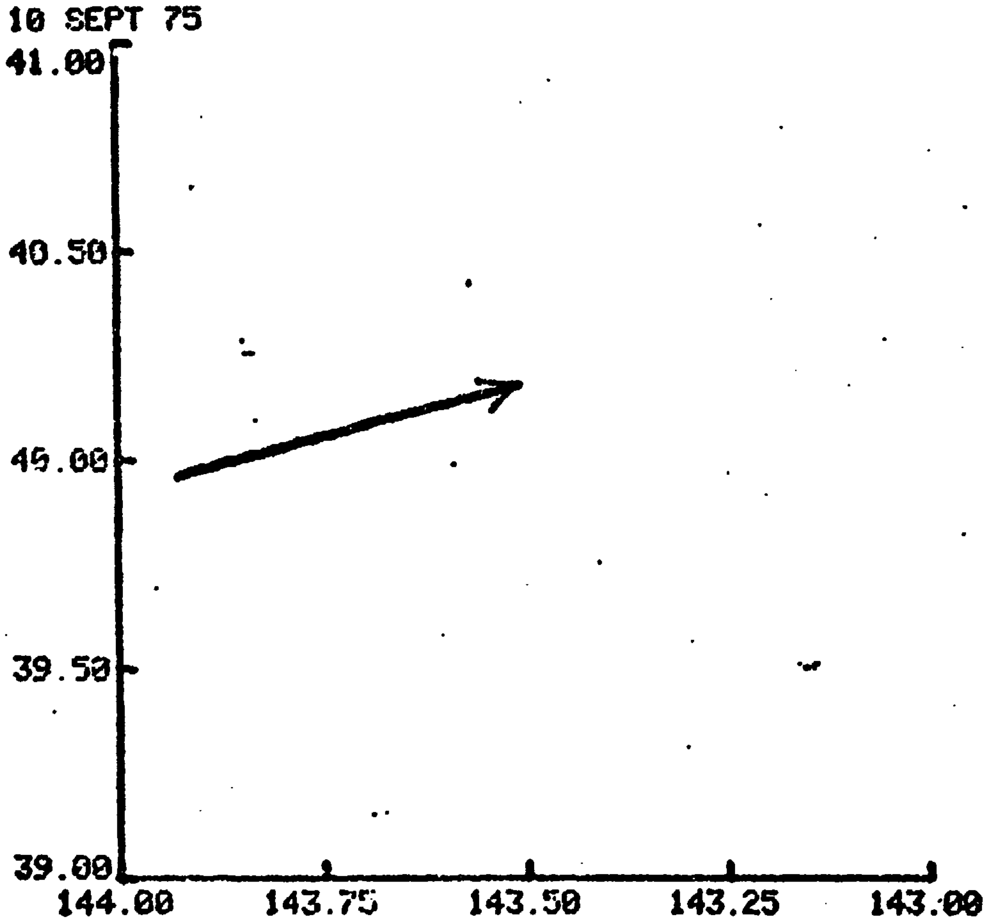

FILES 105 189 TIME 01:00:00 02:14:54 1.25 HOURS 39.97 143.92
SPEED RANGE 12.6 16.0 MIN SNR 13.0 40.18 143.51
AVG SPEED= 14.3 SPEED FROM LSQ= 26.8
AVG SNR= 18.5 AVG RCS= 38.5 RCS S.D.M= .9 AVG SPEED
SPEED FROM LAT/LON= 18.5 HEADING 55.9 DEGREES

> 90%

1 to 3 ships in group

Figure E.1-8

SEP 10 1975

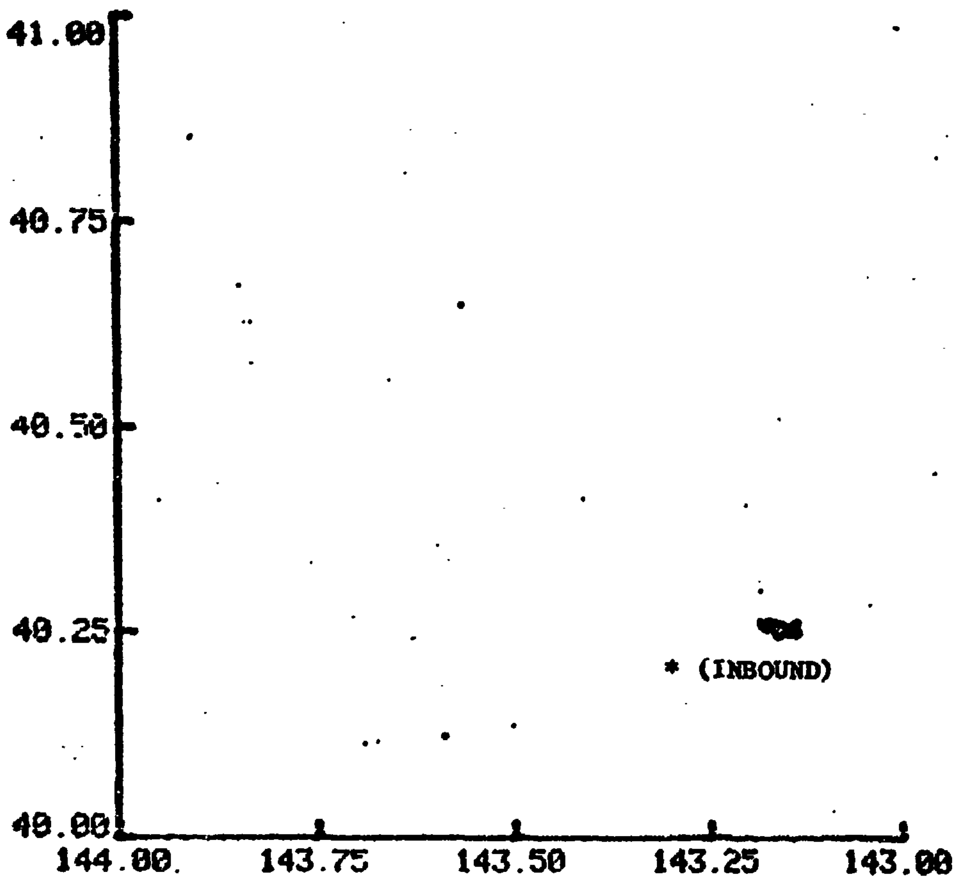

FILES 173 178 TIME 02:00:52 02:05:17 .07 HOURS 40.26 143.17
SPEED RANGE 17.3 20 7 MIN SNR 14.9 40.25 143.14
* AVG SPEED= 18.8 SPEED FROM LSQ= -9.7
AVG SNR= 17.4 AVG RCS= 37.9 RCS S.D.M= -4.0 AVG SPEED

\> 50%

Figure E.1-9

SEP 10 1975

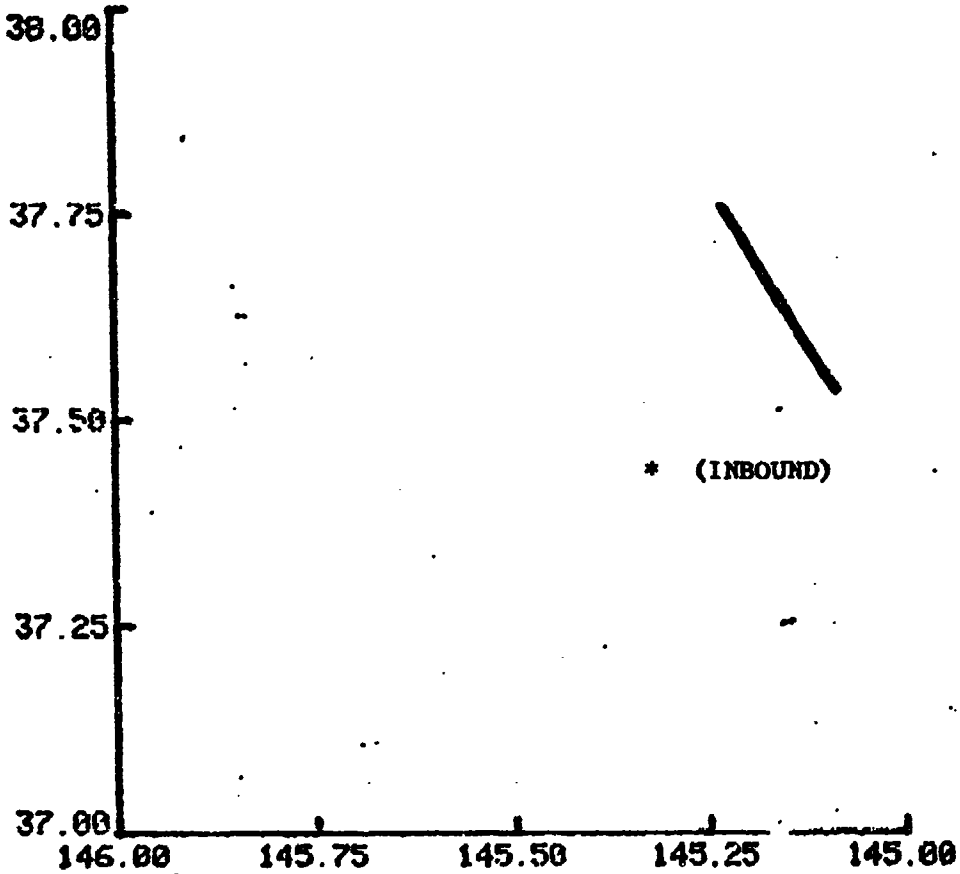

FILES 196 211 TIME 02:24:00 02:39:00 .25 HOURS 37.75 145.22
SPEED RANGE 20.5 25.5 MIN SNR 13.4 37.54 145.08
* AVG SPEED= 22.6 SPEED FROM LSQ= 28.8
AVG SNR= 21.9 AVG RCS= 37.1 RCS S.D.M= 1.2 AVG SPEED

> 50%

Figure E.1-10

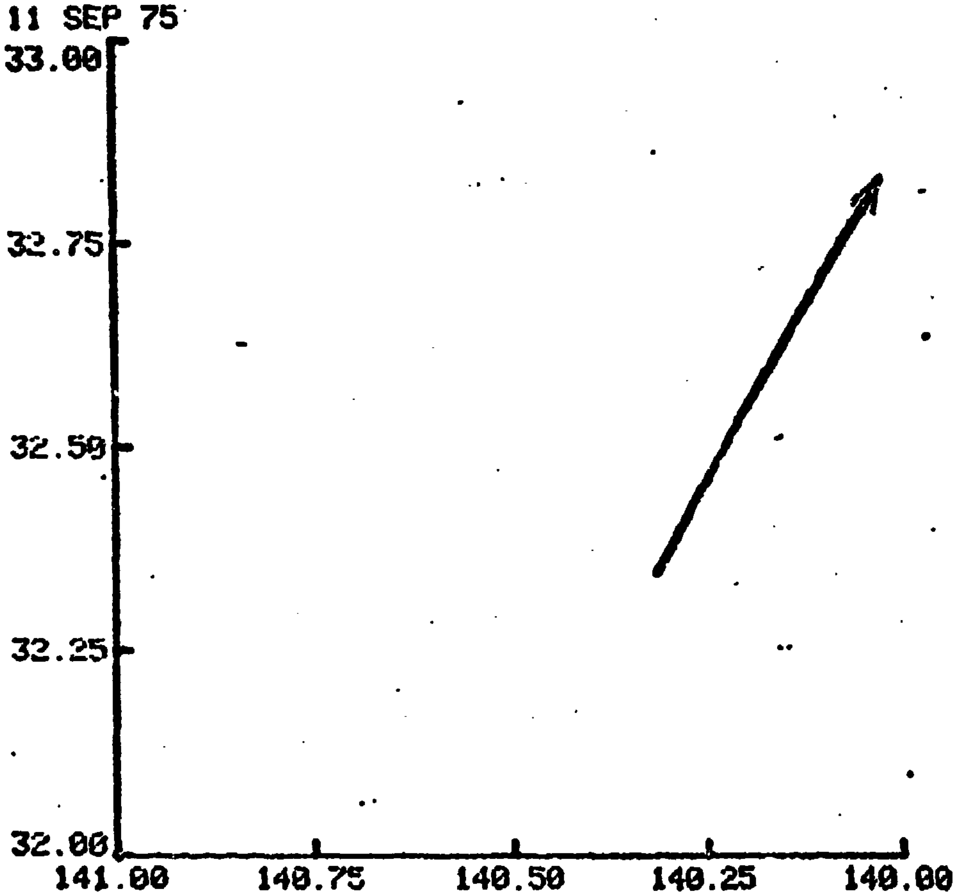

FILES 89 181 TIME 19:05:00 20:44:00 1.65 HOURS 32.35 140.31
SPEED RANGE 13.0 14.4 MIN SNR 13.2 32.83 140.02
AVG SPEED= 13.7 SPEED FROM LSQ= 2.4
AVG SNR= 13.9 AVG RCS= 34.9 RCS S.D.M= -2.7 AVG SPEED
SPEED FROM LAT/LON= 19.7 HEADING 26.8 DEGREES

< 25%

Figure E.1-11

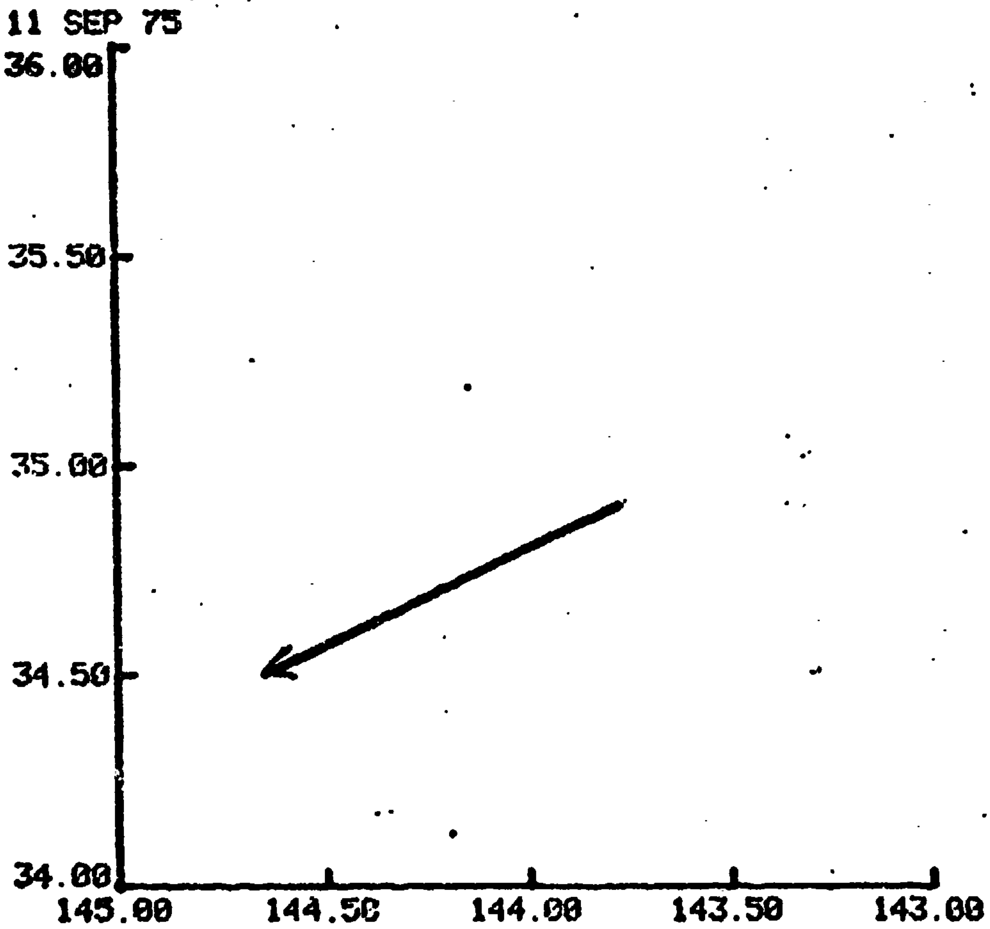


```
FILES  103  341 TIME 19:19:00  23:33:00   4.23 HOURS 34.91 143.76
SPEED RANGE  -13.1 -12.4 MIN SNR 12.4                34.51 144.64
AVG SPEED= -12.7  SPEED FROM LSQ=  -7.7
AVG SNR= 15.4    AVG RCS= 41.9    RCS S.D.M= -2.5    AVG SPEED
SPEED FROM LAT/LON=  13.5 HEADING 241.1 DEGREES
```

< 25%

Figure E. 12

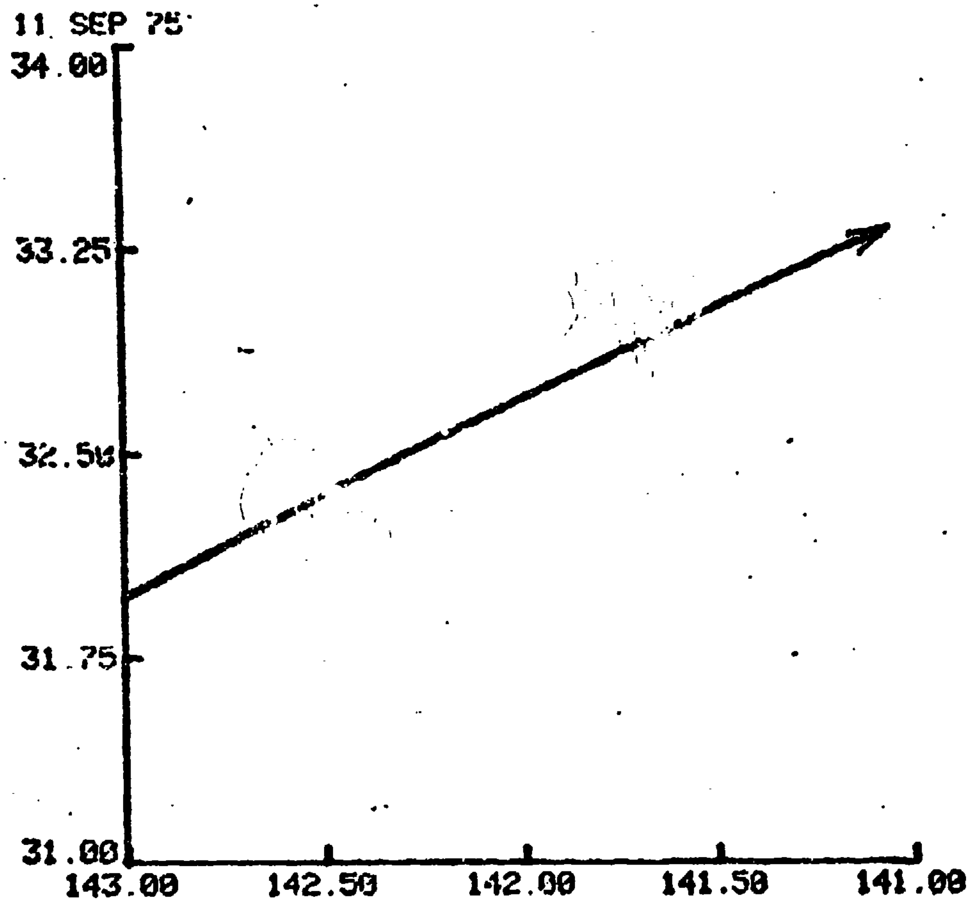

FILES 112 478 TIME 19:20:00 01:58:00 6.50 HOURS 31.98 142.99
SPEED RANGE 16.8 18.8 MIN SNR 14.5 33.32 141.06
AVG SPEED= 17.8 SPEED FROM LSQ= 14.3
AVG SNR= 17.5 AVG RCS= 35.6 RCS S.D.M= -1.0 AVG SPEED
SPEED FROM LAT/LON= 19.5 HEADING 50.1 DEGREES

< 25%

Figure E.1-13

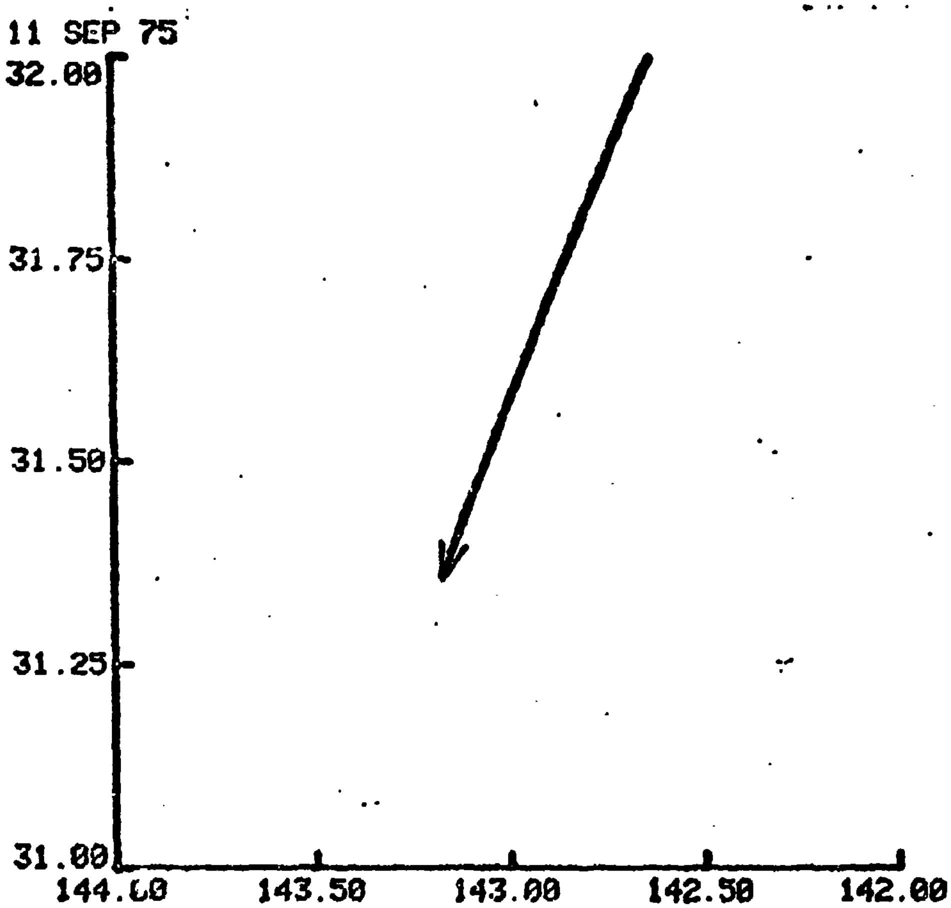

FILES 126 288 TIME 19:42:00 22:38:00 2.93 HOURS 32.00 142.64
SPEED RANGE -14.4 -11.6 MIN SNR 12.2 31.36 143.17
AVG SPEED= -13.0 SPEED FROM LSQ= -15.2
AVG SNR= 12.7 AVG RCS= 45.7 RCS S.D.M= -.5 AVG SPEED
SPEED FROM LAT/LON= 16.0 HEADING 215.6 DEGREES

> 50%

Figure E.1-14

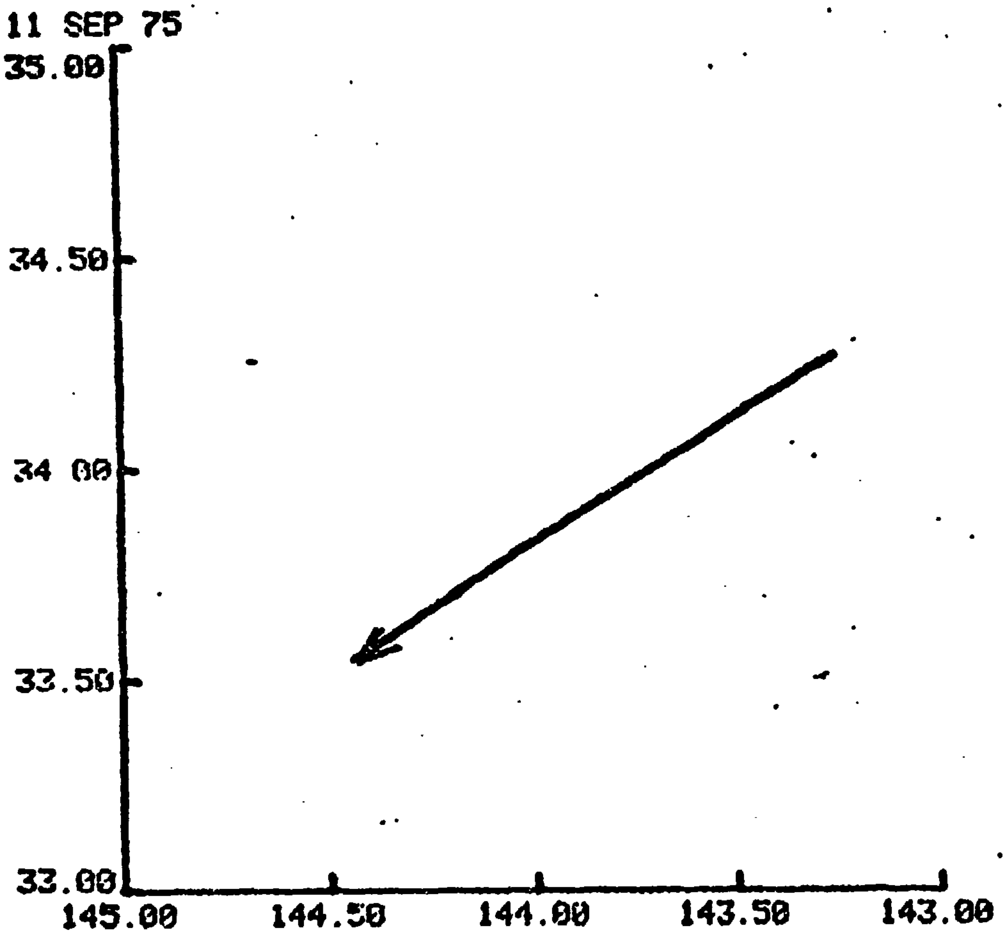

FILES 236 445 TIME 21:44:00 01:24:00 3.67 HOURS 34.27 143.26
SPEED RANGE -18.4 -18.1 MIN SNR 13.1 33.55 144.44
AVG SPEED= -18.3 SPEED FROM LSQ= -16.6
AVG SNR= 14.7 AVG RCS= 43 9 RCS S.D.M= 1.6 AVG SPEED
SPEED FROM LAT/LON= 19.9 HEADING 234.3 DEGREES

> 50%

Figure E.1-15

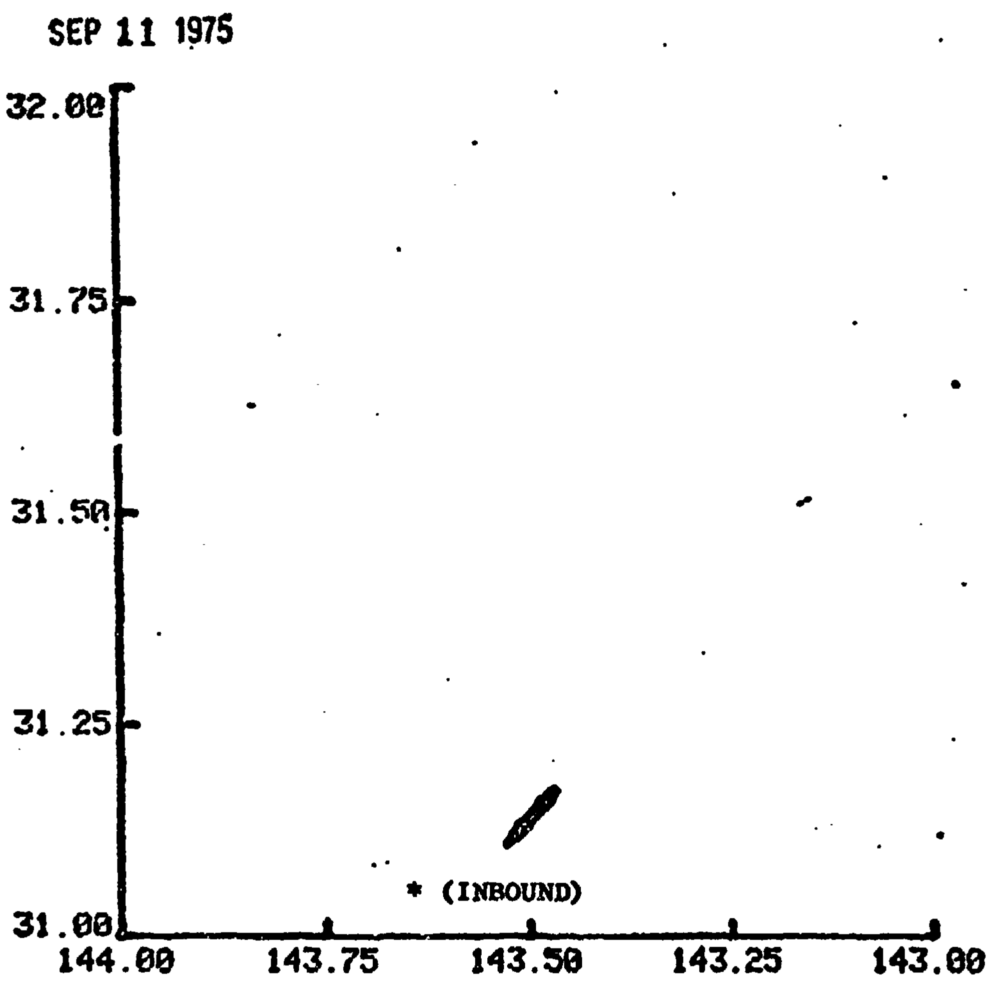

FILES 278 292 TIME 22:28:00 22:42:00 .23 HOURS 31.12 143.52
SPEED RANGE 14.2 17.0 MIN SNR 13.2 31.17 143.47
* AVG SPEED= 15.8 SPEED FROM LSQ= 40.6
AVG SNR= 14.6 AVG RCS= 38.6 RCS S.D.M= -.4 AVG SPEED

> 80%

Figure E.1-16

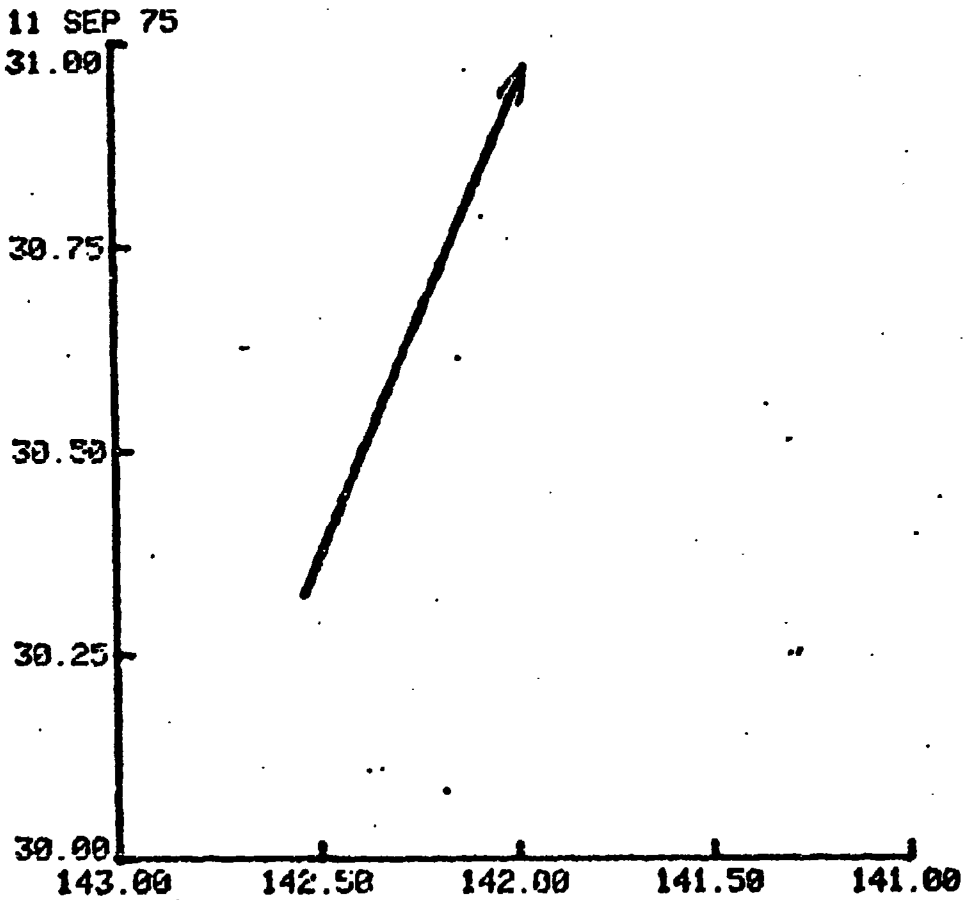

FILES 355 454 TIME 23:47:00 01:33:00 1.77 HOURS 30.33 142.53
SPEED RANGE 22.2 25.1 MIN SNR 13.0 30.97 141.97
AVG SPEED= 23.6 SPEED FROM LSQ= 12.7
AVG SNR= 13.4 AVG RCS= 33.1 RCS S.D.M= .2 AVG SPEED
SPEED FROM LAT/LON= 27.5 HEADING 36.7 DEGREES

< 25%

Figure E.1-17

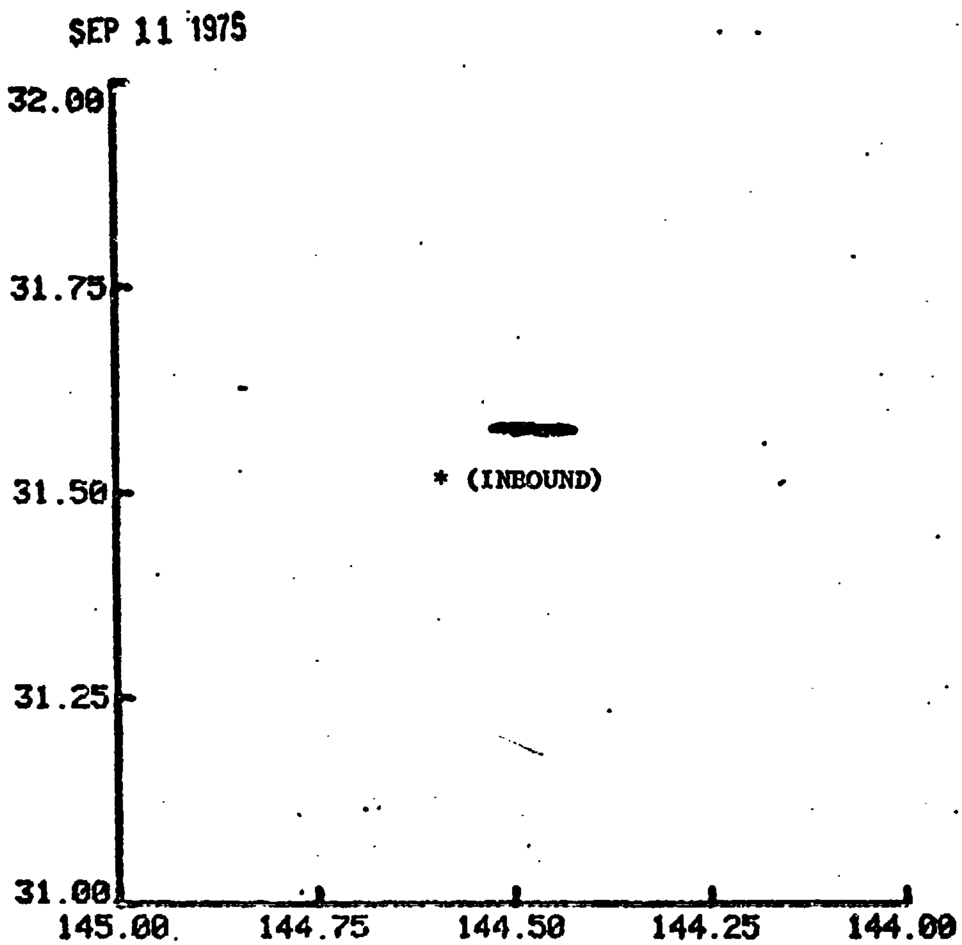


```
FILES  417  433 TIME 00:56:00  01:12:00     .27 HOURS 31.58 144.51
SPEED RANGE   14.9  16.7 MIN SNR 13.8                 31.58 144.42
* AVG SPEED=  15.5  SPEED FROM LSQ=  34.5
AVG SNR=      17.9 AVG RCS=     35.7 RCS S.D.M=     -2.9 AVG SPEED
```

> 90%

Figure E.1-18

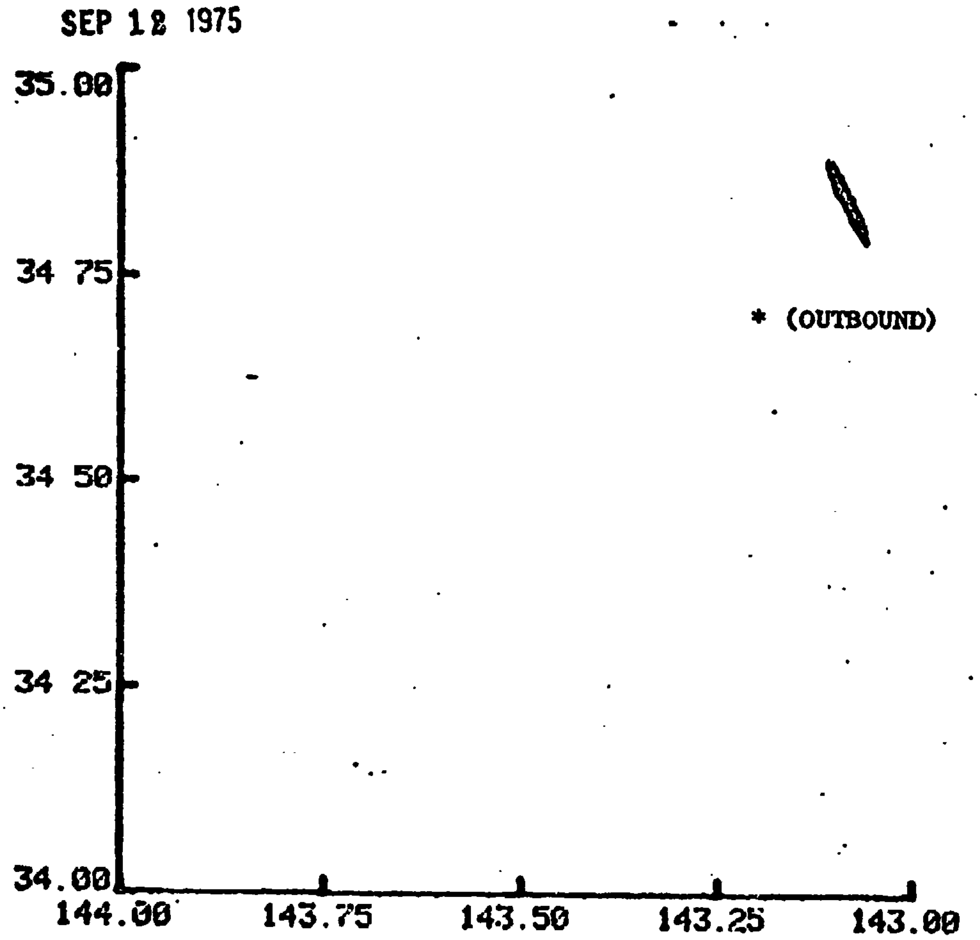

FILES 321 325 TIME 22:38:00 22:42:00 .07 HOURS 34.82 143.07
SPEED RANGE -13.3 -13.1 MIN SNR 11.6 34.89 143.11
* AVG SPEED= -13.2 SPEED FROM LSQ= -60.8
AVG SNR= 13.1 AVG RCS= 42.9 RCS S.D.M= -2.6 AVG SPEED

> 50%

Figure E.1-19

SEP 12 1975

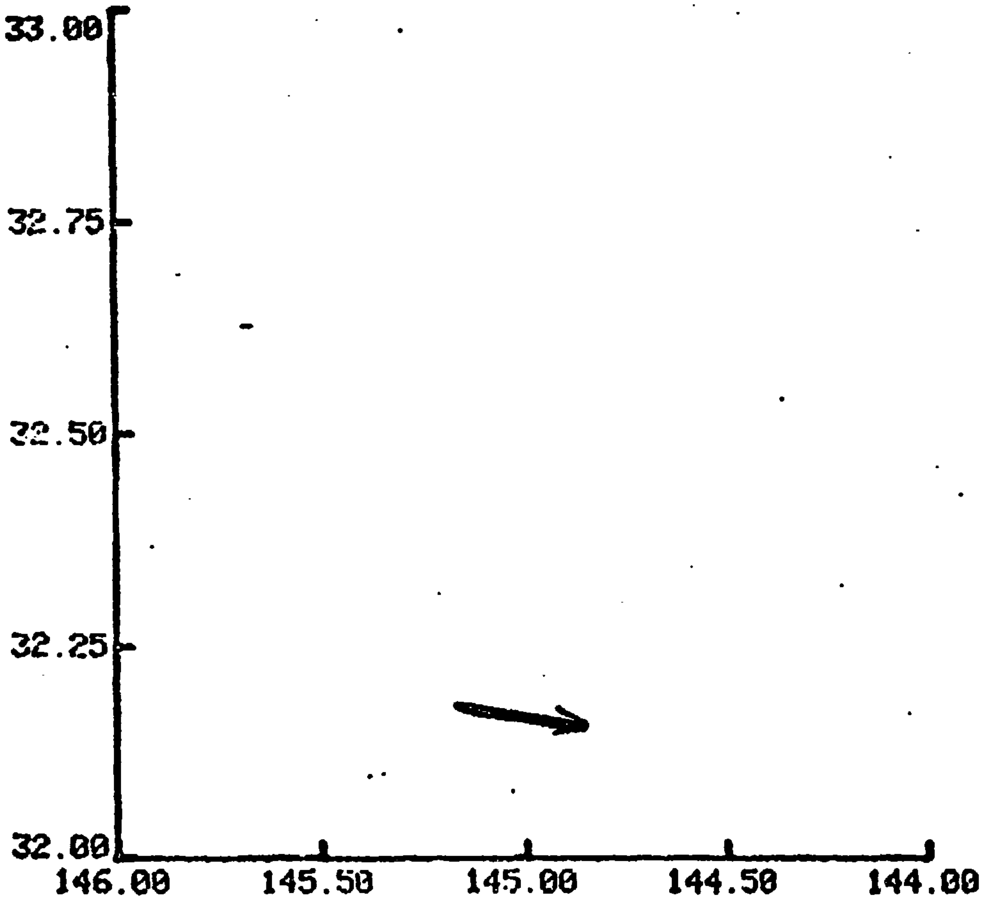

FILES 395 446 TIME 23:54:00 00:48:00 .90 HOURS 32.18 145.15
SPEED RANGE 14.1 15.7 MIN SNR 13.7 32.15 144.86
* AVG SPEED= 14.8 SPEED FROM LSQ= 32.6
AVG SNR= 19.3 AVG RCS= 38.0 RCS S.D.M= 1.6 AVG SPEED
SPEED FROM LAT/LON= 16.1 HEADING 90.0 DEGREES

> 90%

Figure E.1-20

SEP 13 1975

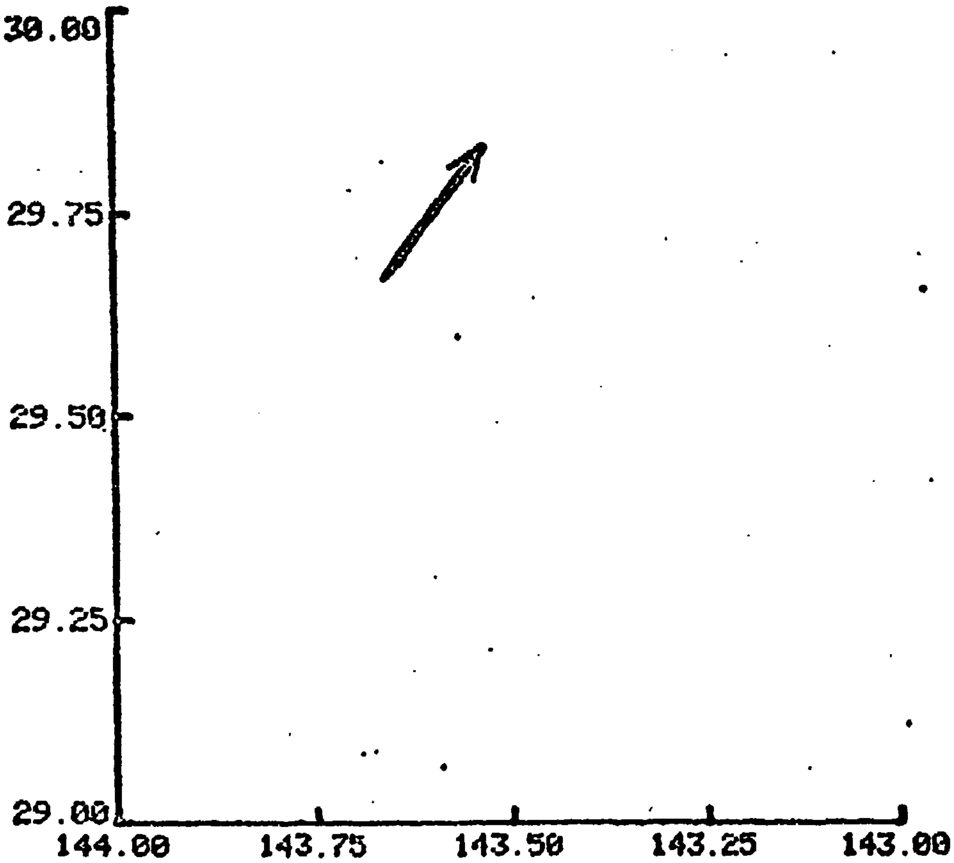

FILES 6 44 TIME 16:36:00 17:14:00 .63 HOURS 29.66 143.65
SPEED RANGE 14.9 15.1 MIN SNR 19.1 29.83 143.53
AVG SPEED= 15.0 SPEED FROM LSQ= 12.9
AVG SNR= 21.0 AVG RCS= 27.4 RCS S.D.M= -8.7 AVG SPEED
SPEED FROM LAT/LON= 17.5 HEADING 34.2 DEGREES

> 50%

Figure E.1-21-A

See 6-240

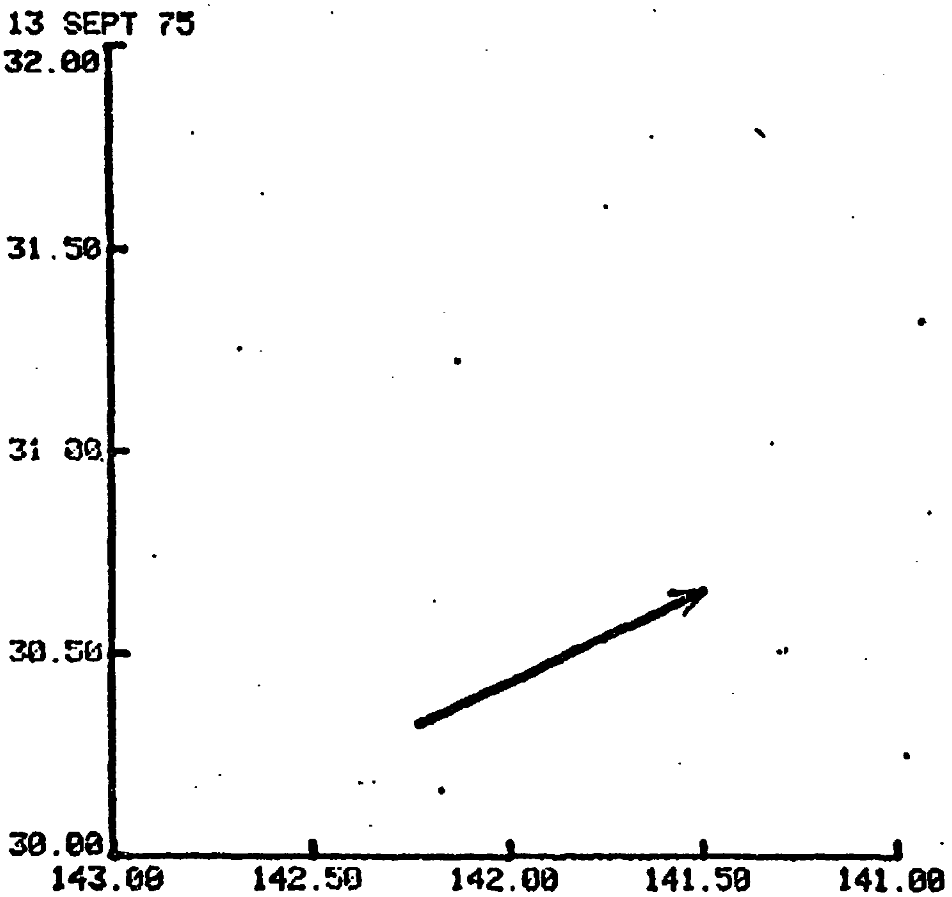

FILES 132 240 TIME 18:47:00 21:29:06 2.70 HOURS 30.33 142.23
SPEED RANGE 13.9 15.7 MIN SNR 12.9 30.66 141.50
AVG SPEED= 15.4 SPEED FROM LSQ= 14.9
AVG SNR= 22.1 AVG RCS= 36.5 RCS S.D.M= 2.8 AVG SPEED
SPEED FROM LAT/LON= 15.7 HEADING 62.2 DEGREES

> 90%

Figure E.1-21-B

See 6-240

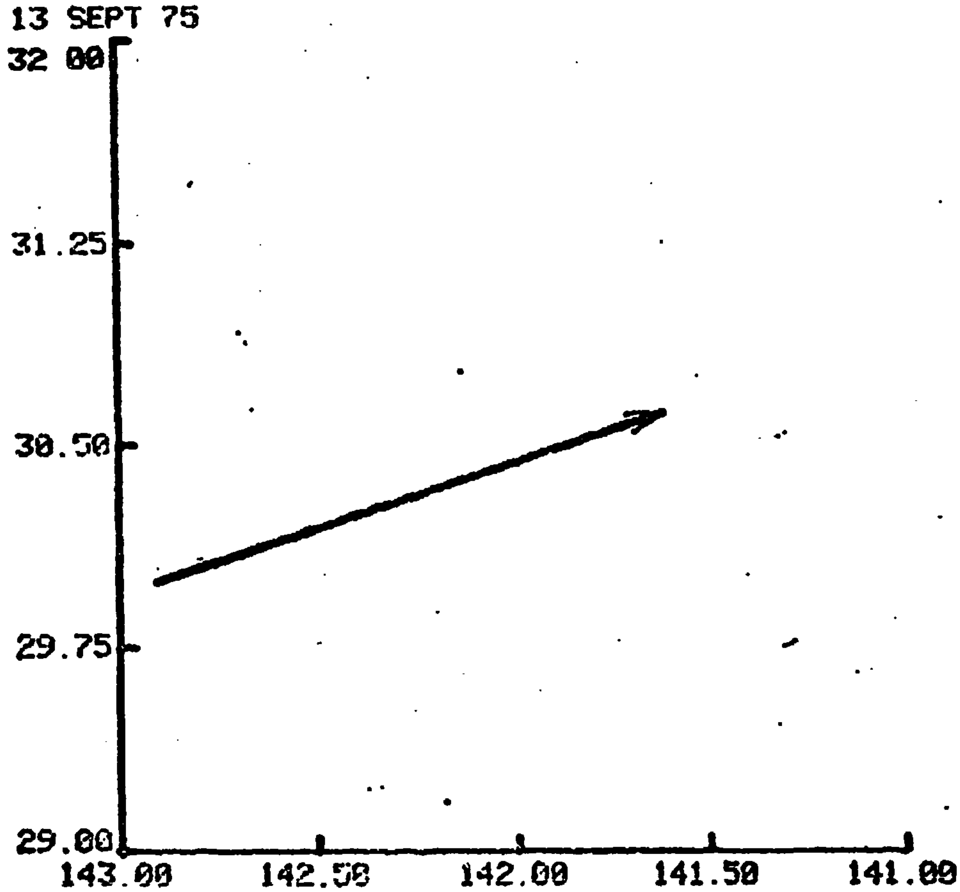

FILES 6 240 TIME 16:36:00 21:29:06 4.89 HOURS 30.00 142.90
SPEED RANGE 13.9 15.7 MIN SNR 12.9 30.62 141.62
AVG SPEED= 15.3 SPEED FROM LSQ= 17.4
AVG SNR= 22.0 AVG RCS= 36.0 RCS S.D.M= 3.0 AVG SPEED
SPEED FROM LAT/LON= 15.7 HEADING 60.2 DEGREES

> 90%

(Combination of last two)

Figure E.1-21-C 4+6

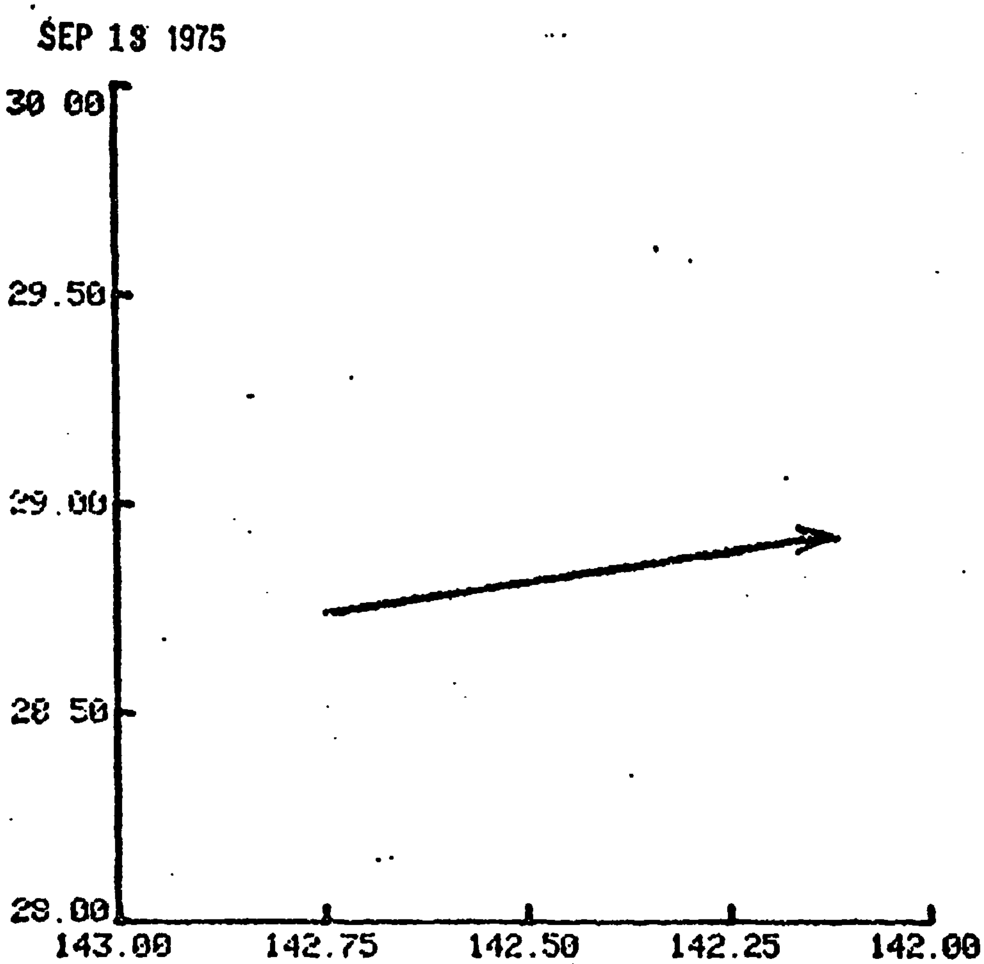

FILES 115 151 TIME 16:41:00 19:06:00 2.42 HOURS 28.74 142.75
SPEED RANGE 13.9 15.5 MIN SNR 13.0 28.93 142.12
AVG SPEED= 14.1 SPEED FROM LSQ= 10.4
AVG SNR= 18.5 AVG RCS= 35.6 RCS S.D.M= 1.4 AVG SPEED
SPEED FROM LAT/LON= 14.5 HEADING 71.1 DEGREES

> 90%

Figure E.1-22

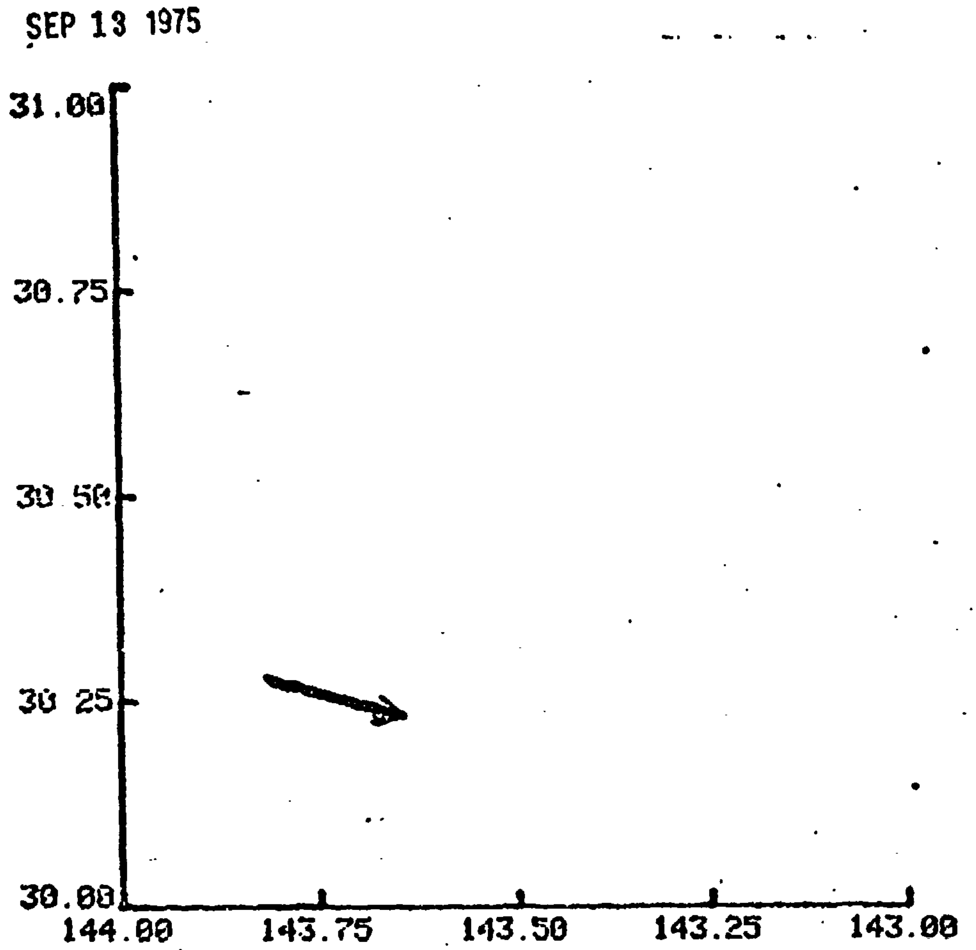

FILES 81 114 TIME 17:53:00 18:29:00 .60 HOURS 30.28 143.81
SPEED RANGE 9.7 12.0 MIN SNR 13.4 30.23 143.65
AVG SPEED= 10.9 SPEED FROM LSQ= 11.0
AVG SNR= 22.5 AVG RCS= 37.8 RCS S.D.M= 1.8 AVG SPEED
SPEED FROM LAT/LON= 14.6 HEADING 105.0 DEGREES

≥ 90%

Figure E.1-23

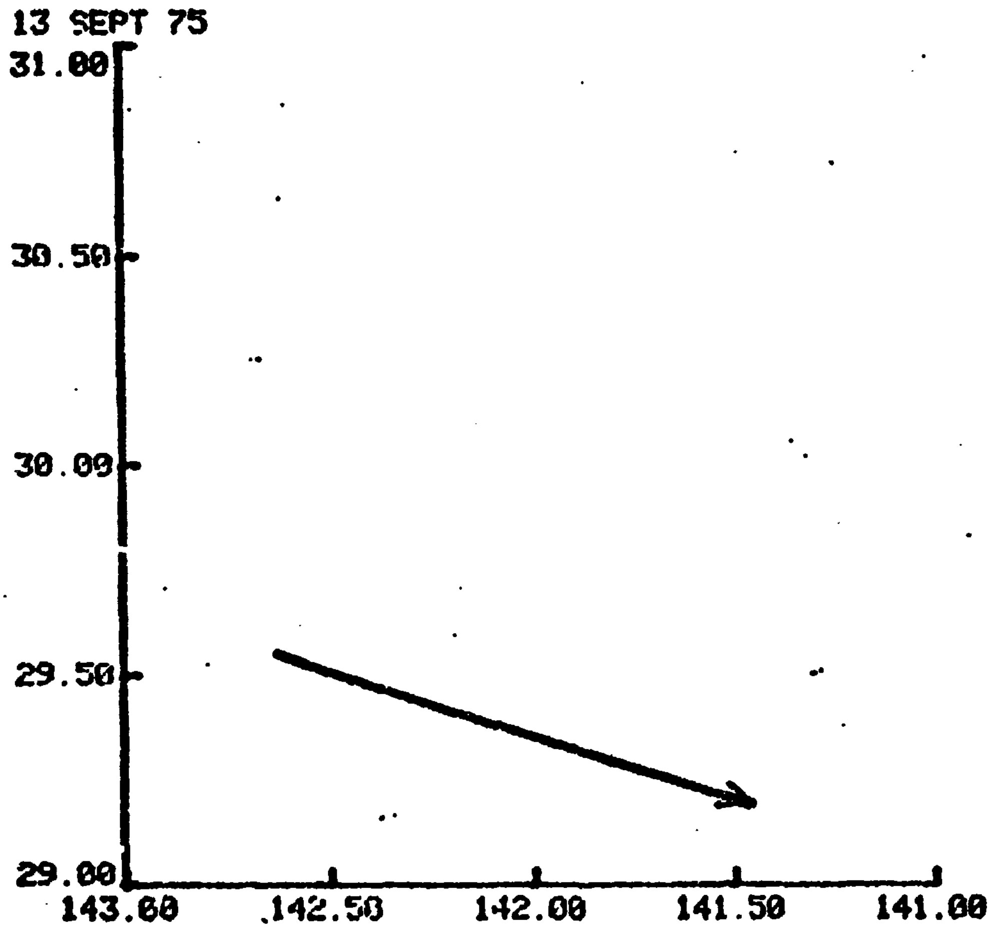

FILES 117 252 TIME 18:32:00 21:39:41 3.13 HOURS 29.55 142.63
SPEED RANGE 13.9 14.3 MIN SNR 14.2 29.20 141.46
AVG SPEED= 14.1 SPEED FROM LSQ= 14.2
AVG SNR= 14.7 AVG RCS= 32.7 RCS S.D.M= -.3 AVG SPEED
SPEED FROM LAT/LON= 20.8 HEADING 108.7 DEGREES

< 25%

Figure E.1-24

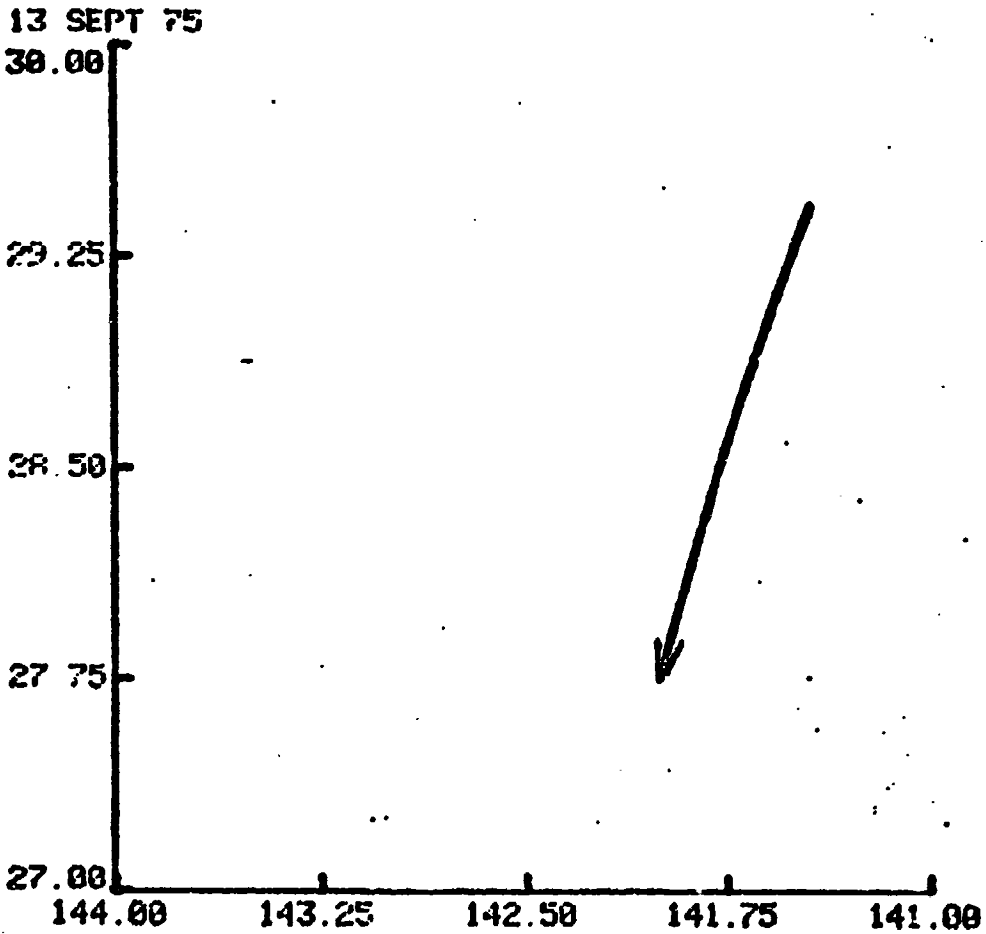

FILES 191 513 TIME 19:49:00 01:45:45 5.95 HOURS 29.43 141.44
SPEED RANGE -14.5 -11.7 MIN SNR 11.8 27.76 142.00
AVG SPEED= -12.4 SPEED FROM LSQ= -13 6
AVG SNR= 13.5 AVG RCS= 43.2 RCS S.D.M= -1.6 AVG SPEED
SPEED FROM LAT/LON= 17.7 HEADING 196.4 DEGREES

> 90%

Figure E.1-25

SEP-13-1975

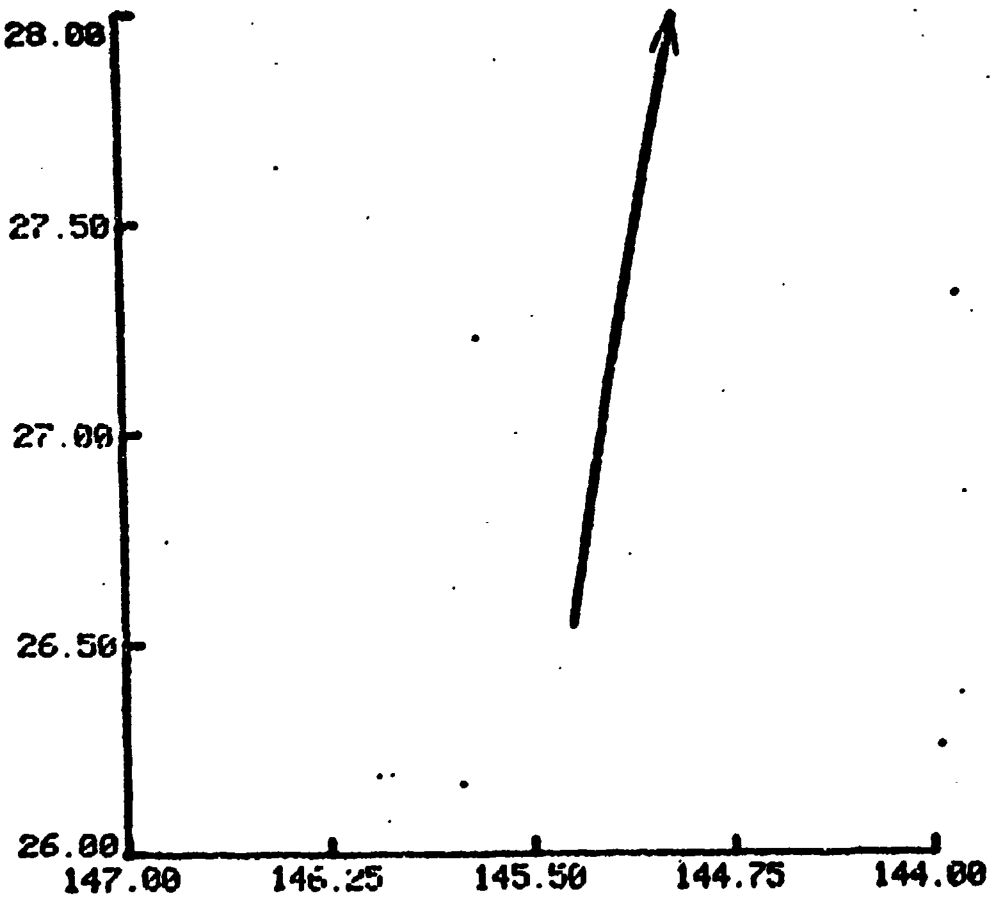

FILES 302 556 TIME 22:30:24 02:27:05 3.94 HOURS 26.56 145.34
SPEED RANGE 15.3 15.8 MIN SNR 13.6 28.00 144.94
AVG SPEED= 15.5 SPEED FROM LSQ= 24.4
AVG SNR= 15.9 AVG RCS= 32.1 RCS S.D.M= -.7 AVG SPEED
SPEED FROM LAT/LON= 22.7 HEADING 13.7 DEGREES

> 50%

Figure E.1-26

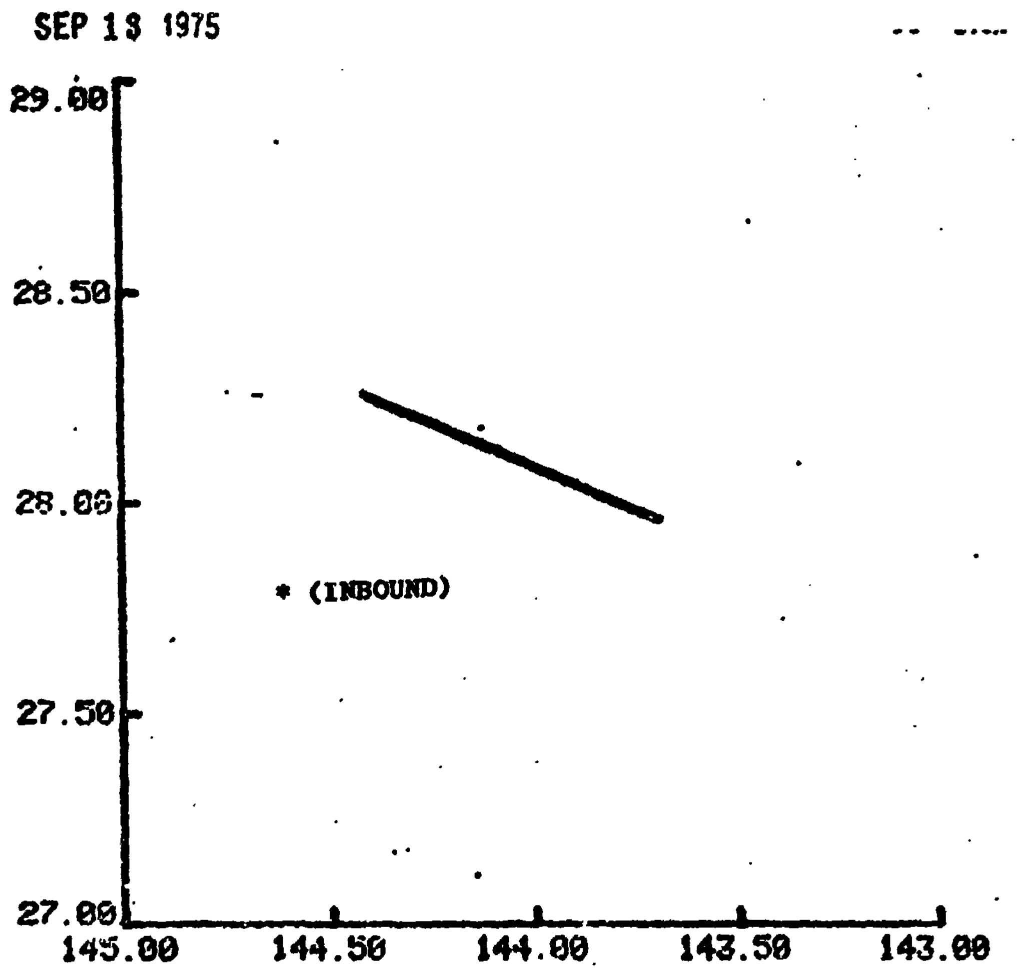

FILES 387 488 TIME 23:48:27 01:23:59 1.59 HOURS 28.26 144.43
SPEED RANGE 15.6 16.0 MIN SNR 13.4 27.96 143.70
* AVG SPEED= 15.8 SPEED FROM LSQ= 10.2
AVG SNR= 13.9 AVG RCS= 33.5 RCS S.D.M= -2.6 AVG SPEED

< 25%

Figure E.1-27

EP 13 1975

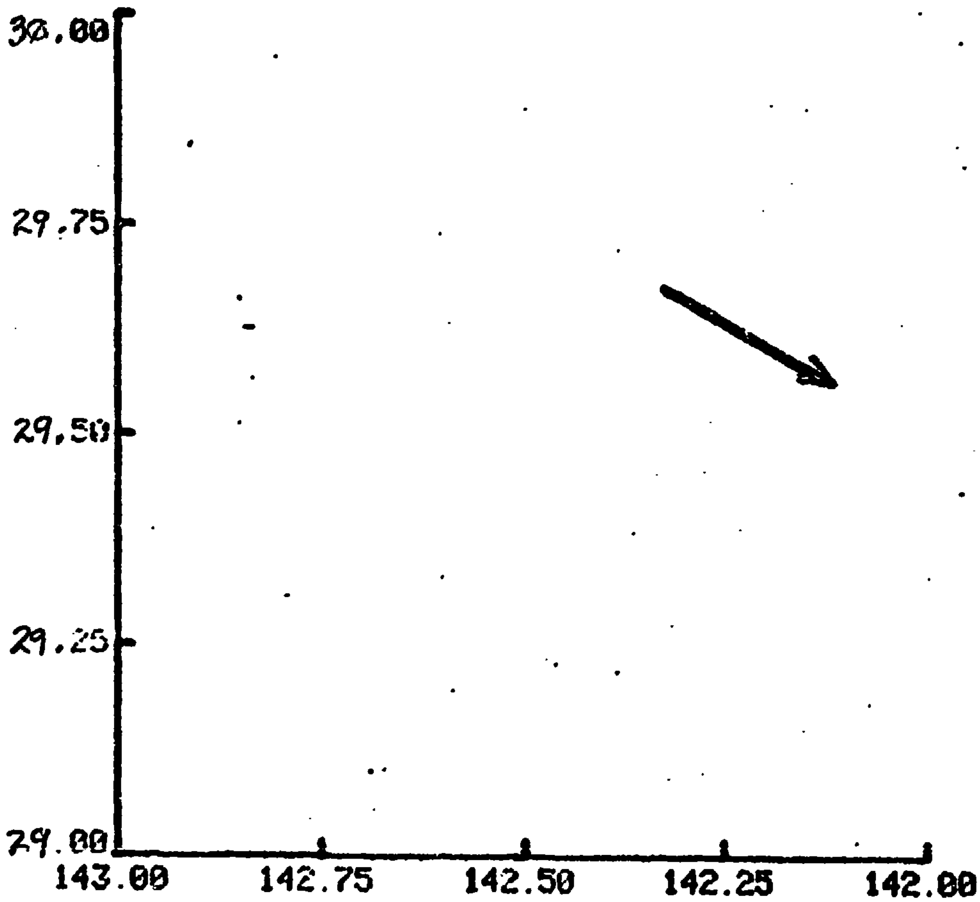

FILES 425 462 TIME 00:25:00 00:59:42 .58 HOURS 29.67 142.32
SPEED RANGE 10.0 11.7 MIN SNR 13.9 29.57 142.12
AVG SPEED= 11.1 SPEED FROM LSQ= 14.2
AVG SNR= 16.2 AVG RCS= 38.7 RCS S.D.M= -2.0 AVG SPEED
SPEED FROM LAT/LON= 21.2 HEADING 120.4 DEGREES

> 50%

Figure E.1-28

SEP 18 1975

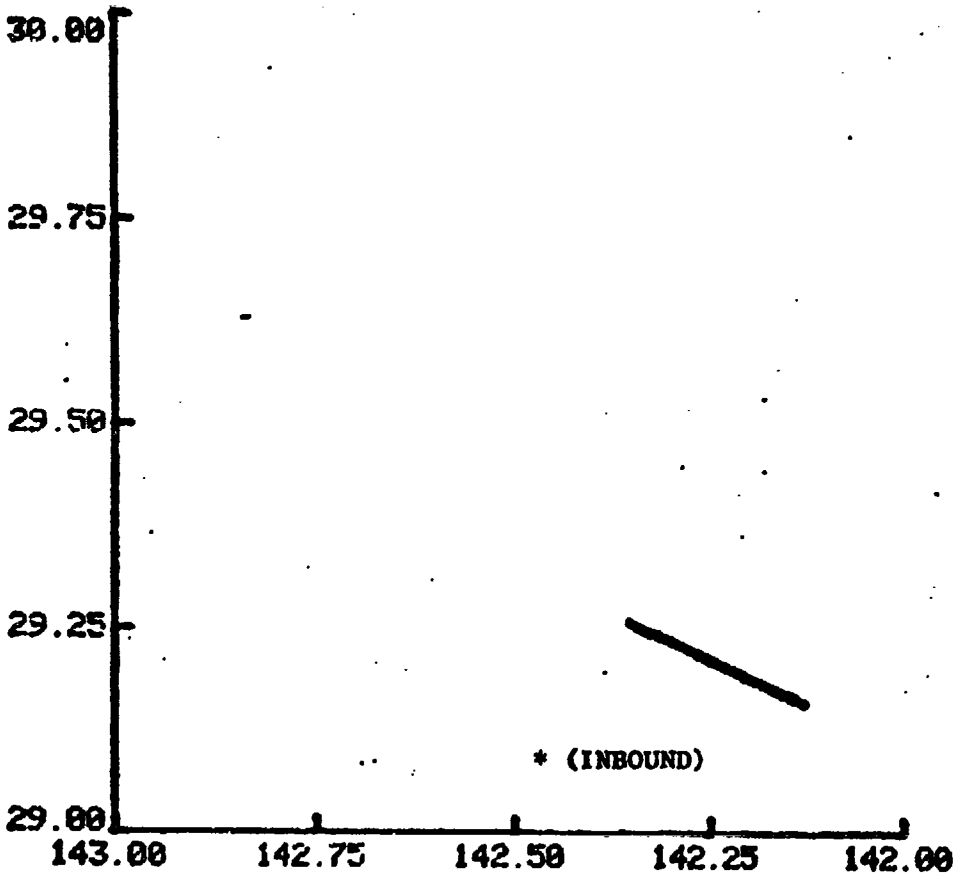

FILES 426 459 TIME 00:26:00 00:57:06 .52 HOURS 29.26 142.35
SPEED RANGE 14.4 14.6 MIN SNR 13.4 29.16 142.13
* AVG SPEED= 14.5 SPEED FROM LSQ= 15.6
AVG SNR= 13.6 AVG RCS= 35.4 RCS S.D.M= -2.6 AVG SPEED

< 25%

Figure E.1-29

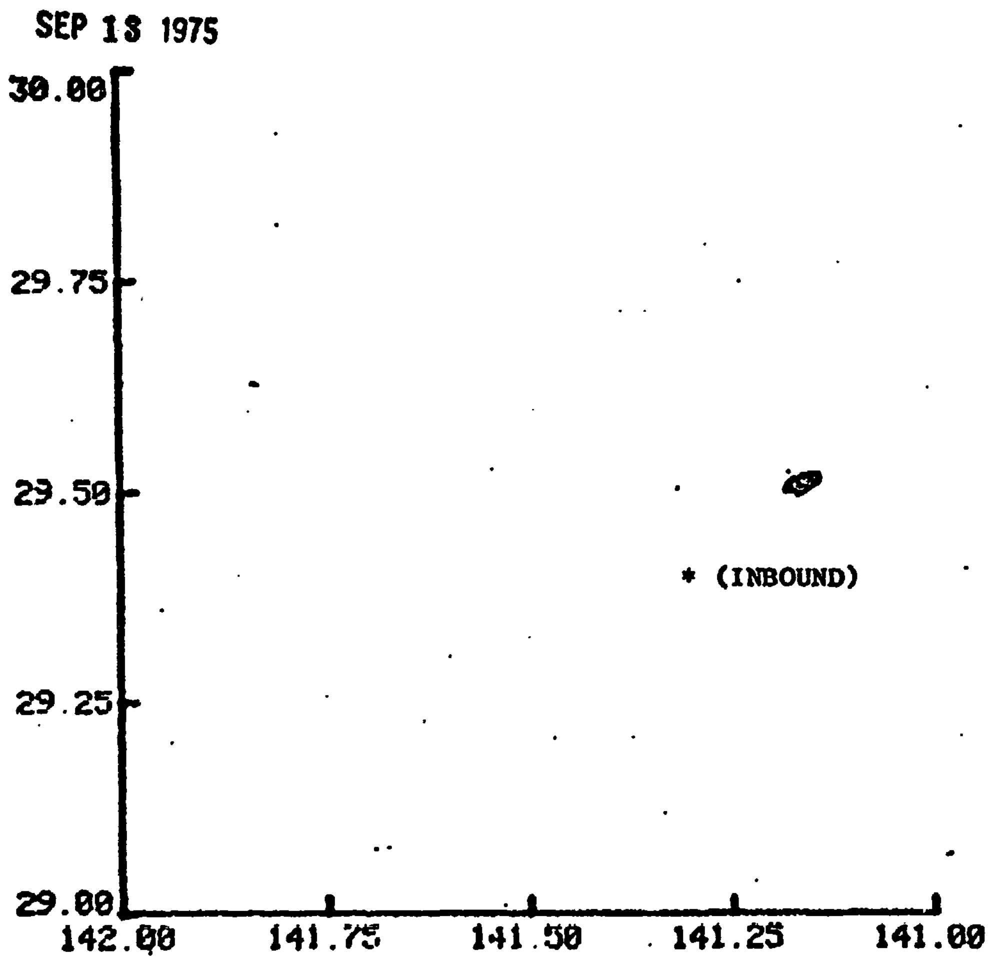

FILES 468 473 TIME 01:04:53 01:09:15 .07 HOURS 29.51 141.16
SPEED RANGE 14.4 14.6 MIN SNR 15.4 29.52 141.14
* AVG SPEED= 14.5 SPEED FROM LSQ= 210.5
AVG SNR= 19.3 AVG RCS= 37.0 RCS S.D.M= -3.0 AVG SPEED

< 25%

Figure E.1-30

SEP 14 1975

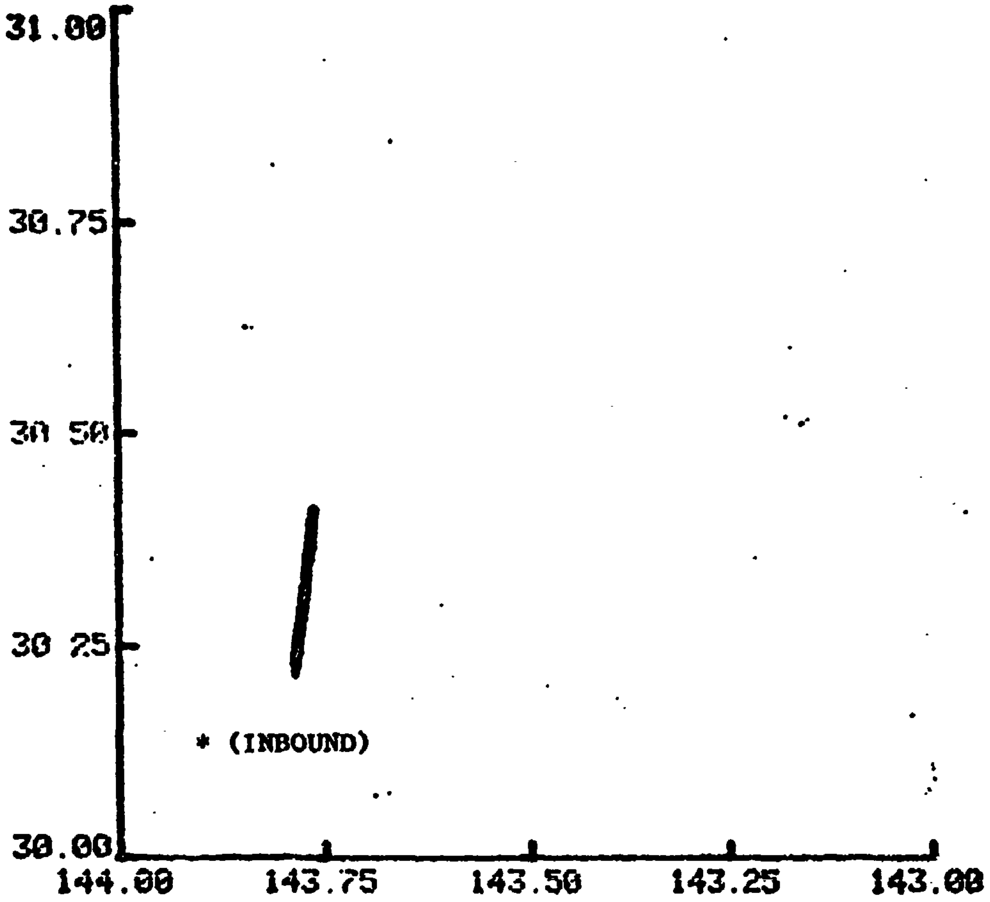

FILES .7 38 TIME 16:39:00 17:09:31 .51 HOURS 30.22 143.79
SPEED RANGE 9.7 12.7 MIN SNR 13.0 30.41 143.76
* AVG SPEED= 11.0 SPEED FROM LSQ= .6
AVG SNR= 15.6 AVG RCS= 40 3 RCS S.D.M= -1.1 AVG SPEED

1 to 3 ships in group

> 90%

Figure E.1-31-A (see 7-482)

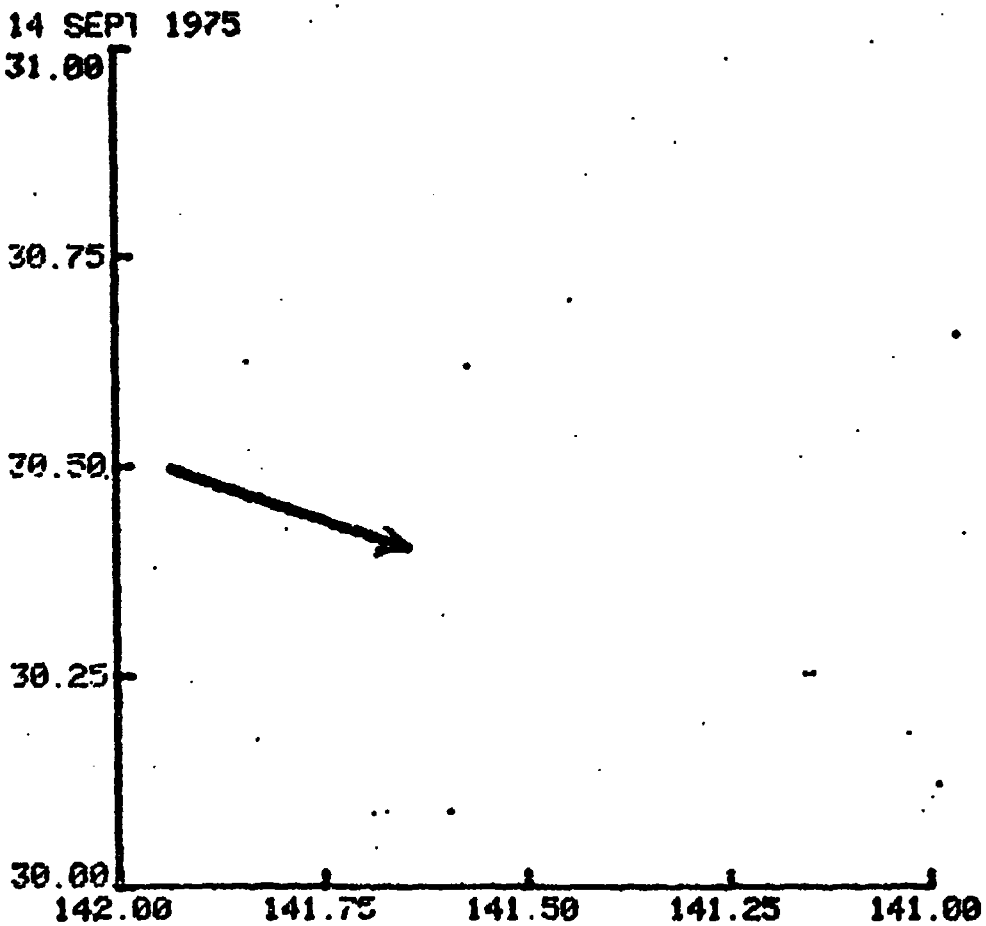

FILES 422 482 TIME 23:47:00 00:48:22 1.02 HOURS 30.50 141.93
SPEED RANGE 9.7 12.4 MIN SNR 13.6 30.40 141.65
AVG SPEED= 10.8 SPEED FROM LSQ= 21.4
AVG SNR= 19.5 AVG RCS= 36.8 RCS S.D.M= -.9 AVG SPEED
SPEED FROM LAT/LON= 15.5 HEADING 109.6 DEGREES

1 or 2 ships in group > 90%

Figure E.1-31-B

(see 7-482)

14 SEPT 1975

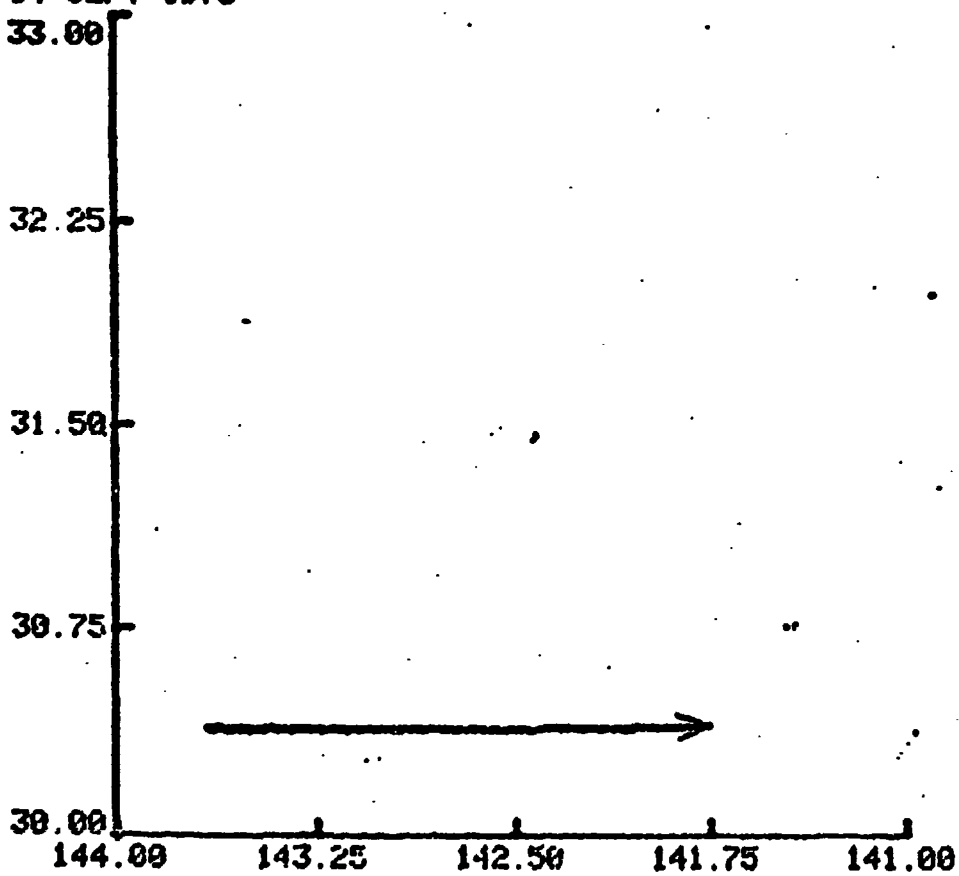

FILES 7 482 TIME 16:39:00 00:48:22 8.16 HOURS 30.39 143.65
SPEED RANGE 9.7 12.7 MIN SNR 13.7 30.40 141.76
AVG SPEED= 10.8 SPEED FROM LSQ= 11.2
AVG SNR= 18.5 AVG RCS= 38.3 RCS S.D.M= .0 AVG SPEED
SPEED FROM LAT/LON= 12.0 HEADING 90.0 DEGREES

1 to 3 ships in group > 90%

(combination of last 2 tra

Figure E.1-31-C

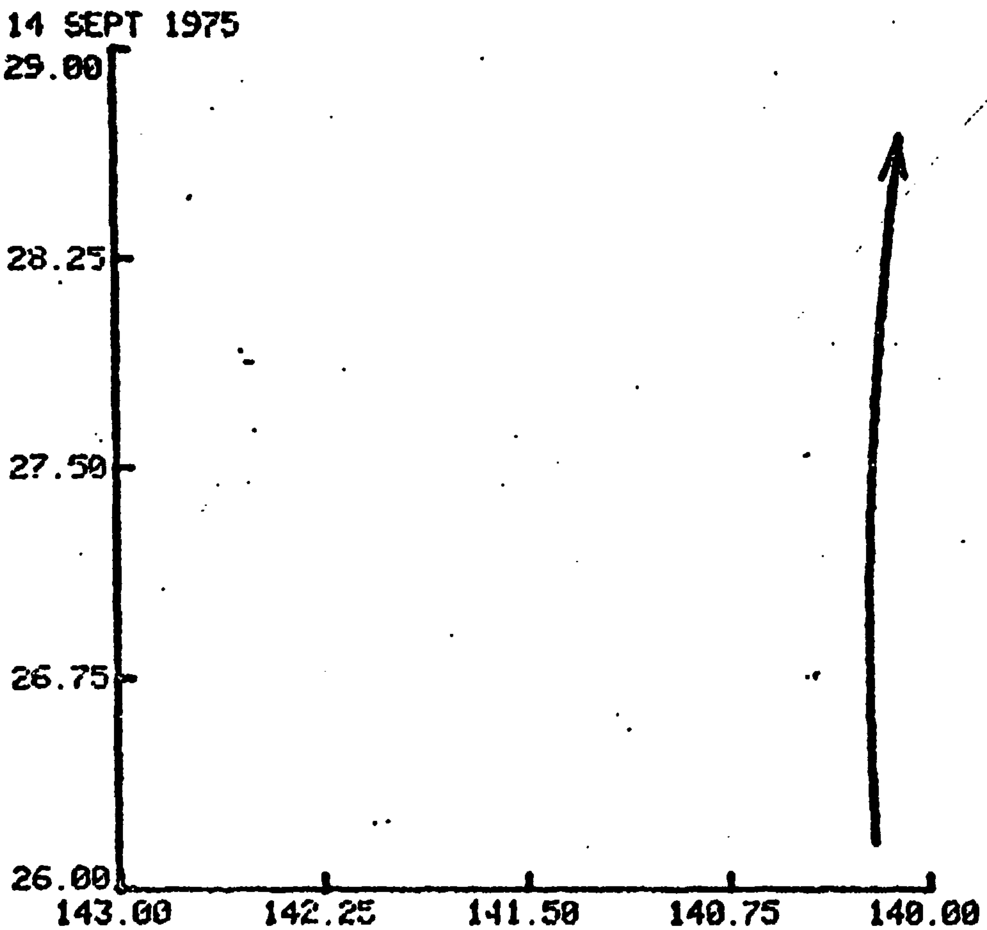

FILES 62 498 TIME 17:31:25 01:02:21 7.52 HOURS 26.18 140.20
SPEED RANGE 10.4 13.6 MIN SNR 13.3 28.68 140.10
AVG SPEED= 11.5 SPEED FROM LSQ= 10.9
AVG SNR= 15.4 AVG RCS= 35.3 RCS S.D.M= -2.1 AVG SPEED
SPEED FROM LAT/LON= 20.3 HEADING 2.0 DEGREES

> 50%

Figure E.1-32

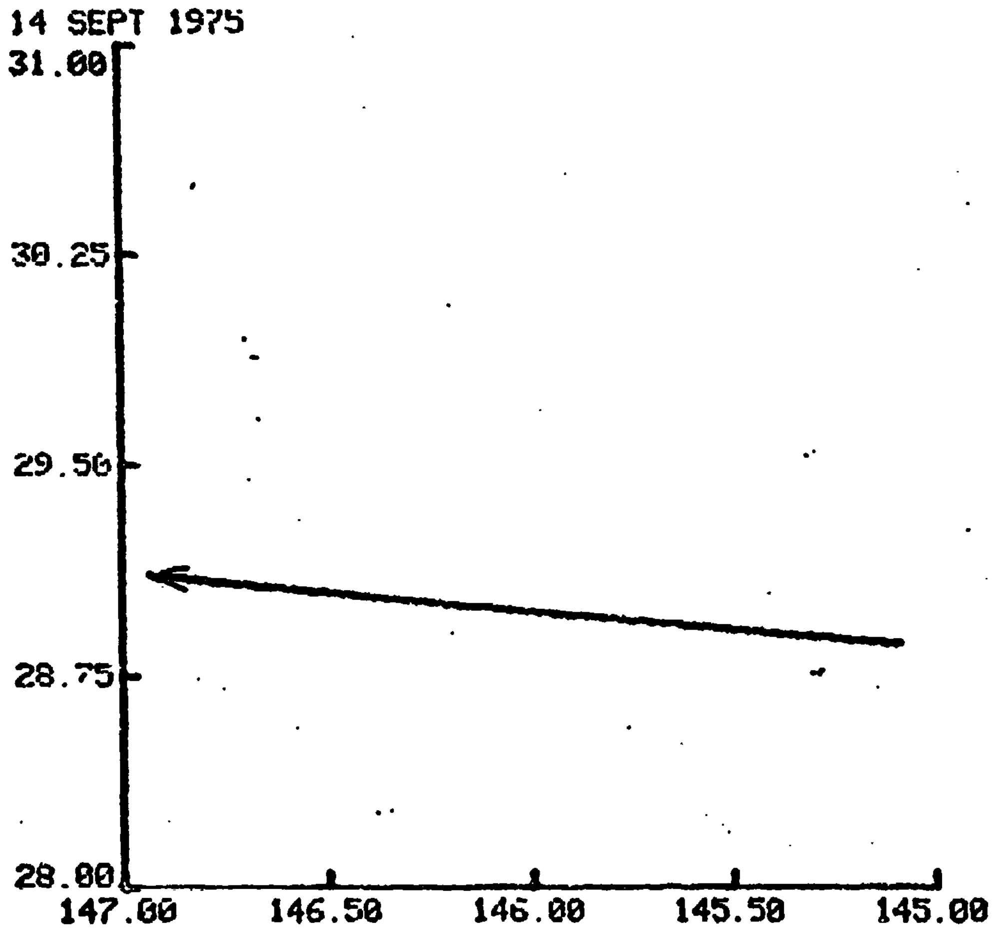


```
FILES  106  407 TIME 18:19:24  23:29:50   5.17 HOURS 28.87 145.09
SPEED RANGE  -17.5 -14.0 MIN SNR 12.3                29.11 146.93
AVG SPEED= -15.5  SPEED FROM LSQ= -12.0
AVG SNR= 15.5    AVG RCS= 34.9    RCS S.D.M=  1.7     AVG SPEED
SPEED FROM LAT/LON=  18.9 HEADING 279.0 DEGREES
```

> 90%

Figure E.1-33

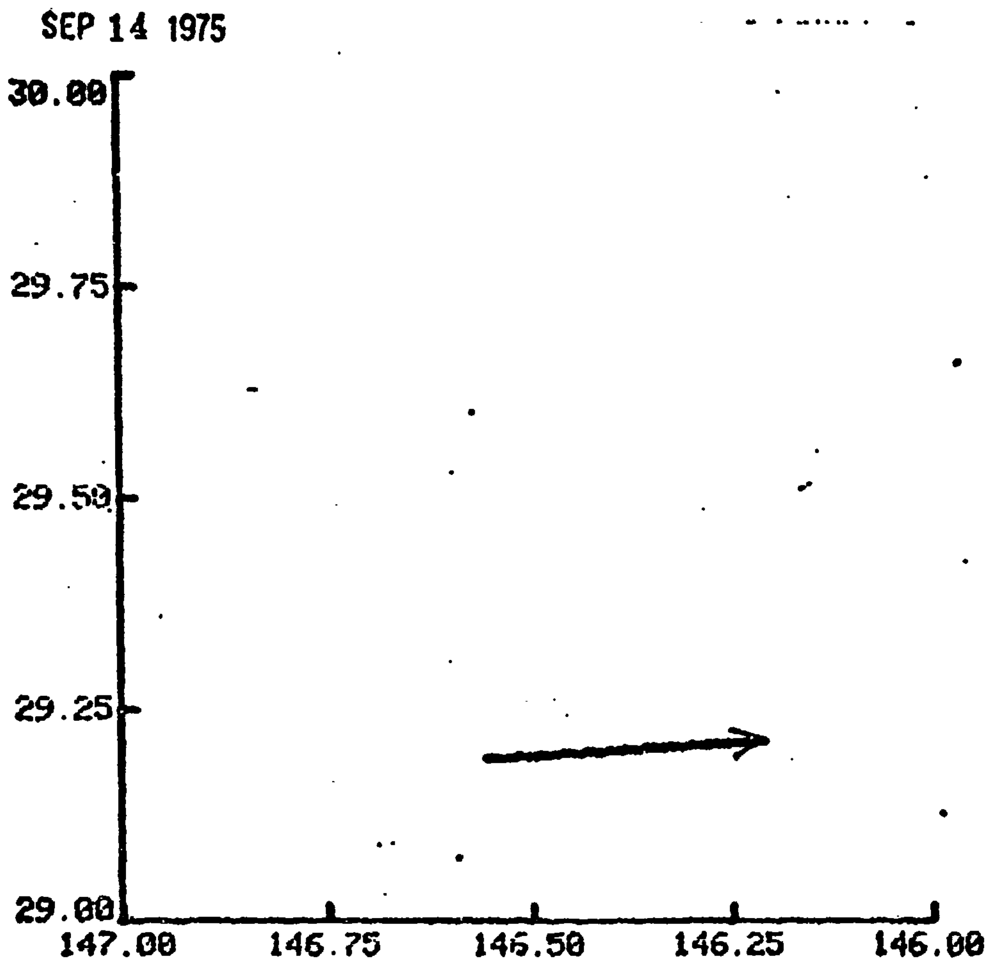

FILES 316 399 TIME 22:06:00 23:22:53 1.28 HOURS 29.19 146.55
SPEED RANGE 11.9 13.8 MIN SNR 12.0 29.21 146.21
AVG SPEED= 12.9 SPEED FROM LSQ= 16.2
AVG SNR= 13.0 AVG RCS= 24.5 RCS S.D.M= -.5 AVG SPEED
SPEED FROM LAT/LON= 14.0 HEADING 87.1 DEGREES

> 50%

Figure E.1-34

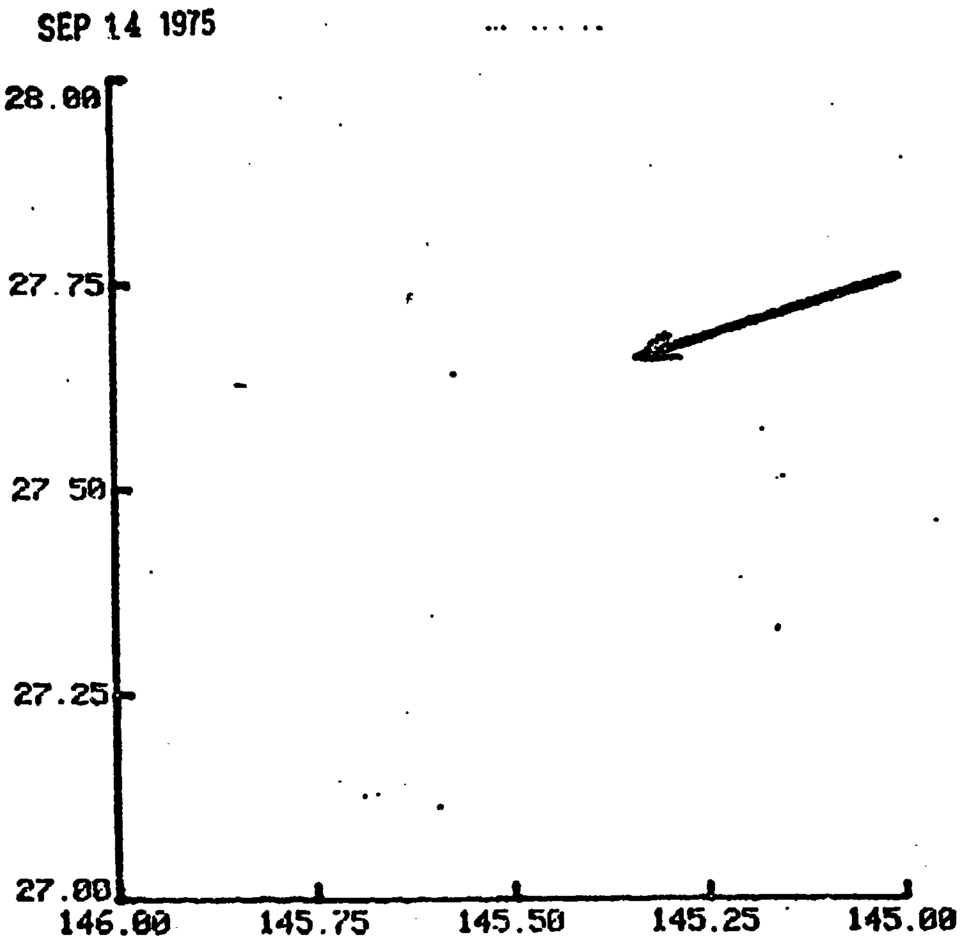

FILES 321 387 TIME 22:11:00 23:12:30 1.02 HOURS 27.76 145.01
SPEED RANGE -17.5 -16.0 MIN SNR 12.6 27.66 145.33
AVG SPEED= -17.1 SPEED FROM LSQ= -8 2
AVG SNR= 18.5 AVG RCS= 32.4 RCS S.D.M= -.6 AVG SPEED
SPEED FROM LAT/LON= 17.6 HEADING 251.7 DEGREES

> 90%

Figure E.1-35

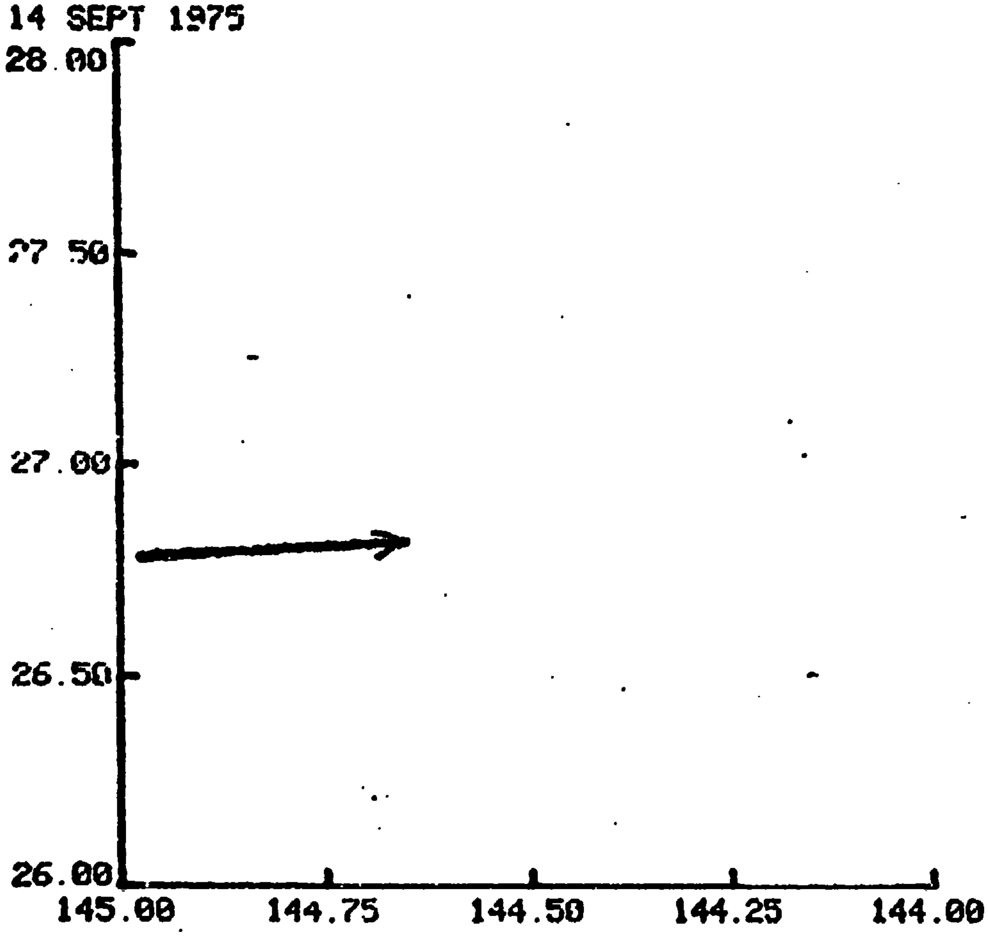

FILES 322 371 TIME 22:12:00 22:58:22 .77 HOURS 26.78 144.97
SPEED RANGE 19.2 20.7 MIN SNR 15.0 26.82 144.66
AVG SPEED= 20.1 SPEED FROM LSQ= 23.8
AVG SNR= 25.6 AVG RCS= 34.2 RCS S.D.M= .7 AVG SPEED
SPEED FROM LAT/LON= 22.2 HEADING 37 2 DEGREES

> 90%

Figure E.1-36

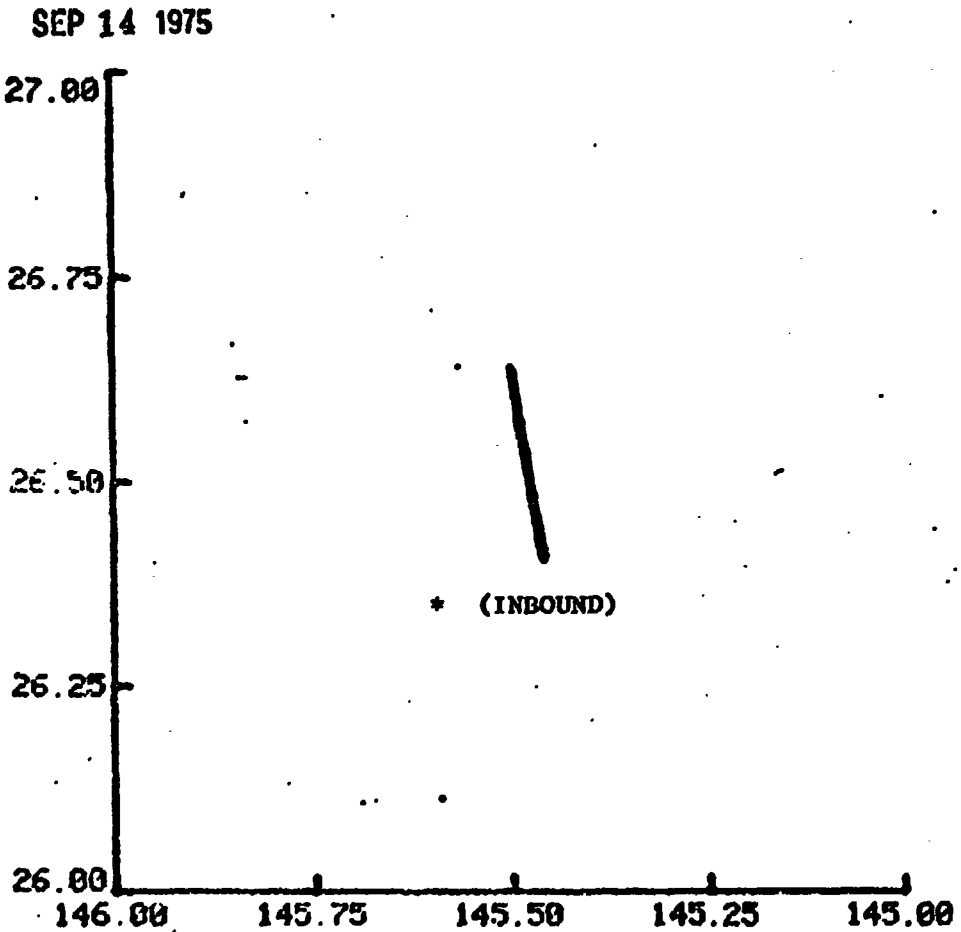


```
 FILES   323   352 TIME 22:13:00  22:40:28     .46 HOURS 26.41 145.46
 SPEED RANGE    11.3  11.5 MIN SNR 13.2                  26.64 145.50
*AVG SPEED=   11.4  SPEED FROM LSQ=   8.7
 AVG SNR=     14.2 AVG RCS=    36.3 RCS S.D.M=    -1.2 AVG SPEED
```

< 25%

Figure E.1-37

APPENDIX E.2

APPENDIX E.2

OTH RADAR SHIP-DISTRIBUTION MEASUREMENTS: SEPTEMBER 1975

1. (U) INTRODUCTION (U)

(U) Surface shipping surveillance tests were conducted with the SEA ECHO over-the-horizon (OTH) radar at San Clement Island during the period from September 20-24, 1975, for a project sponsored by the Office of Naval Research. The survey was made by daily scans of specified areas in the Gulf of Alaska with the objective of defining shipping density distributions in support of analyses being conducted by Planning Systems Incorporated of McLean, Virginia. This report gives the results of this investigation together with a description and some discussion of the experimental parameters.

2. (C) TASK OBJECTIVES (U)

(C) The objective of the OTH surveillance tests was to provide information on the density distribution of surface shipping in a specified area and for specified times for comparison and use in theoretical models for ship distribution. More specifically the scope of this specific work was categorized as a test of the capability of OTH radar systems to provide ship surveillance data of adequate utility for such comparison. The test requirements called for a daily snapshot of specified 5° x 5° (lat.-long.) areas to be performed with a spatial resolution which should be adequate for a reasonable detail of target distribution within this area, and an exposure time was to be consistent with a reasonable freezing of 15 kt ship motion. These objectives were achieved.

3. (C) TEST DETAILS (U)

(C) Two test areas were specified, namely a region bounded by 140° and 145°W and by 45° and 50°N, and a second region bounded by 140° and 145°W and by 50° and 55°N. The first of these, Area 1, was specified for surveillance on September 22 and 23, and the second, Area 2, on September 20, 21 and 24. By agreement with PSI, the daily time of each surveillance — for this initial exercise — was to be determined at the SEA ECHO site on a criterion of best-ionospheric propagation conditions. Accordingly the surveillance scans were conducted generally at mid-day. Data were taken for the specified areas on September 21, 22 and 24.

(U) System difficulties prohibited useful measurements on September 20 and 23. Two scans are presented for different times, however, on September 21.

(U) The SEA ECHO radar was set up for the maximum spatial resolution (smallest cell size) for maximum signal-to-clutter ratio. The cell size used was a nominal 2° in beam width and 15 km (8.09 nm) in range. The data is reported on the basis of this resolution. (Note: In the accompanying graphical representations, for convenience in plotting the range-wise grid size is shown in steps of 10 nm.) In presenting the data, each target is shown in the center of each resolution cell. However, no further resolution can be assigned than the presence of a target in a cell. (Identification of more than one target per cell is readily possible if their doppler signatures differ, however.)

(U) In a scan of a given area, 20 consecutive range cells were interrogated simultaneously in successive azimuthal beam positions. The system was then reset for the second (more distant) set of 20 range cells and again sequenced at these ranges through the successive six beams. Each 20-cell, six-beam scan required about 10 minutes. Re-set to the new ranges also required about 10 minutes. Therefore an entire scan was accomplished in 30 minutes.

(C) Since the radar spatial resolution cell size is much larger than that of individual ships (both in physical and radar cross-section), doppler - or velocity - processing must be invoked to discriminate the targets of interest from the sea return (clutter). For these tests, the SEA ECHO processor was arranged to acquire at each beam position for approximately 25 seconds producing a 256 point Fourier transform for each resolution cell in that beam before sequencing to the next beam. The sum of four such transforms, taken at intervals of the beam revisit time, were averaged and presented on a CRT for display. Each display presented spectral plots of radar cross-section vs. doppler frequency (target velocity) for ten consecutive range cells. Each display was photographed, and the resulting Polaroid print was used in a visual examination for the presence of ship targets All data acquired in these tests were digitally recorded in a f. mat which is suitable for more sophisticated machine processing for discrimination and detection of targets. While such processing is beyond the scope of the tasks defined in this preliminary work, it is recommended. Details of this and the data parameters are discussed in a later section of this report.

4. (S) RESULTS (U)

(U) Results are displayed in the attached charts each of which is identified by area, date and time. These charts are to scale. Latitude and longitude in truee coordinates are given in a 1 x 1° grid. Radar coordinates are given in nautical miles and true bearings from the SEA ECHO site. The radar azimuthal grid is given in a 2° resolution corresponding to the half-power points of the radiated beams — i.e., each beam lies within adjacent labeled grid lines.

(S) Each target identified is shown by an arrow whose direction indicates whether the velocity vector was generally away from or toward the radar. Further, a discrimination is shown between targets whose radar cross section is estimated to be either greater or less than $10,000M^2$, i.e., 40 dB greater than on square meter (40 dBsm). A double-line arrow indicates a radar cross section which is greater than 40 dBsm and one with a single line, a target smaller than 40 dBsm. (For reference, the cross-section of a large U.S. Navy destroyer is approximately 33 dBsm at HF wave lengths.)

5. (S) DISCUSSION (U)

(C) A large ship (i.e., larger than a destroyer but smaller than an aircraft carrier) can be generally categorized in the 10,000 square meter HF radar cross section range.

(S) The competing signal return from the minimum radar resolution cell (at a range of 1500 nm) is of the order of $1.4 \times 10^9 M^2$. Doppler processing is utilized to extract targets of interest from this significantly larger clutter. The following details are pertinent.

(S) The spectra produced by the doppler processing represent a continuous set of values of radar cross-section as a function of doppler frequency (target velocity). The SEA ECHO display has been implemented to show both receding and approaching doppler. (Thus processed, clutter return from the sea always appears as two spectral lines symetrically disposed about zero doppler frequency. These lines represent sea waves receding and approaching the radar. Because of spatial ("Bragg") resonance, the waves producing these spectral lines are those components whose wave length is exactly half of the electromagnetic wave length corresponding to the frequency selected for the radar operation.) Furthermore, because of the dispersion relation between ocean wave lengths and their felocity, the doppler frequency (velocity) produced by these waves are exactly determined. For example, at the (approximate) SEA ECHO frequency of 16.0 MHZ used in these tests the sea resonant spectral (Braff) lines peak at ±0.41 Hz, representing a radial velocity of ±7.44 kts. Hard targets such as ships, whose radial velocity is at or near this value, will be masked by the effects of clutter, particularly in the case of the dominant Braff line, i.e., the one which is being produced by the wind-driven sea which produces resultingly high cross-section.

(C) Choice of operation with two or more simultaneous radar frequencies (a process which is uniquely possible with the SEA ECHO system) will produce target spectra in which the Bragg lines are shifted <u>relative</u> to the doppler produced by a hard target. Use of this technique, while straightforward, requires some operationally subtle strategies not invoked in the limited scope of these initial tests. (Braff line widths are determined in part by the Fourier data integration period, and this in turn must be chosen with carc lest doppler smearing is introduced by movement of or multi-path effects in theionosphere.) In short, in the somewhat simplified data processing used here, $10^4 M^2$ (and somewhat smaller) targets are detectable in the prosence of clutter if their doppler signatures (radial velocities) are sufficiently different from the clutter doppler.

(U) In the data presented here, analysis criteria (necessarily somewhat subjective) were used which opted for a minimization of false alrams, hence toward a reduced probability of detection.

(S) The following characteristics represent thresholds either of which, in the analysis used, would have obscured a target.

1. Radar cross section less than 30 dBsm (1000 M^2).
2. A radial velocity component of less than approximately 13 kts. (The doppler spectrum between the Bragg lines does provide a window for low velocity targets of something more than minimal cross section, but this spectral region was discounted in these data.)

6. (C) TARGET CROSS SECTION (U)

(C) Estimation of the radar cross section values for targets plotted in the charts was performed by comparison with the principal clutter Bragg line. Given the condition that at least one Bragg line was produced by a fully-arisen sea, the albedo (σ° in radar parlance) for those waves has been shown to be a fixed value of -17 dB. Since the resolution cell area is known, the sea thus provides a built-in calibration. The requirement for the fully arisen sea applies only to the wave lengths selected by the radar frequency. That is, for the September 20-24 period, full sea saturation would have called for a wind component of 7.4 kts in a radial direction for a few hours. To the degree that this was not the case, the (absolute) value for σ° would be greater than 17 dB, and target cross-section should be estimated as proportionately higher.

7. (C) RECOMMENDATIONS (U)

(C) Based on the results achieved in the tests described in the foregoing, NRL recommends two further approaches to the ONR ship-density surveillance task.

1. Re-examination of the September 21-24 data using machine processing.

   All data were recorded in such digital format that complete flexibility in reprocessing the data can be accomplished — i.e., in terms of Fourier integration lengths and averaging. Since a characteristic of ionospheric propagation is a time-dependent Faraday rotation of the EM plane of polarization, fading of target signals arises as a result of target cross-section changes with polarization. (This is particularly true for small craft whose mast-head height is critical to cross section.) The four-integral 100 sec. average time selected a priori for the tests is somewhat in excess of the facing period. It is proposed that the individual 25 sec. spectra be separately displayed and examined for target appearance on a shorter-time but enhanced signature basis.

   Further, the 25-second integration period was selected on a synoptic understanding of ionospheric time-dependence. It is proposed that the data be reprocessed for a higher doppler resolution with the objective of increasing the velocity range of detectable targets.

   On the assumption that for the areas surveyed there are targets of 30 dBsm or greater cross-section broadly distributed in velocity from 5 to 25 kts along a general great circle trans-Pacific route to the Far East, the refinement of the above analysis techniques for September

1975 could increase detected targets by an amount of the order of 30%.

2. It is also proposed that further surveys of the north Pacific shipping densities be conducted with the following optimizing changes in procedure:

With due recognition that the surveillance areas specified for September 1975 were selected in consonance with other related activities, it should be noted that the resulting radar gound range of 1200 to 1700 nm presents the maximum difficulty to the SEA ECHO system (and OTH radars in general) in terms of clean ionospheric propagation. While our results show that ship detection is not prohibited at these ranges, it is suggested that considerable benefits could accrue to a correlation of theoretical prediction and direct measurement if investigations were made at ranges of the order of 700 to 1200 nm. The reasons for this are beyond the scope of this report but generally have to do with the more or less unique layers of the ionosphere associated with propagation to specific ground ranges. SEA ECHO is unique in an antenna design which capitalizes on the use of the lower layers of the ionosphere — with resulting freedom from the interfering effects of multiple propagation paths. This capability was confirmed in fact by a test survey measurement made on September 24 at ranges of the order of 800 nm in which E-layer propagation produced extremely clean, narrow clutter spectra.

It is further proposed that such measurements be performed using multiple radar frequencies to provide redundant looks at each range cell with separated Bragg clutter lines.

Thirdly, by performing area scans in a regular and continued time sequence, e.g., at a rate of one per hour for several hours, it will be possible to apply track correlation techniques. By associating successive target hits in progressively adjacent range and/or azimuthal cells with the intrinsic doppler velocity information, target absolute velocity vectors can be established. Furthermore, target track techniques can greatly improve the ratio of probability of detection to probability of false alarm.

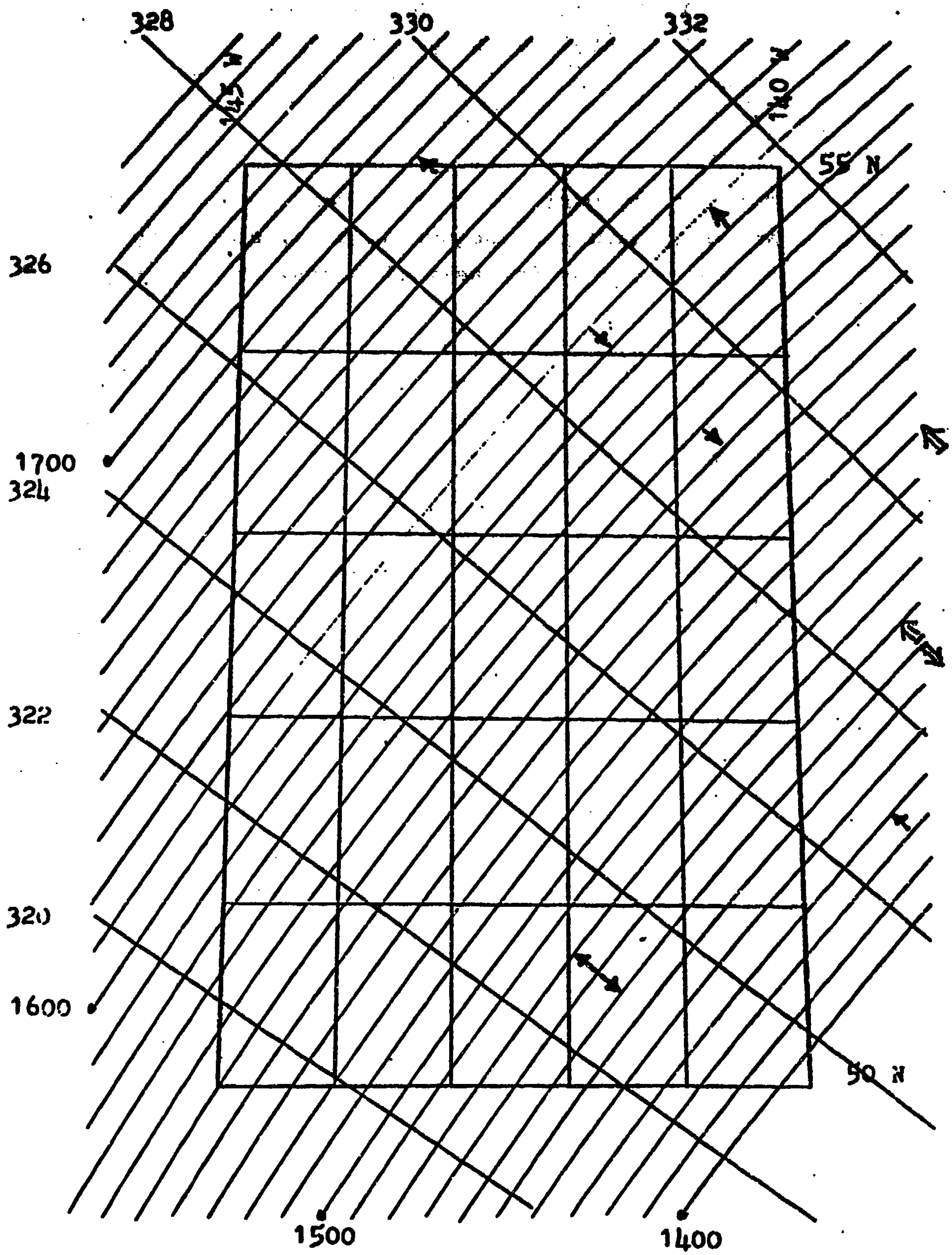

AREA 2

9/21/75 1700 - 1730 Z

FIGURE E.2-1

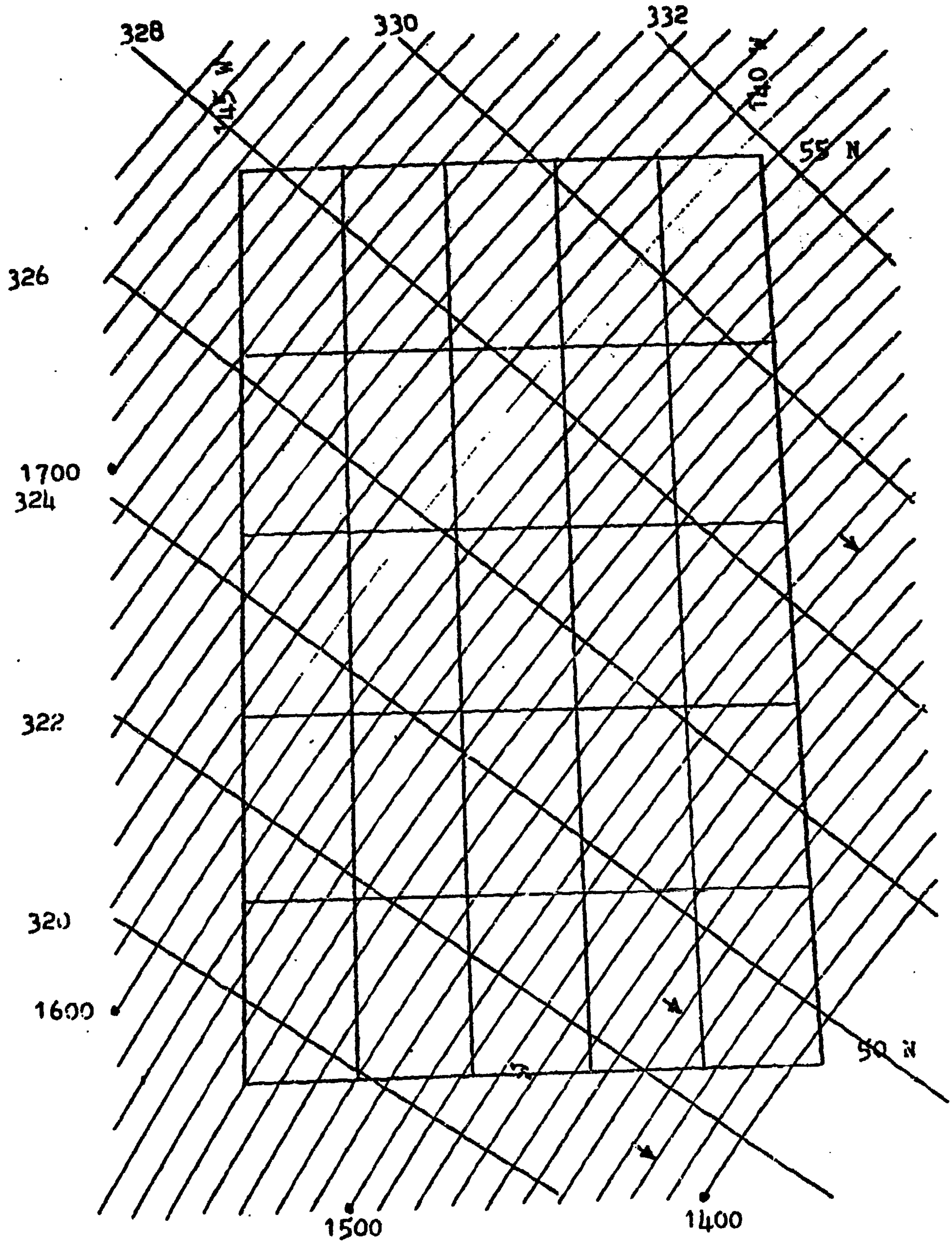

AREA 2

9/21/75 2100 - 2130 Z

FIGURE E.2-2

SECRET

(This page is unclassified)

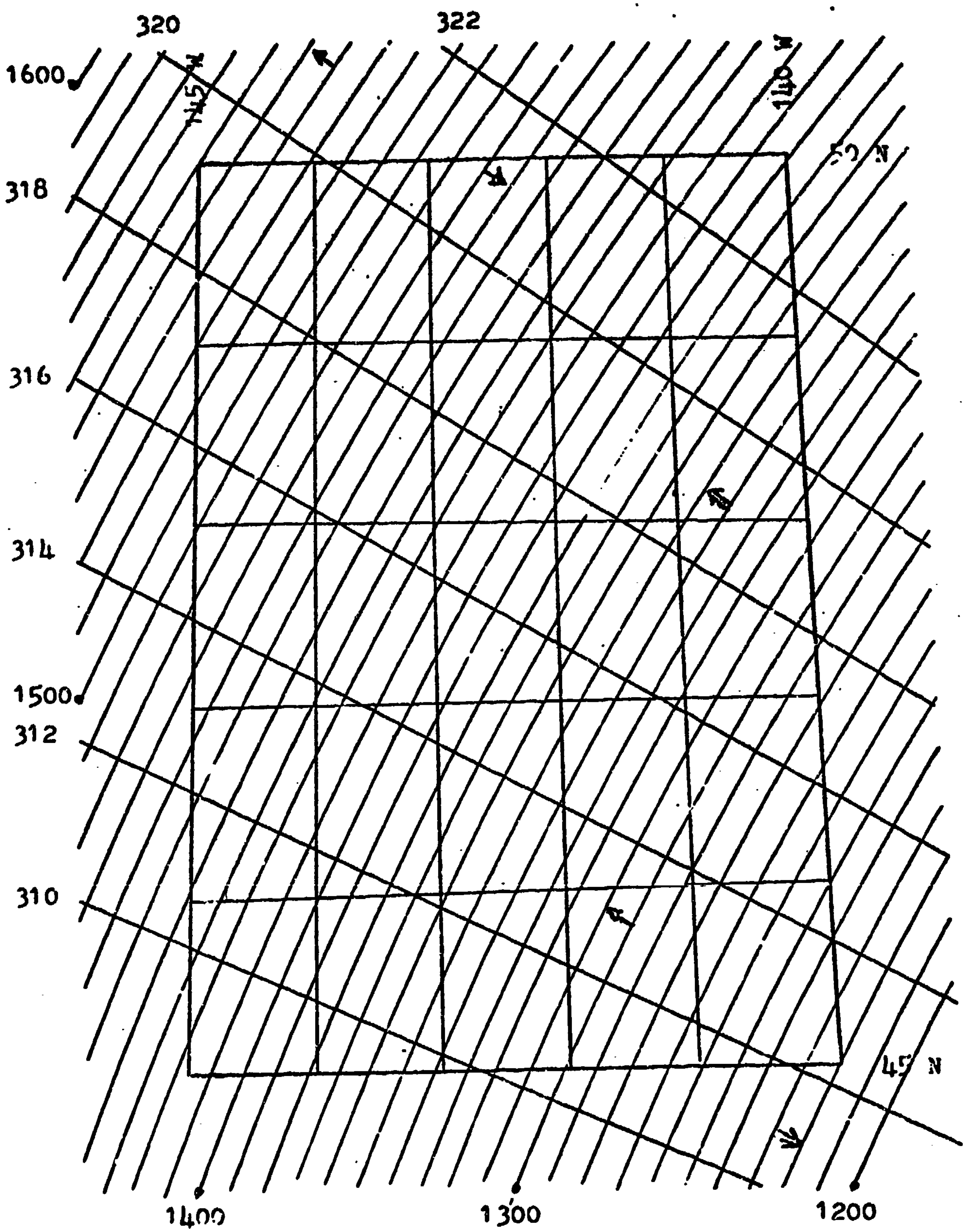

AREA 1

9/22/75 1800 - 1830 Z

FIGURE E.2-3

SECRET

(This page is unclassified)

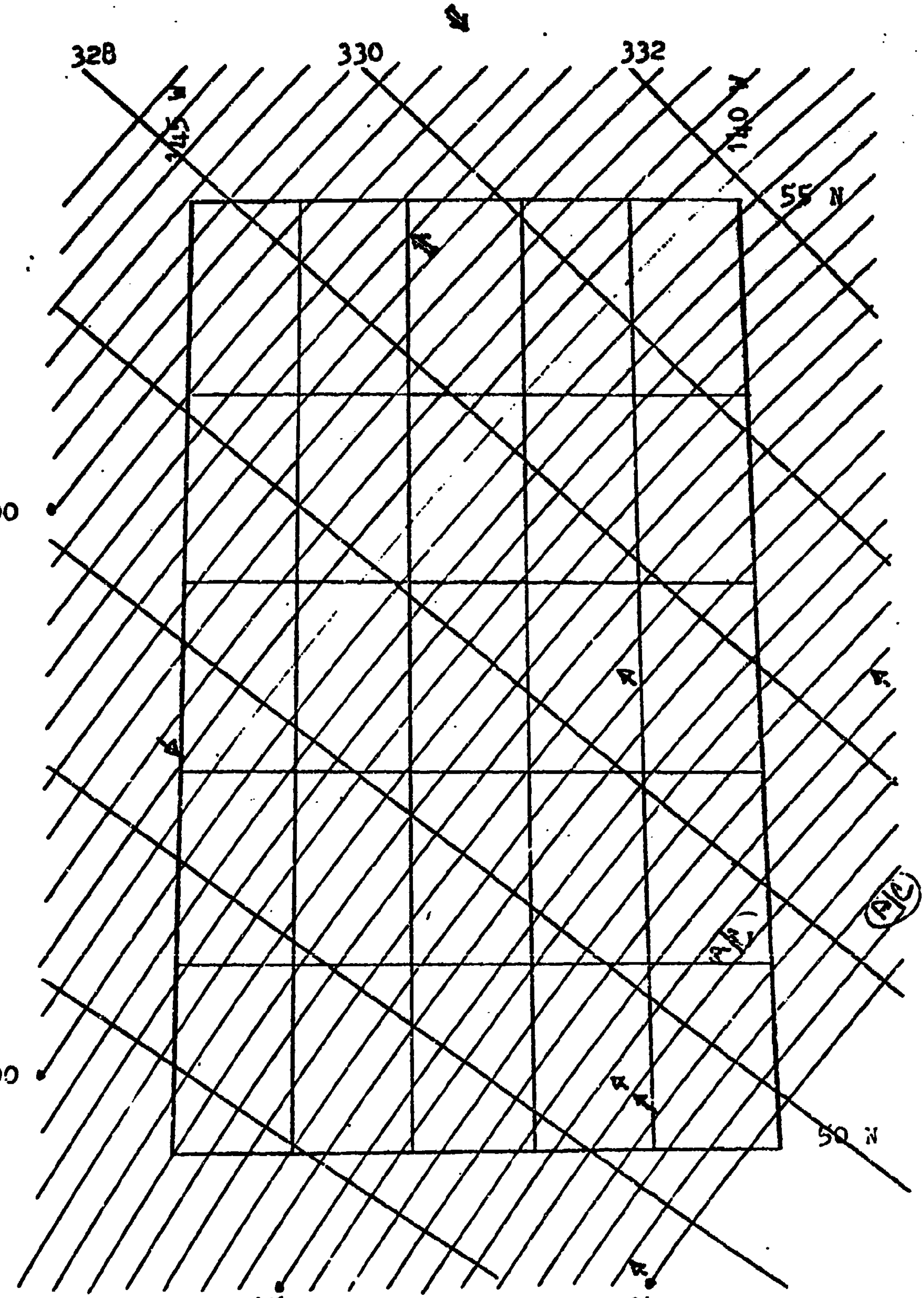

AREA 2

9/24/75 1430 - 1500 Z

FIGURE E.2-4

DEPARTMENT OF THE NAVY
OFFICE OF NAVAL RESEARCH
800 NORTH QUINCY STREET
ARLINGTON, VA 22217-5660

IN REPLY REFER TO
5510/1
Ser 43/885
03 Dec 03

MEMORANDUM FOR DISTRIBUTION LIST

Subj: DECLASSIFICATION OF CHURCH OPAL DOCUMENTS

Ref: (a) SECNAVINST 5510.36

Encl: (1) Partial List of CHURCH OPAL Documents

1. In accordance with reference (a), a declassification review has been conducted on a number of classified CHURCH OPAL documents.

2. The CHURCH OPAL documents listed in Part 1 of enclosure (1) have been downgraded to UNCLASSIFIED and have been approved for public release. These documents should be remarked as follows:

> Classification changed to UNCLASSIFIED by authority of the Chief of Naval Operations (N774) letter N774D/3U630173, 11 September 2003.
>
> DISTRIBUTION STATEMENT A: Approved for Public Release; Distribution is unlimited.

3. If other CHURCH OPAL documents are located in your repositories, their markings should be changed and a copy of the title page and a notation of how many pages the documents contained should be provided to Chief of Naval Research (ONR 43) 800 N. Quincy Street, Arlington, VA 22217-5660. This will enable me to maintain a master list of downgraded/declassified CHURCH OPAL reports.

4. Questions may be directed to the undersigned on (703) 696-4619, DSN 426-4619.

Peggy Lambert

PEGGY LAMBERT
By direction

DISTRIBUTION LIST:
See page 2

Subj: DECLASSIFICATION OF CHURCH OPAL DOCUMENTS

DISTRIBUTION LIST:
NAVOCEANO (Code N121LC - Jaime Ratliff)
NRL Washington (Code 5596.3 - Mary Templeman)
PEO LMW Det San Diego (PMS 181-1) (LTJG Ken Larson, USN)
DTIC-OCQ (Larry Downing)
ARL, U of Texas (David Knobles)
BlueSea Corporation (Roy Gaul)
ONR 32B (CAPT Houtman)
ONR 321 (Dr. Livingston)
ONR 03B (Mr. Lackie)

Title: CHURCH OPAL: SURVEILLANCE OF SHIPPING, 15 January 1976 - Turk, LA, Barnes, AE, and Solomon, LP; PSI TR-036027, PSI IS-391
DTIC No.: AD C007 024
Available at NRL (522316)

Title: VERIFICATION OF CHURCH OPAL DATA ANALYSIS AND TAPE REDUCTION PROBLEMS
Classification: UNCLASSIFIED
Author: Shooter, JA
Originator: ARL:UT
Ref. No.: TL-CS-76-2 Date: 12 November 1976
Available at ARL:UT (49698)

Title: REPORT OF A CW WORKSHOP (Held at NORDA, Bay St Louis, MS, 28-29 Sep 1976)
Classification: UNCLASSIFIED
Author: Wallace, WE, Weinstein, MS, and Wittenborn, AF
Originator: Tracor, Inc, and Underwater Systems, Inc
Ref. No.: USI 564-1-77 Date: 24 January 1977
Available at NRL (531773)

Title: AMBIENT NOISE AS A FUNCTION OF WIND SPEED
Classification: UNCLASSIFIED
Author: Wittenborn, AF.
Originator: [31st Navy Symposium on Underwater Acoustics?]
Ref. No.: unknown Date: 1976
Available at NRL (524574)

Title: DEPTH DEPENDENCE OF NOISE RESULTING FROM SHIP TRAFFIC AND WIND
Classification: UNCLASSIFIED
Author: Shooter, JA.
Originator: ARL:UT
Ref. No.: unknown Date: 1978
Available at NRL (533930) and presumably ARL:UT (??)